Central China
Center for Nuclear Theory
华中核理论中心

JETSCAPE

Quantifying the impact of longitudinal information on ultra-relativistic collision measurements across systems at the RHIC top energy with a 3D Bayesian calibration

Andi Mankolli

Vanderbilt University

NSF
SFP_300495

Heavy Ion Collisions Modeling

Pre-hydro

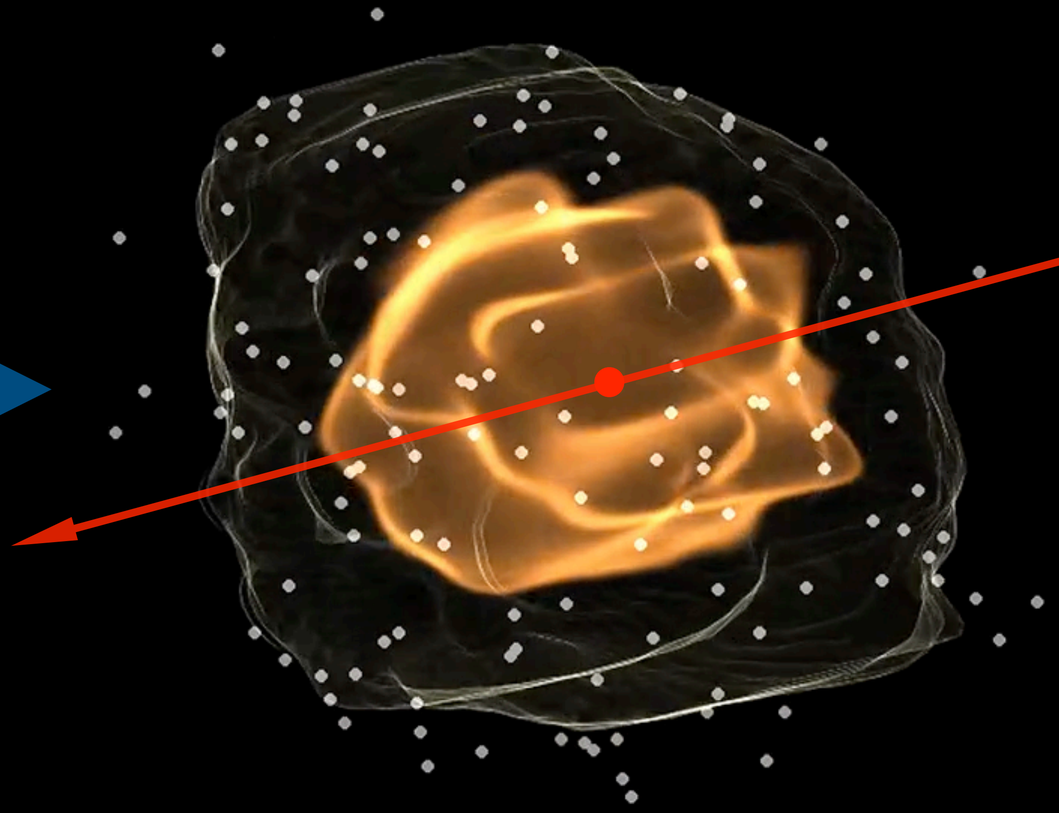

Post-hydro

Chun Shen: iEBE MUSIC

3D Calibration with RHIC top energy data

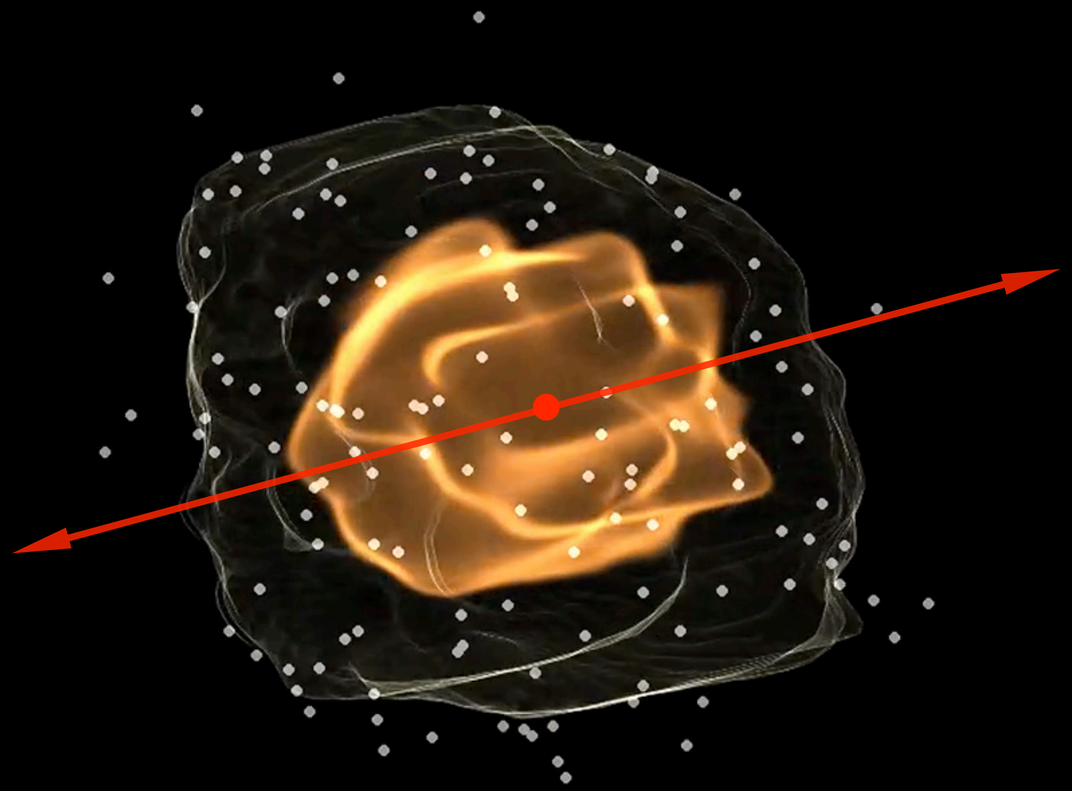

Chun Shen: iEBE MUSIC

3D Calibration with RHIC top energy data

- Learn about longitudinal dynamics from 3D data
- Comprehensive high-energy dataset
- RHIC data: weaker boost invariance and variety of asymmetric systems
- Top energy: fewer uncertainties from finite μ_B

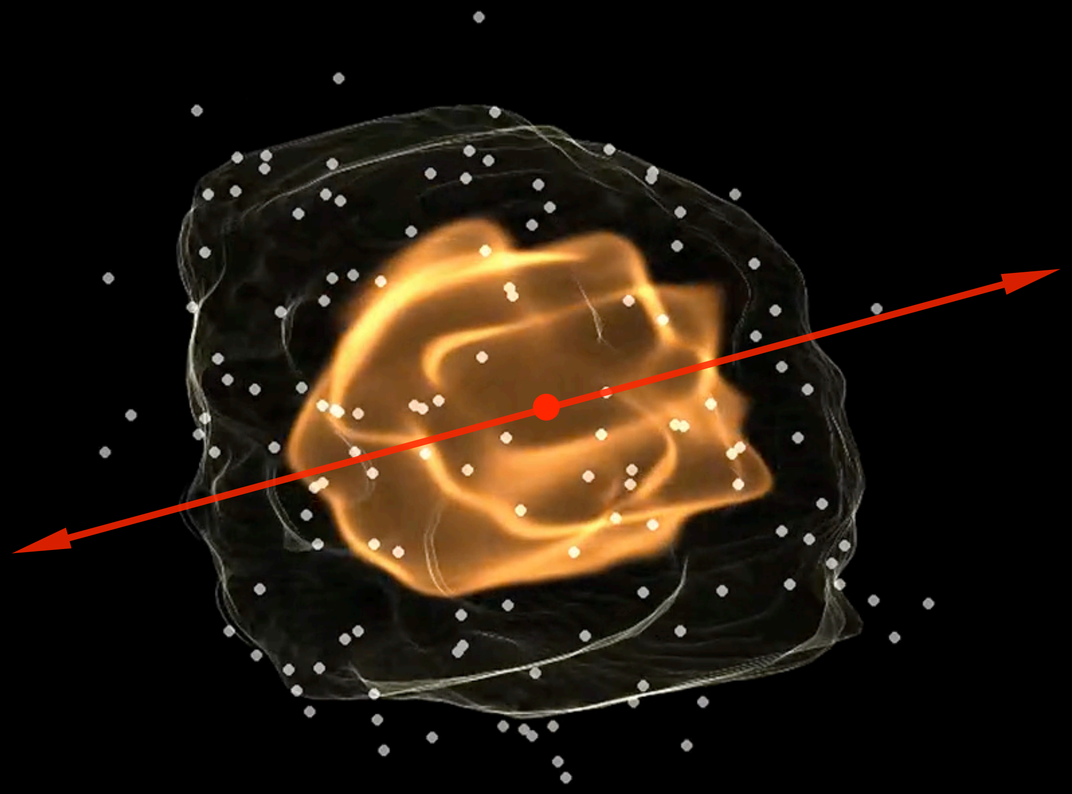

Chun Shen: iEBE MUSIC

3D Calibration with RHIC top energy data

- Learn about longitudinal dynamics from 3D data
- Comprehensive high-energy dataset
- RHIC data: weaker boost invariance and variety of asymmetric systems
- Top energy: fewer uncertainties from finite μ_B

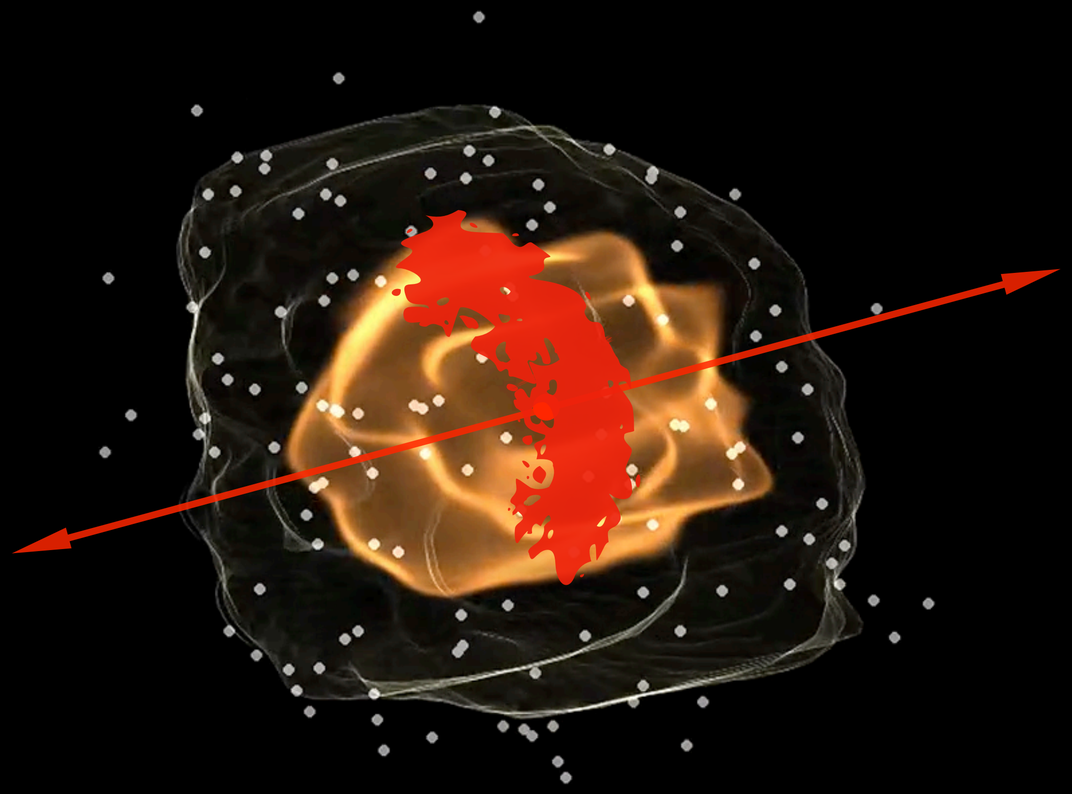

Chun Shen: iEBE MUSIC

The Model: 3D Initial State and Hydrodynamics

Initial State

Hydrodynamics

Hadronic Transport

3D MCGlauber

MUSIC + UrQMD

The Model: 3D Initial State and Hydrodynamics

Initial State

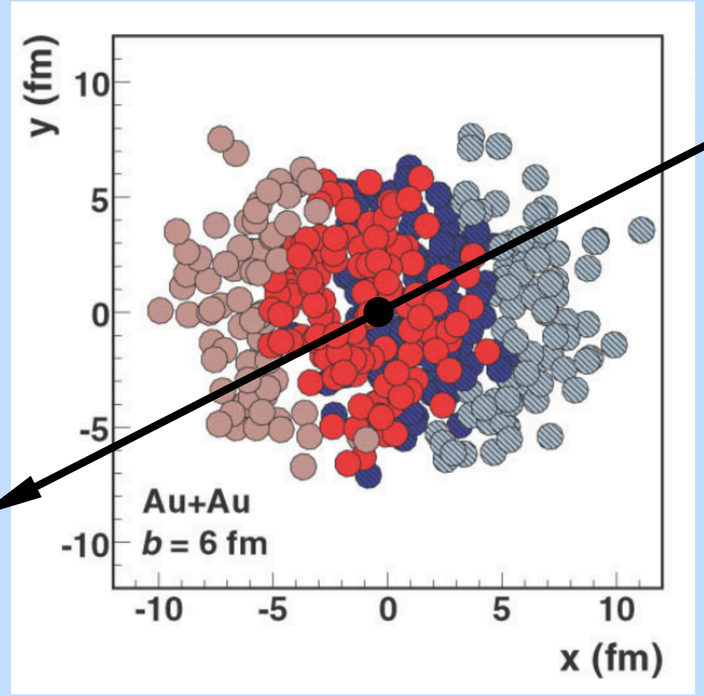

3D MCGlauber

The Model: 3D Initial State and Hydrodynamics

Initial State

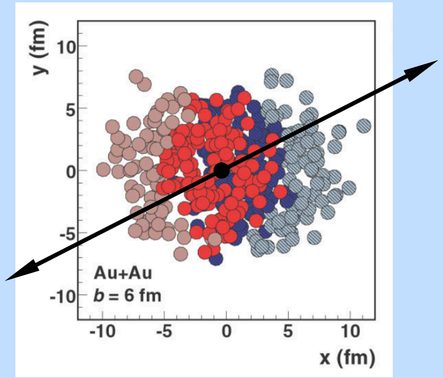

3D MCGlauber

The Model: 3D Initial State and Hydrodynamics

Initial State

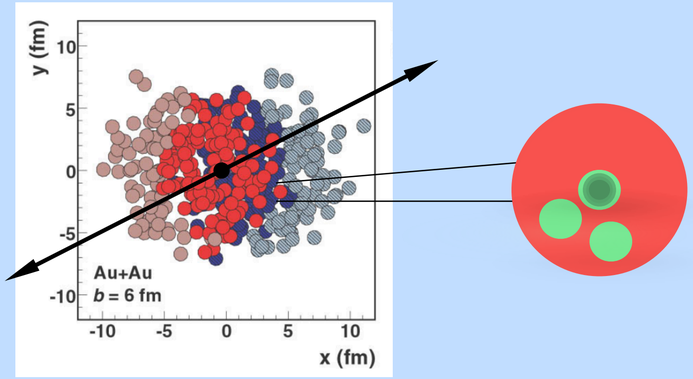

3D MCGlauber

The Model: 3D Initial State and Hydrodynamics

Initial State

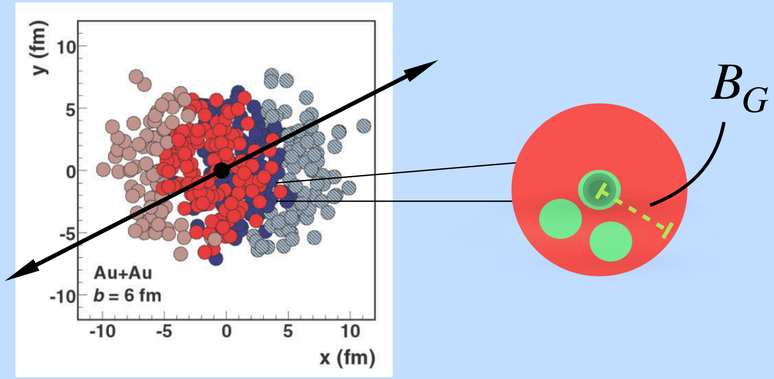

$$P(\vec{r}) \propto e^{-r^2/(2B_G)}$$

3D MCGlauber

The Model: 3D Initial State and Hydrodynamics

Initial State

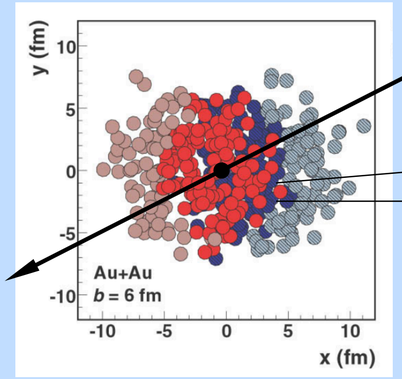

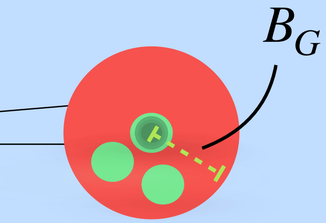

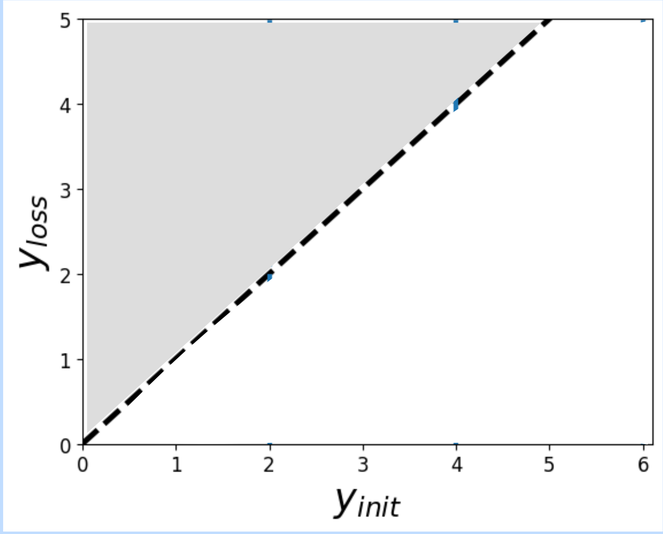

3D MCGlauber

The Model: 3D Initial State and Hydrodynamics

Initial State

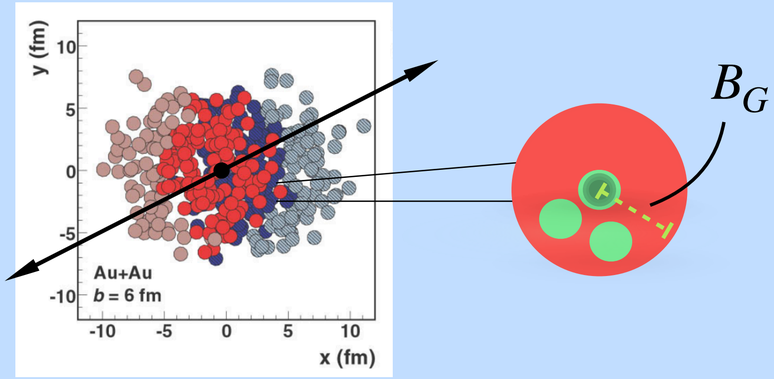

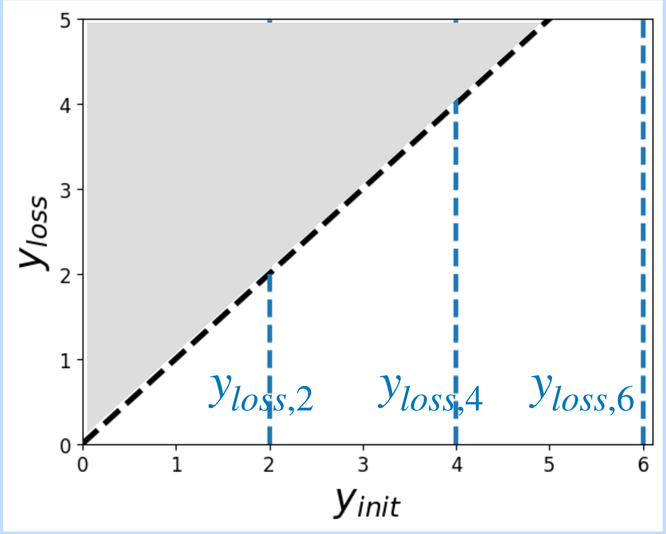

3D MCGlauber

The Model: 3D Initial State and Hydrodynamics

Impose energy momentum conservation

α_{rem} (Remnant energy loss fraction)

Initial State

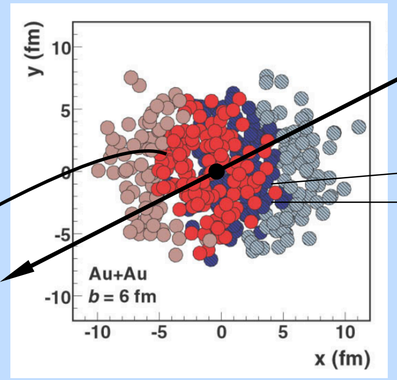

B_G

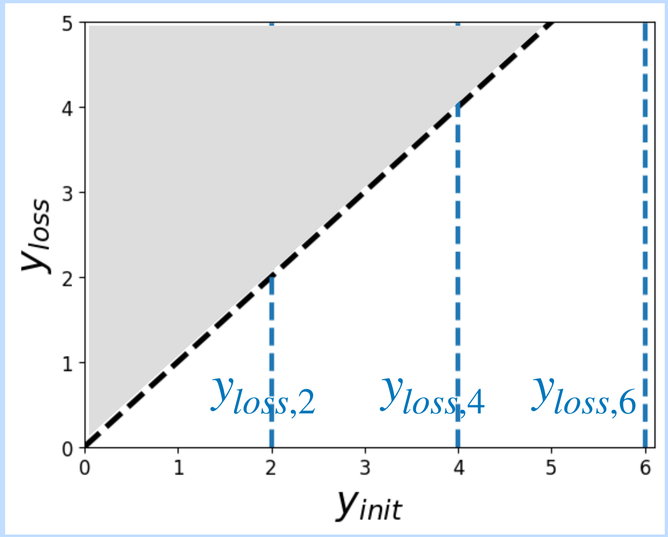

3D MCGlauber

The Model: 3D Initial State and Hydrodynamics

Impose energy momentum conservation

α_{rem} (Remnant energy loss fraction)

Initial State

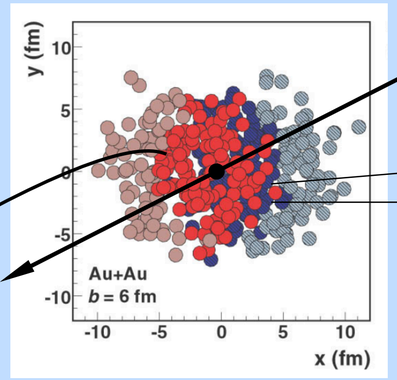

B_G

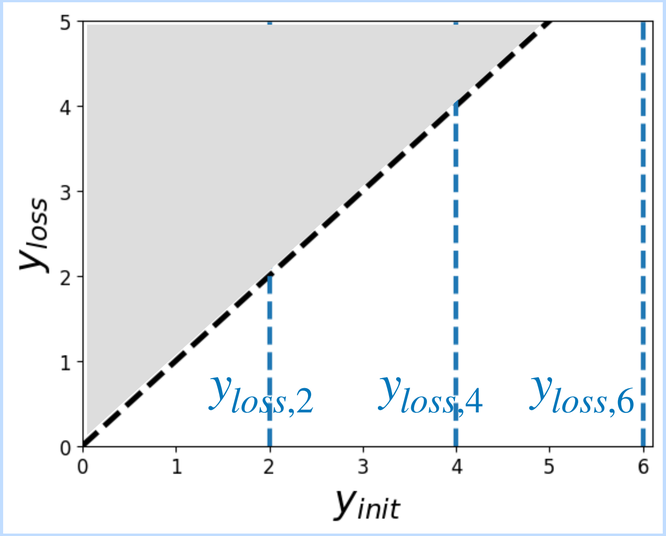

Schenke, Shen, Zhao.

Phys. Rev. C 105, 064905 (2022)

Phys. Rev. C 97, 024907 (2018)

3D MCGlauber

The Model: 3D Initial State and Hydrodynamics

Impose energy momentum conservation

α_{rem} (Remnant energy loss fraction)

Initial State

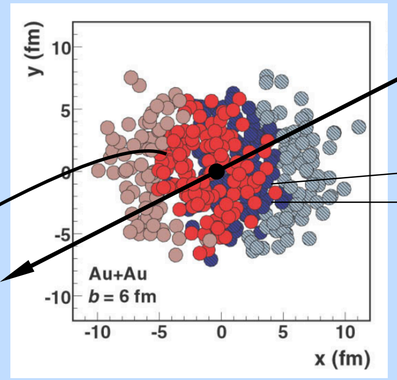

B_G

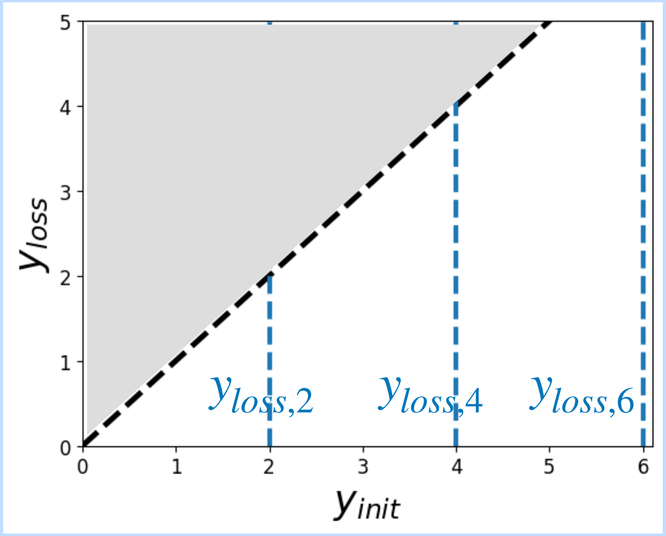

Schenke, Shen, Zhao.

Phys. Rev. C 105, 064905 (2022)

Phys. Rev. C 97, 024907 (2018)

Hydrodynamics

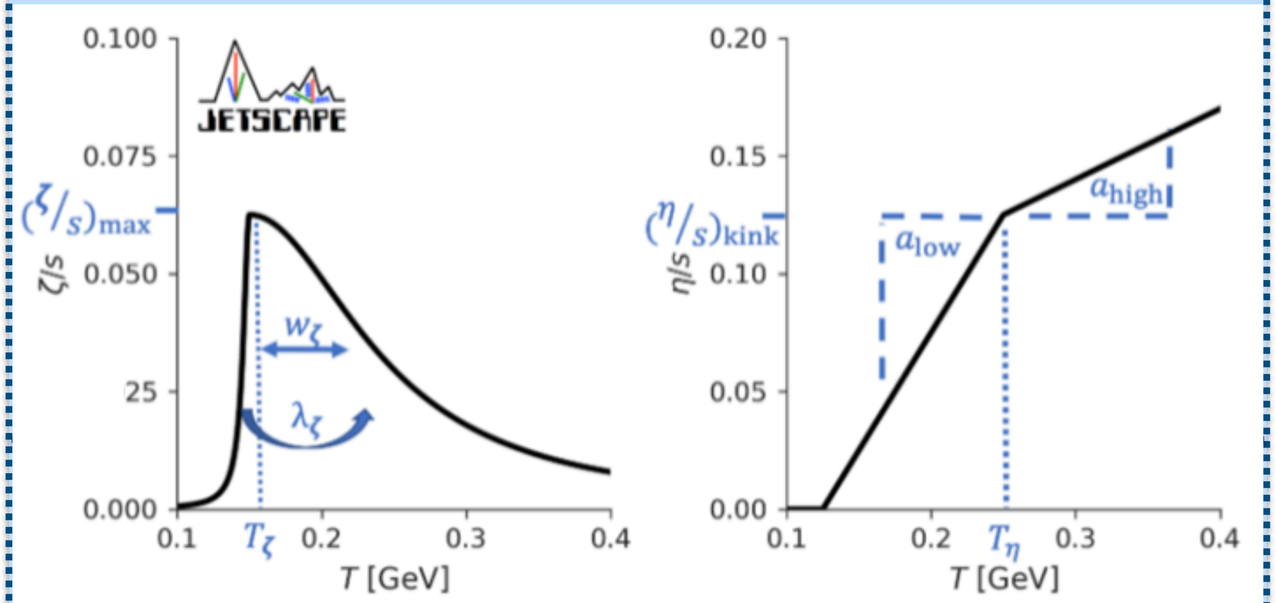

3D MCGlauber

MUSIC

The Model: 3D Initial State and Hydrodynamics

Impose energy momentum conservation

α_{rem} (Remnant energy loss fraction)

Initial State

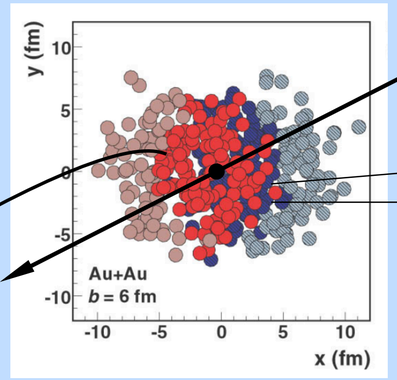

B_G

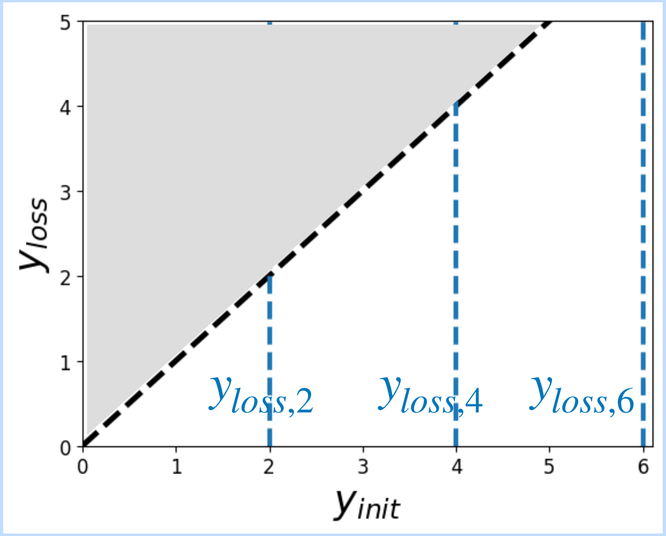

Schenke, Shen, Zhao.

Phys. Rev. C 105, 064905 (2022)

Phys. Rev. C 97, 024907 (2018)

Hydrodynamics

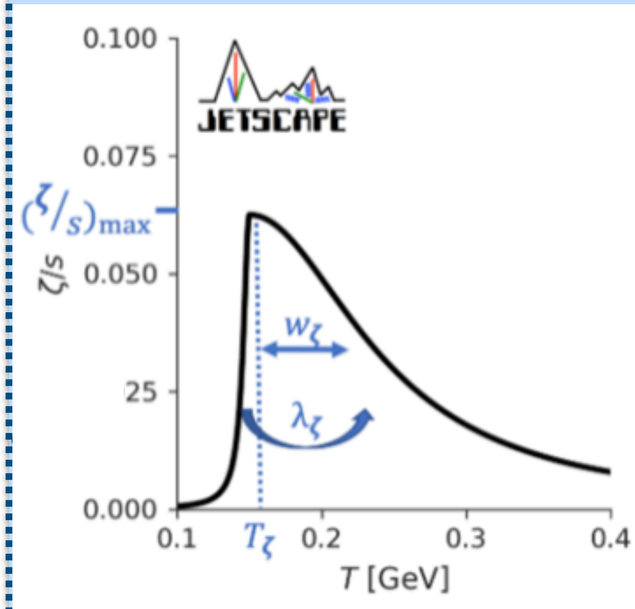

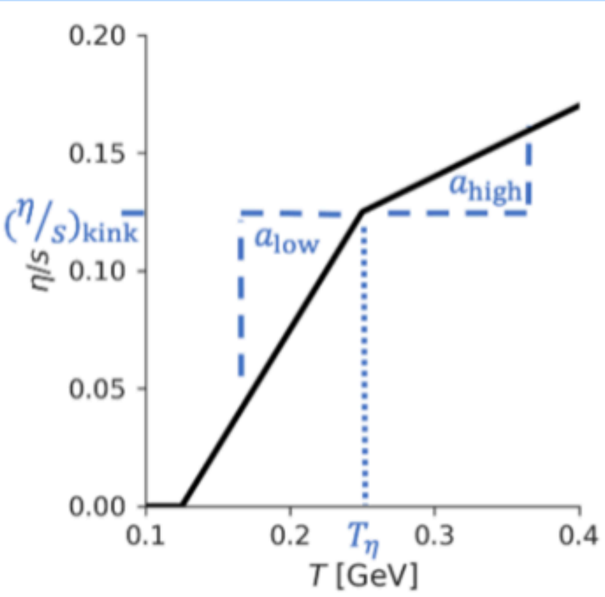

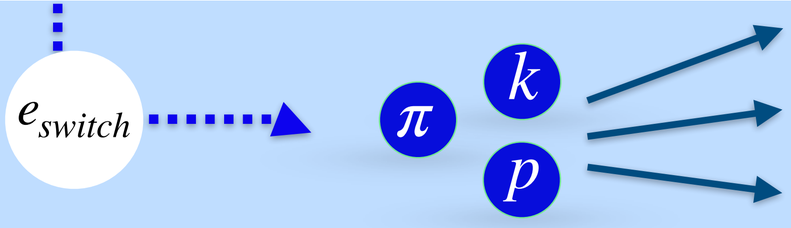

Hadronic Transport

3D MCGlauber

MUSIC + UrQMD

Experimental data

Experimental data

Au-Au 200 GeV

- $v_2(\eta)$ **STAR**
- $v_2(\eta)$ **PHOBOS**
- $\langle p_T \rangle$ π, k **STAR**
- $\langle p_T \rangle$ **k, p PHENIX**
- $\langle p_T \rangle$ p STAR
- $\langle p_T \rangle$ π PHENIX
- $dN_{ch}/d\eta(\eta)$ **PHOBOS**
- v_2**(cent) STAR**
- v_3**(cent) STAR**
- $v_2(p_T)$ **PHENIX**
- $v_2(p_T)$ **STAR**
- $v_3(p_T)$ PHENIX
- $v_4(p_T)$ PHENIX
- $dN_{ch}/d\eta(\eta)$ BRAHMS
- $r_2(\eta)$ STAR
- $r_3(\eta)$ STAR
- $dE_T/d\eta$(cent) PHENIX

d-Au 200 GeV

- $dN_{ch}/d\eta(\eta)$ PHOBOS
- $dN_{ch}/d\eta(\eta)$ **PHENIX**
- $v_2(p_T)$ **PHENIX**
- $v_2(p_T)$ **STAR**
- $v_2(\eta)$ **PHENIX**
- $v_3(p_T)$ STAR
- $v_3(p_T)$ PHENIX
- $dE_T/d\eta$(cent) PHENIX

Experimental data: a note on azimuthal anisotropy

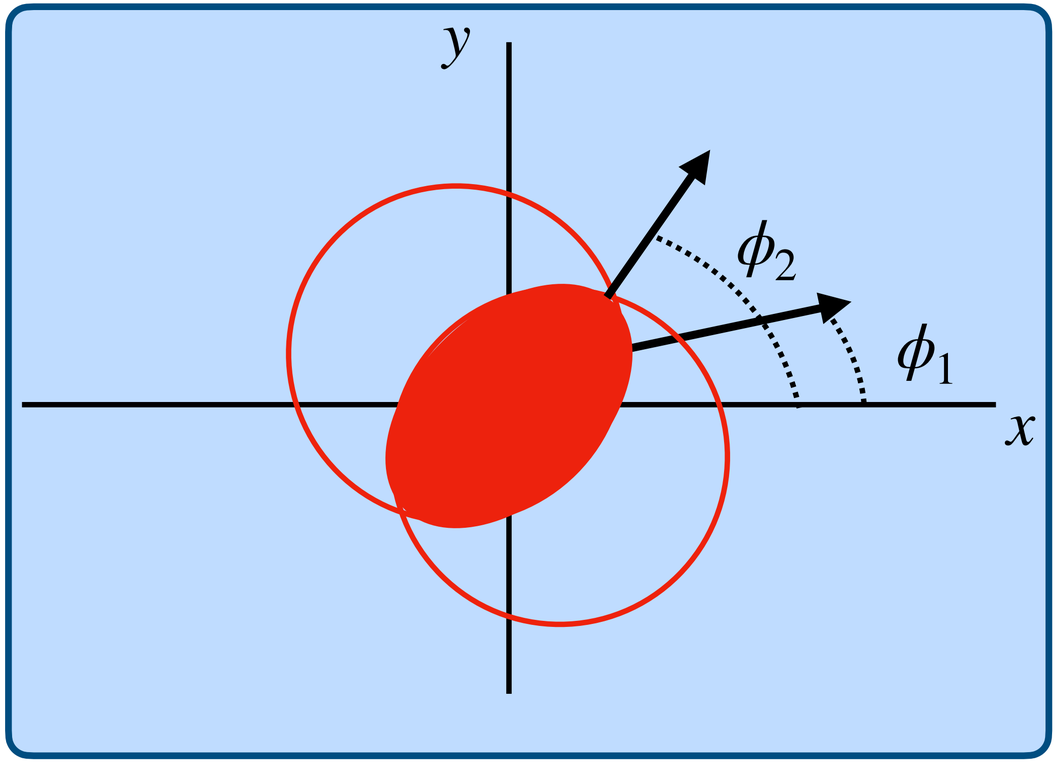

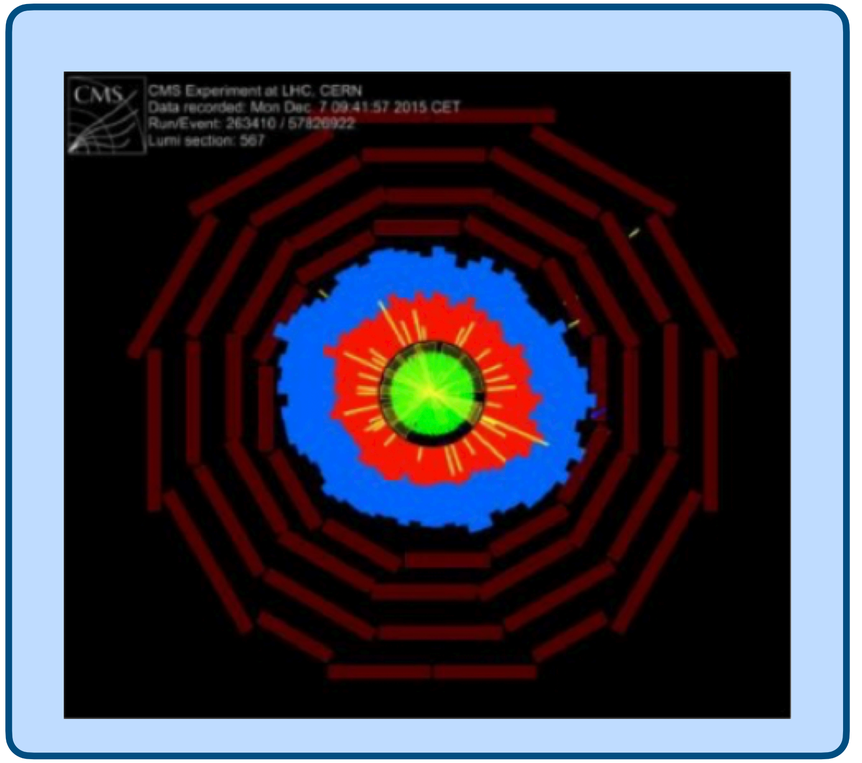

Experimental data: a note on azimuthal anisotropy

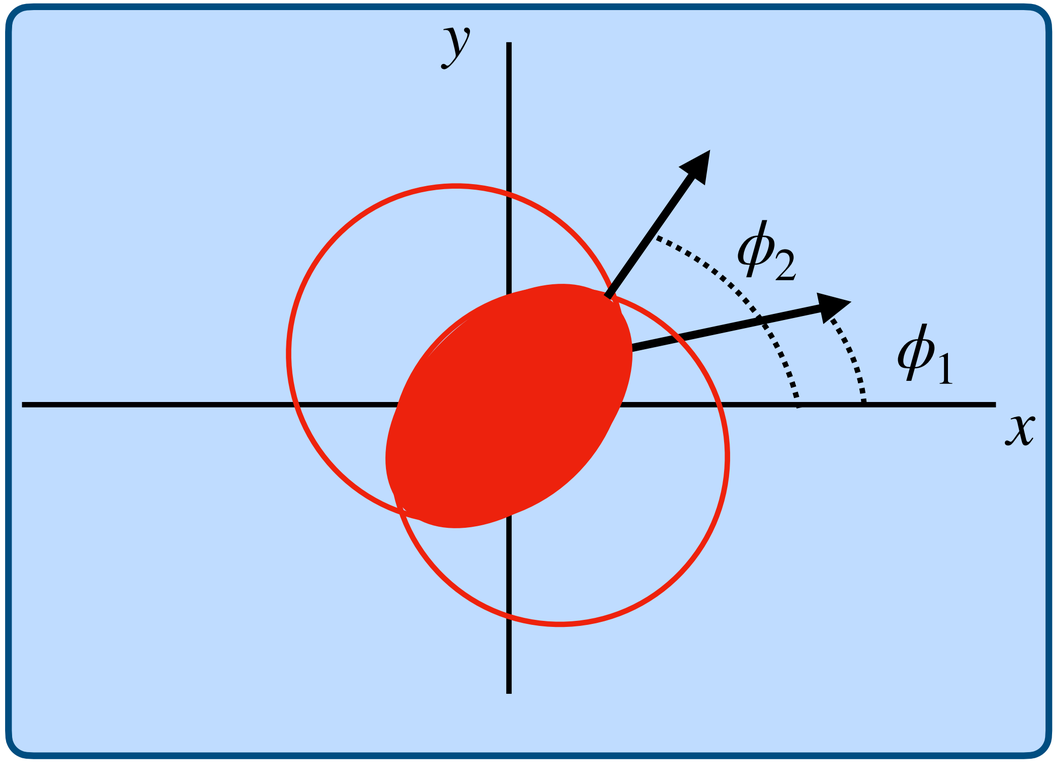

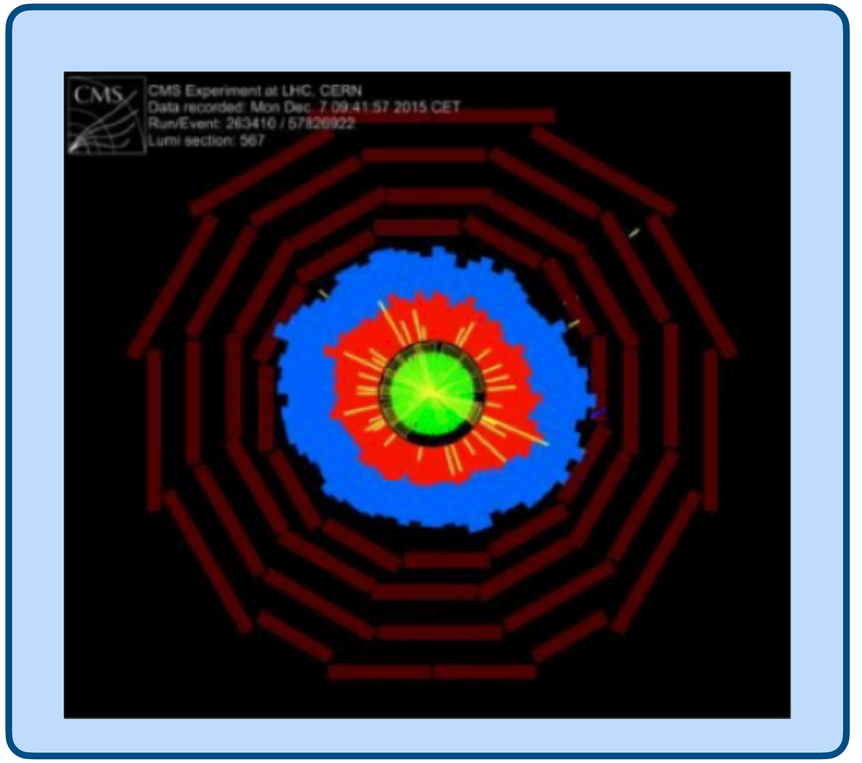

Two-particle spectrum

$$\frac{dN_{pair}}{d\Delta\phi} \propto 1 + 2\sum V_n cos(n\Delta\phi)$$

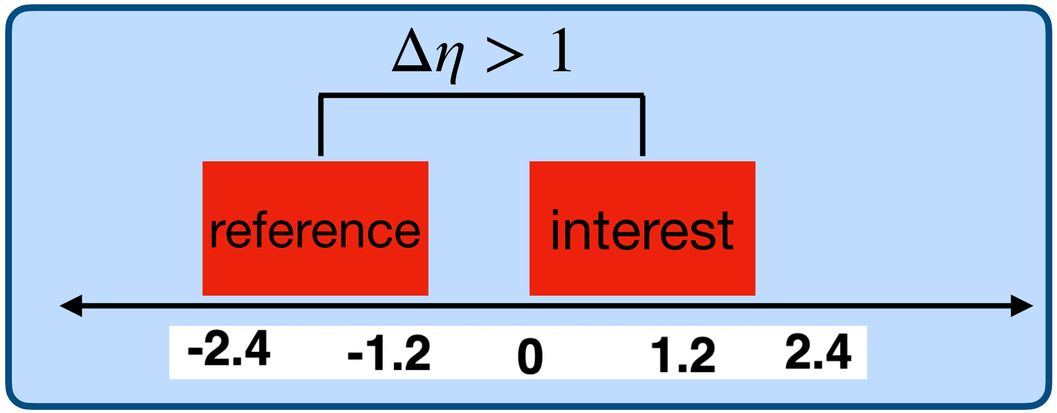

Experimental data: a note on azimuthal anisotropy

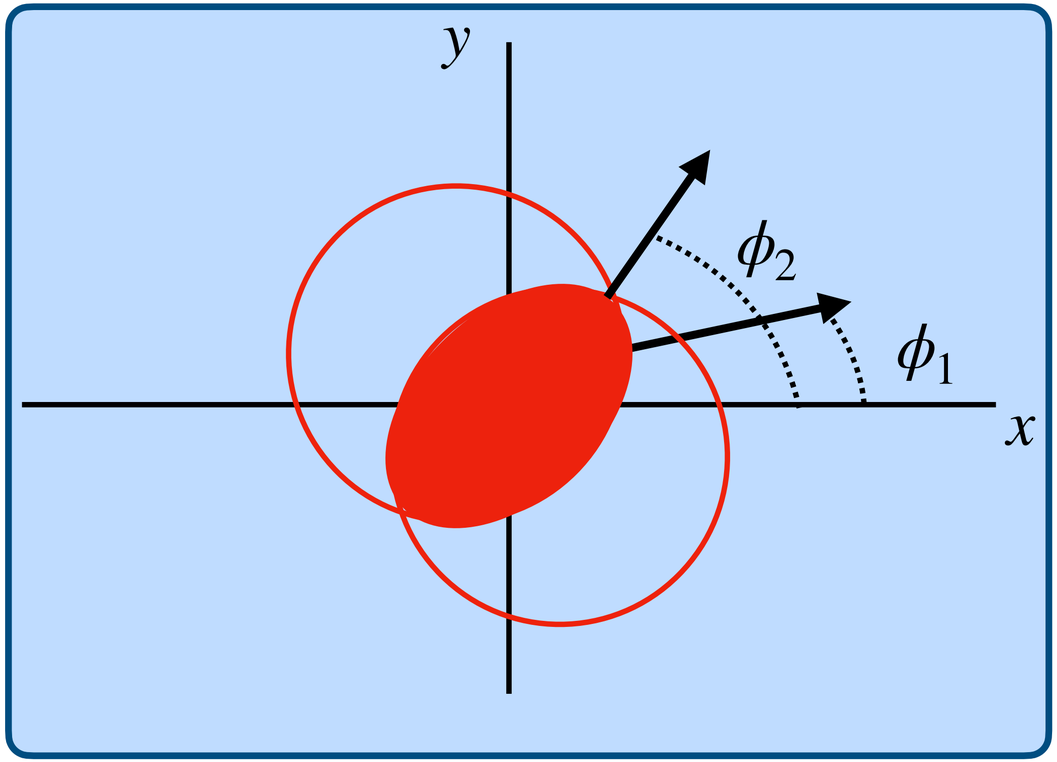

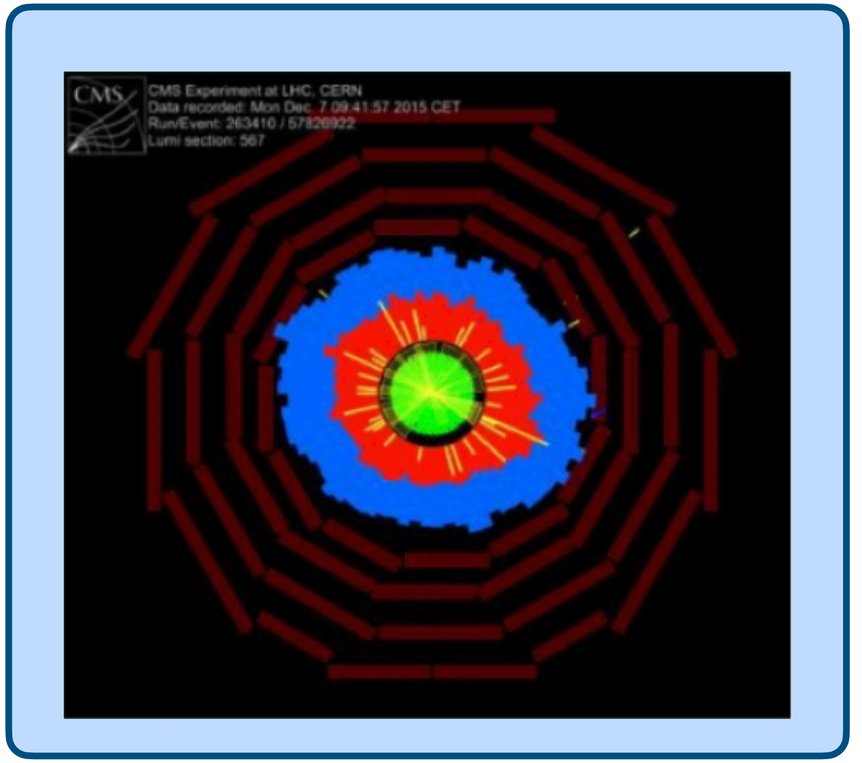

Two-particle spectrum

$$\frac{dN_{pair}}{d\Delta\phi} \propto 1 + 2\sum V_n cos(n\Delta\phi)$$

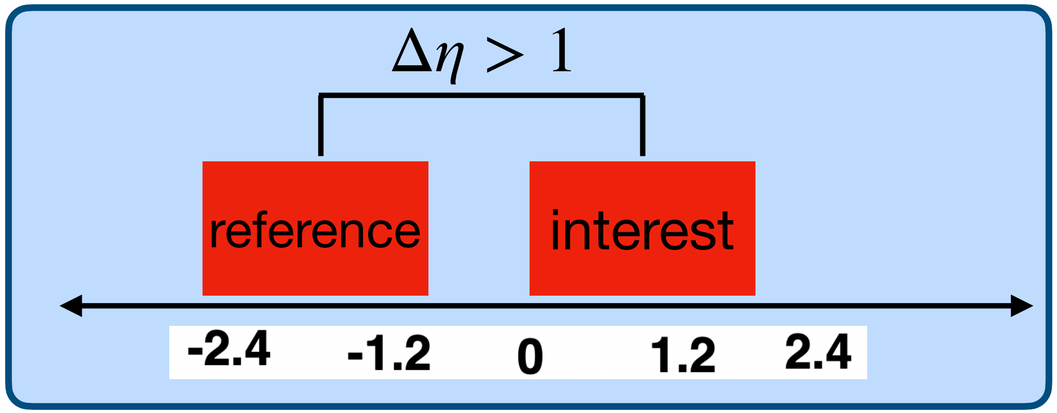

Experimental data: modeling the observables

Example:

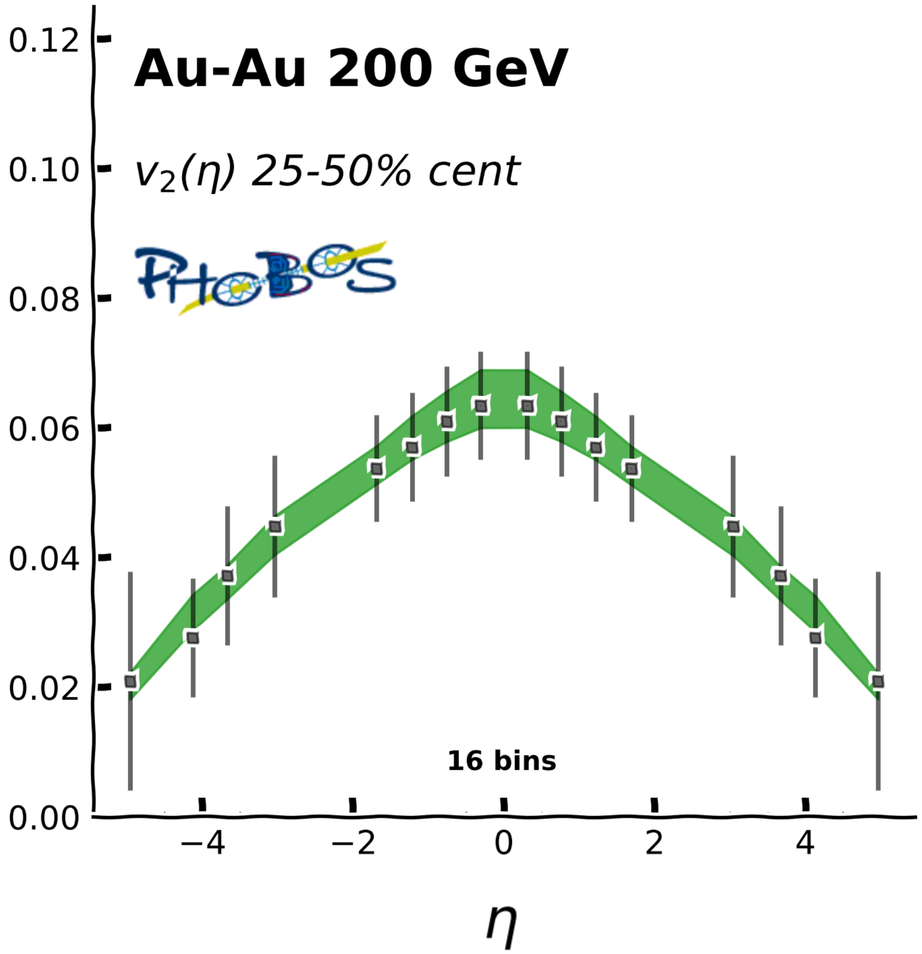

- "Mid-rapidity" measurements contain forward/backward information
- Centrality selection
  - $3.5 < |\eta| < 4.5$
- Event plane determination
  - $2.05 < |\eta| < 3.2$

Experimental data: modeling the observables

Example:

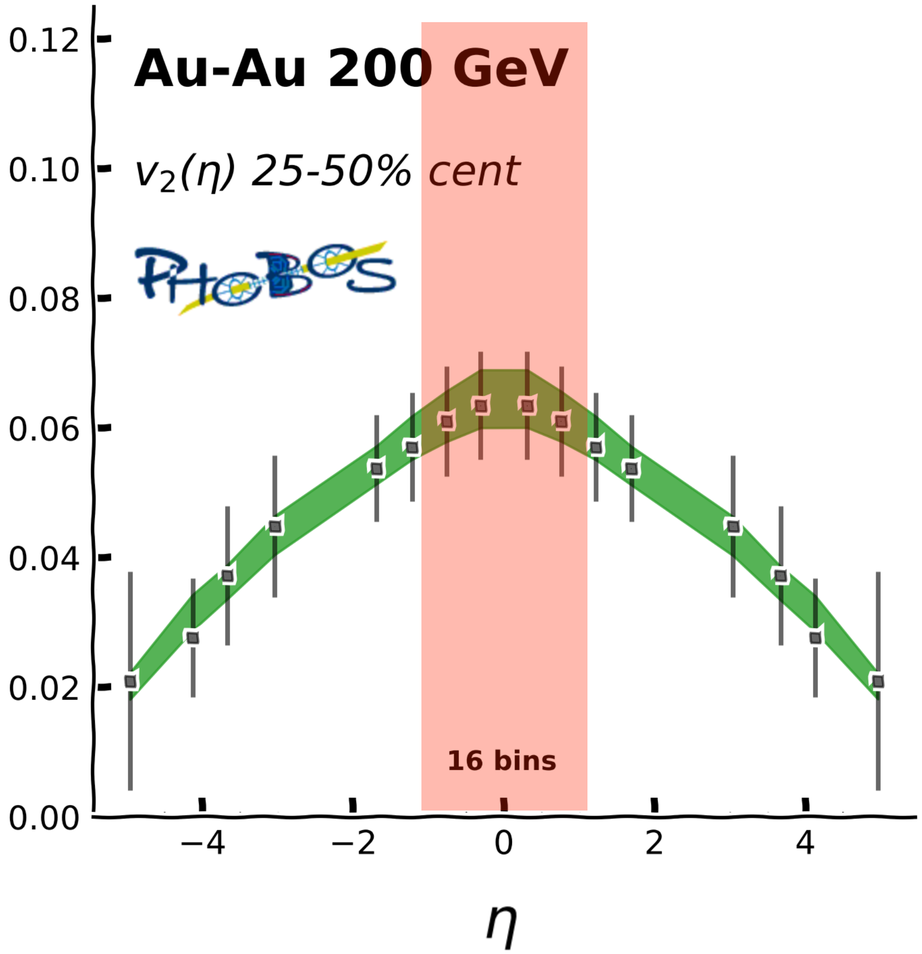

- "Mid-rapidity" measurements contain forward/backward information
- Centrality selection
  - $3.5 < |\eta| < 4.5$
- Event plane determination
  - $2.05 < |\eta| < 3.2$

Experimental data: modeling the observables

Example:

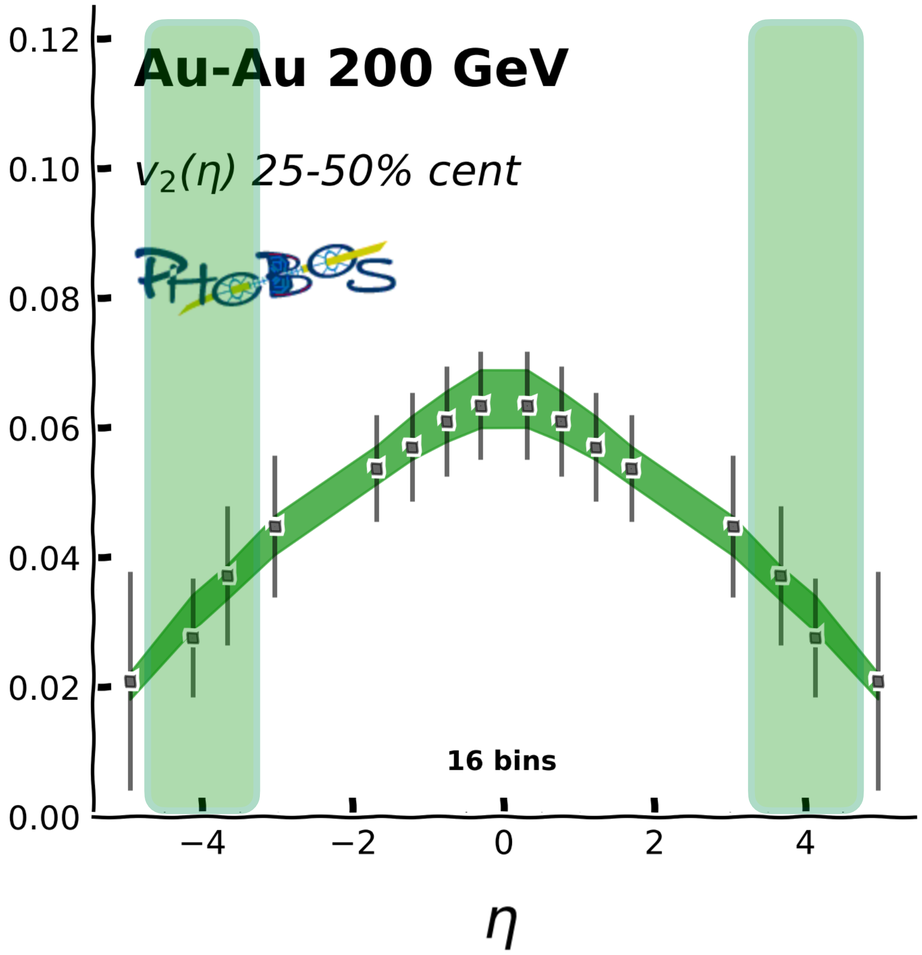

- "Mid-rapidity" measurements contain forward/backward information
- Centrality selection
  - $3.5 < |\eta| < 4.5$
- Event plane determination
  - $2.05 < |\eta| < 3.2$

Experimental data: modeling the observables

Example:

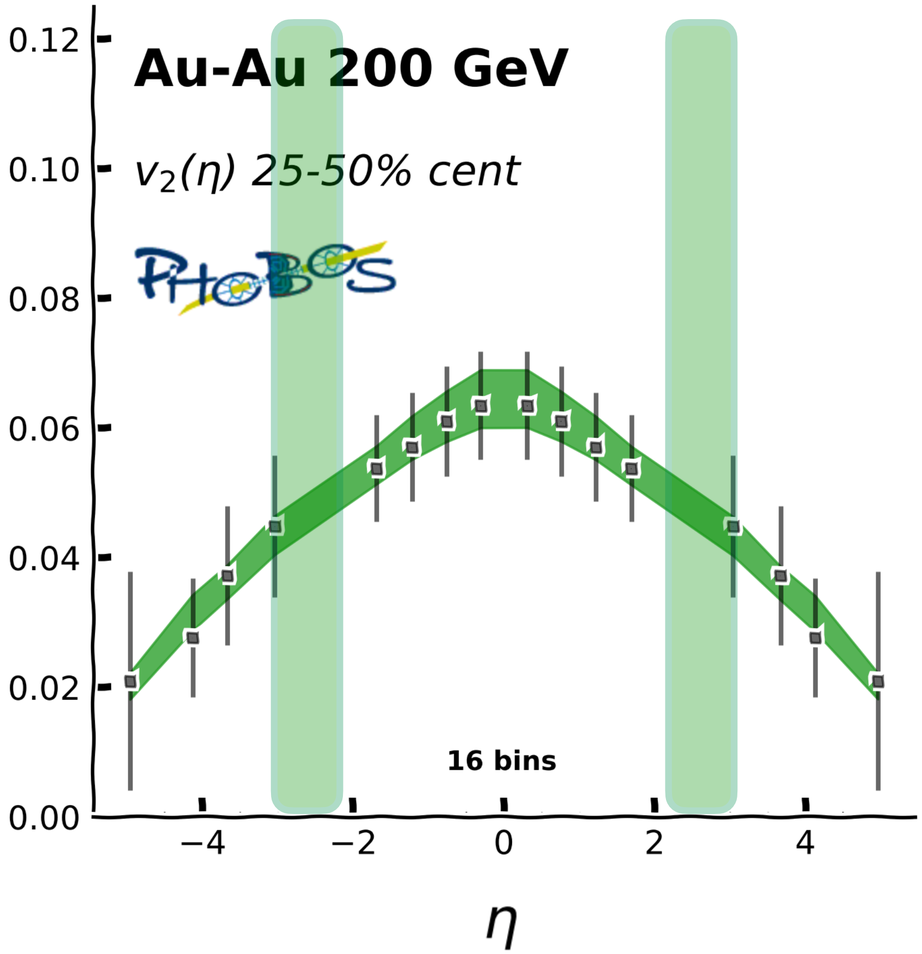

- "Mid-rapidity" measurements contain forward/backward information
- Centrality selection
  - $3.5 < |\eta| < 4.5$
- Event plane determination
  - $2.05 < |\eta| < 3.2$

Model emulation and validation of sensitivity

- ~1000 observable bins → 20 principal components

- 400 parameter training points for Gaussian Process with ~2000 events each

Closure tests throughout parameter space:

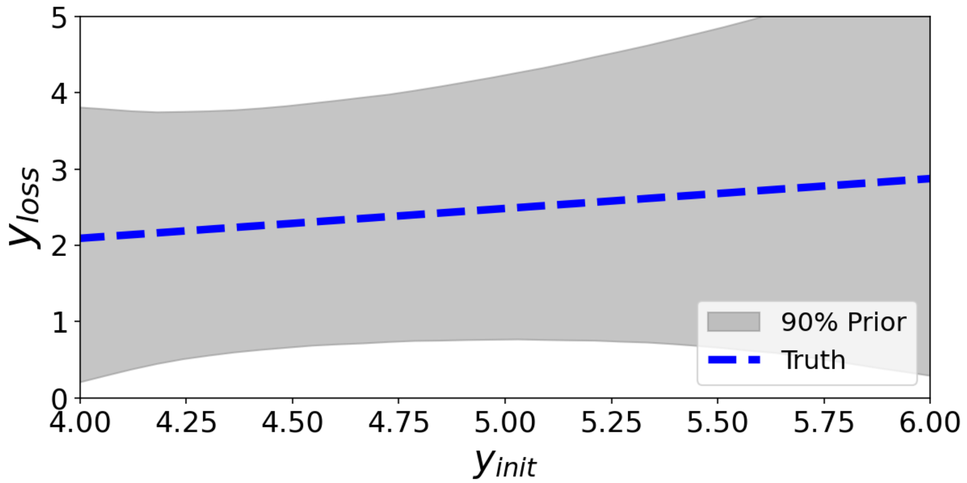

Model emulation and validation of sensitivity

- ~1000 observable bins → 20 principal components

- 400 parameter training points for Gaussian Process with ~2000 events each

Closure tests throughout parameter space:

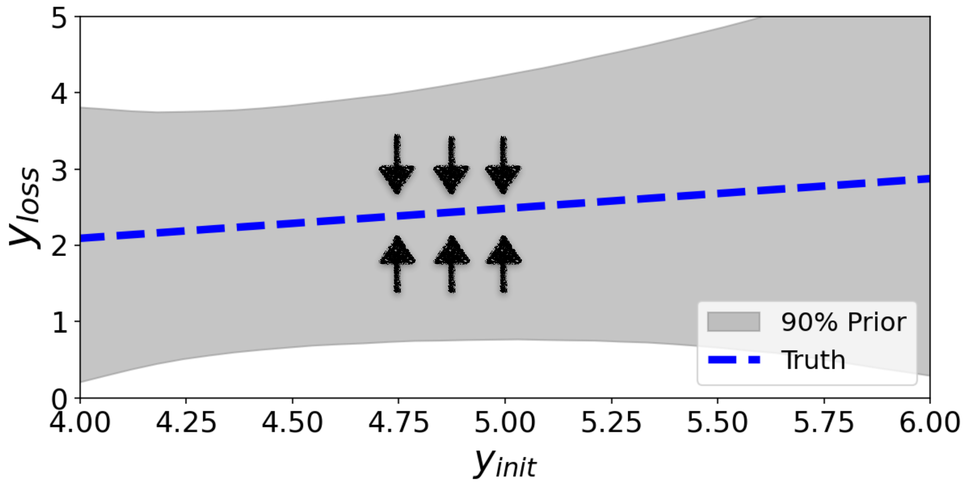

Model emulation and validation of sensitivity

- ~1000 observable bins → 20 principal components
- 400 parameter training points for Gaussian Process with ~2000 events each

Closure tests throughout parameter space:

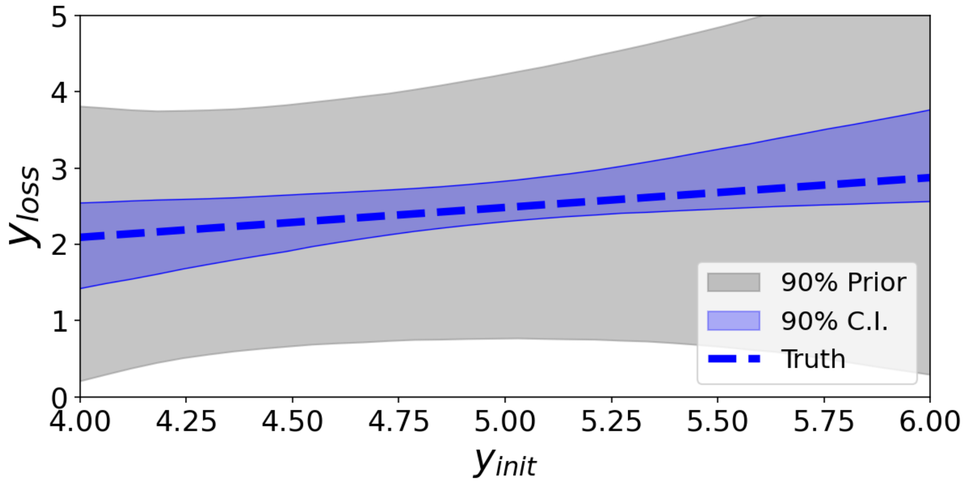

Model emulation and validation of sensitivity

- ~1000 observable bins → 20 principal components
- 400 parameter training points for Gaussian Process with ~2000 events each

Closure tests throughout parameter space:

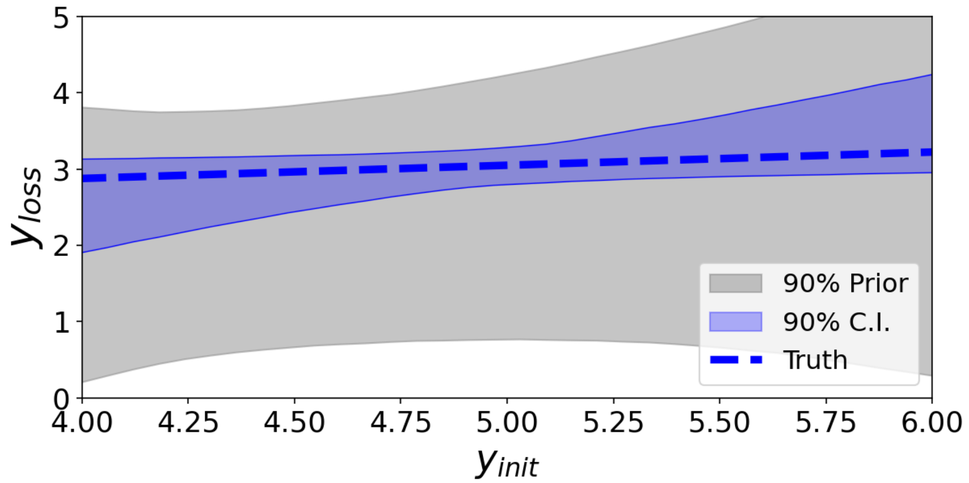

Model emulation and validation of sensitivity

- ~1000 observable bins → 20 principal components
- 400 parameter training points for Gaussian Process with ~2000 events each

Closure tests throughout parameter space:

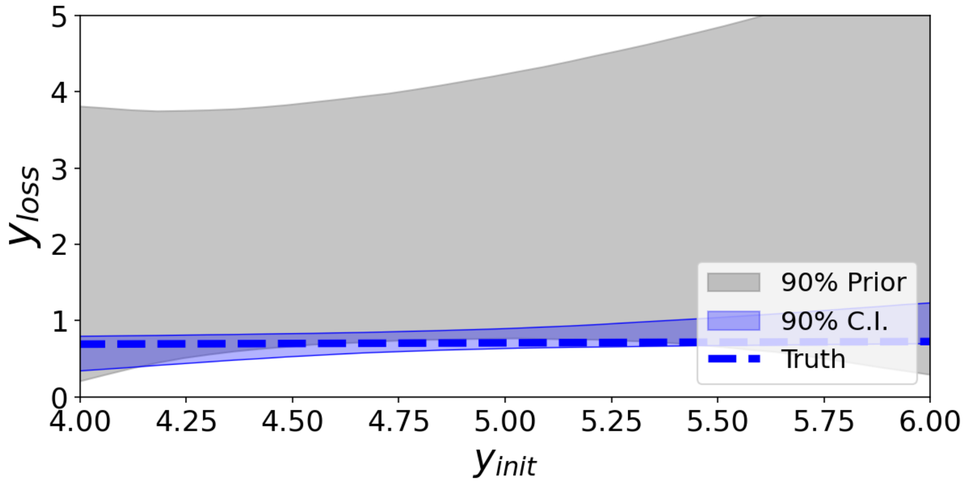

Model emulation and validation of sensitivity

- ~1000 observable bins → 20 principal components
- 400 parameter training points for Gaussian Process with ~2000 events each

Closure tests throughout parameter space:

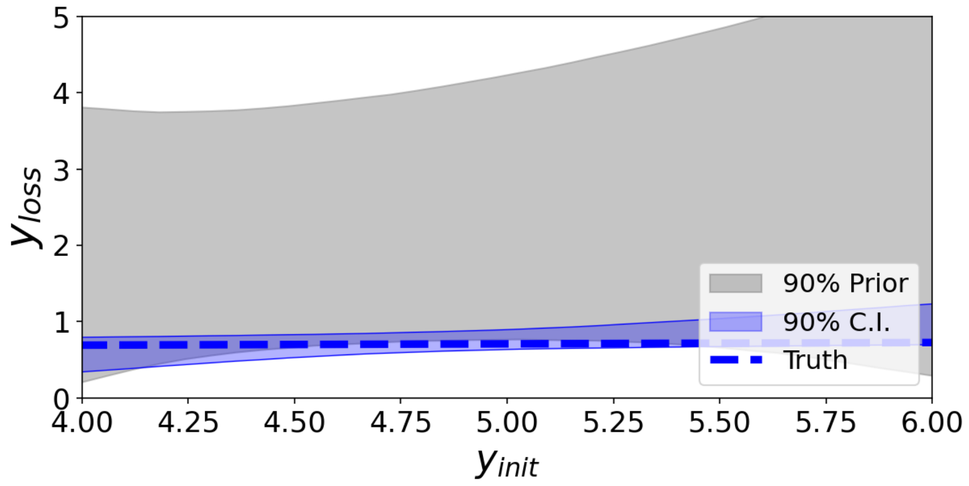

Closure tests around particular region of parameter space:

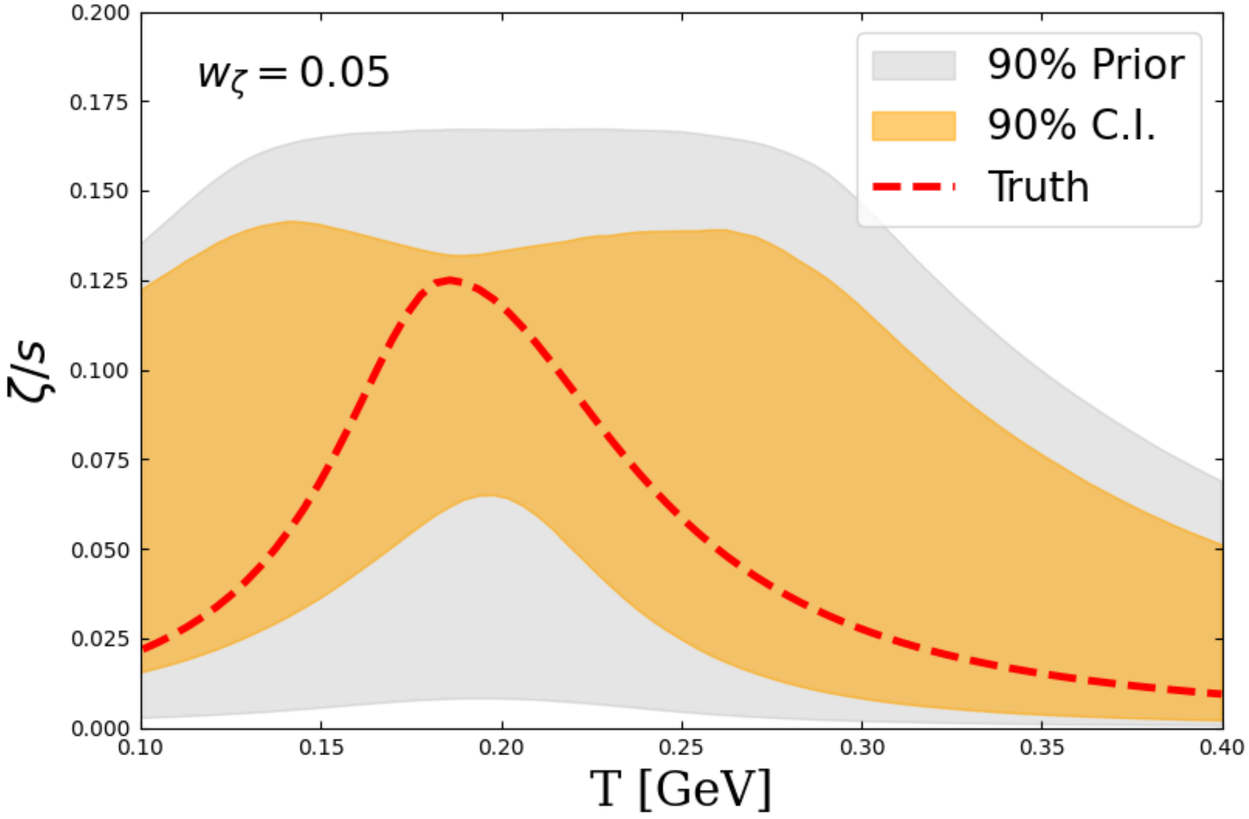

Model emulation and validation of sensitivity

- ~1000 observable bins → 20 principal components
- 400 parameter training points for Gaussian Process with ~2000 events each

Closure tests throughout parameter space:

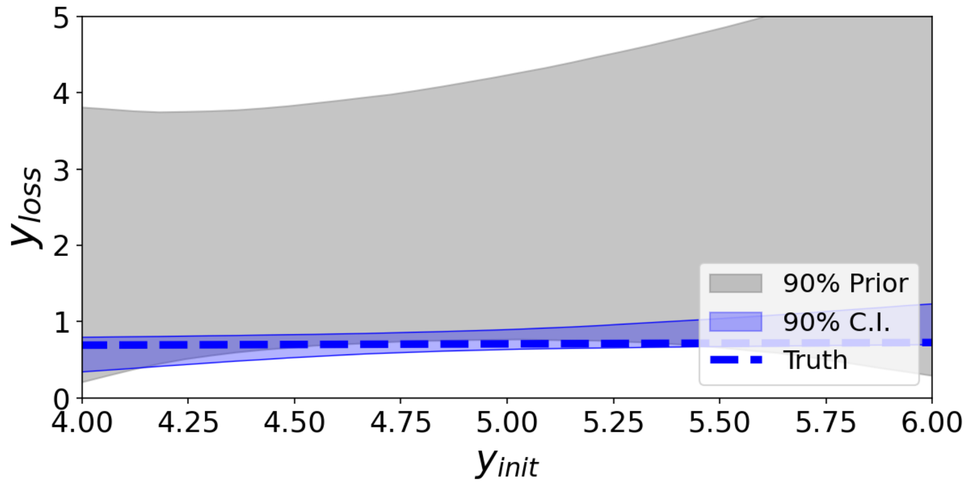

Closure tests around particular region of parameter space:

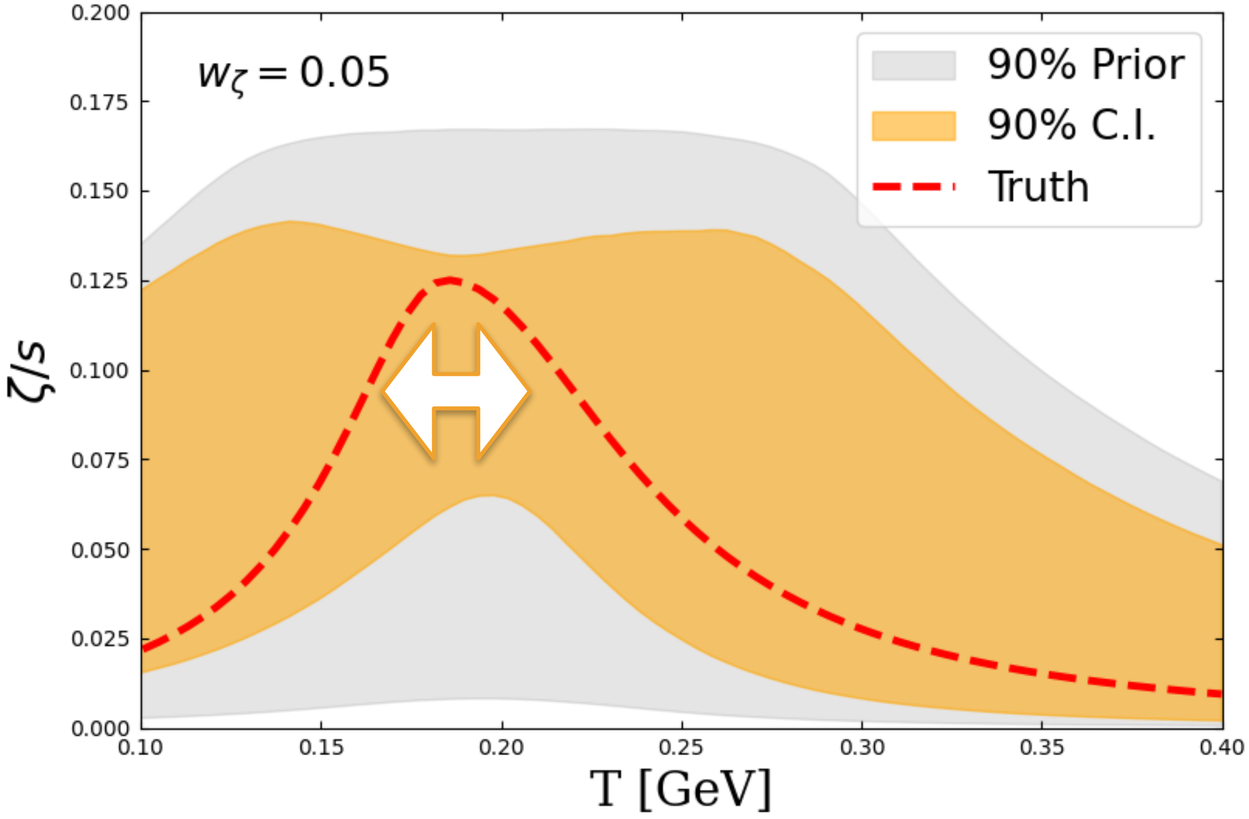

Model emulation and validation of sensitivity

- ~1000 observable bins → 20 principal components
- 400 parameter training points for Gaussian Process with ~2000 events each

Closure tests throughout parameter space:

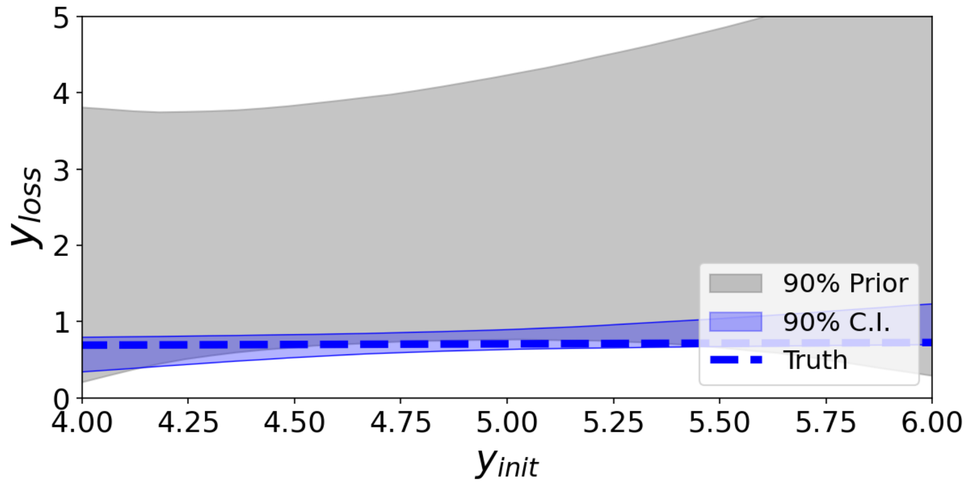

Closure tests around particular region of parameter space:

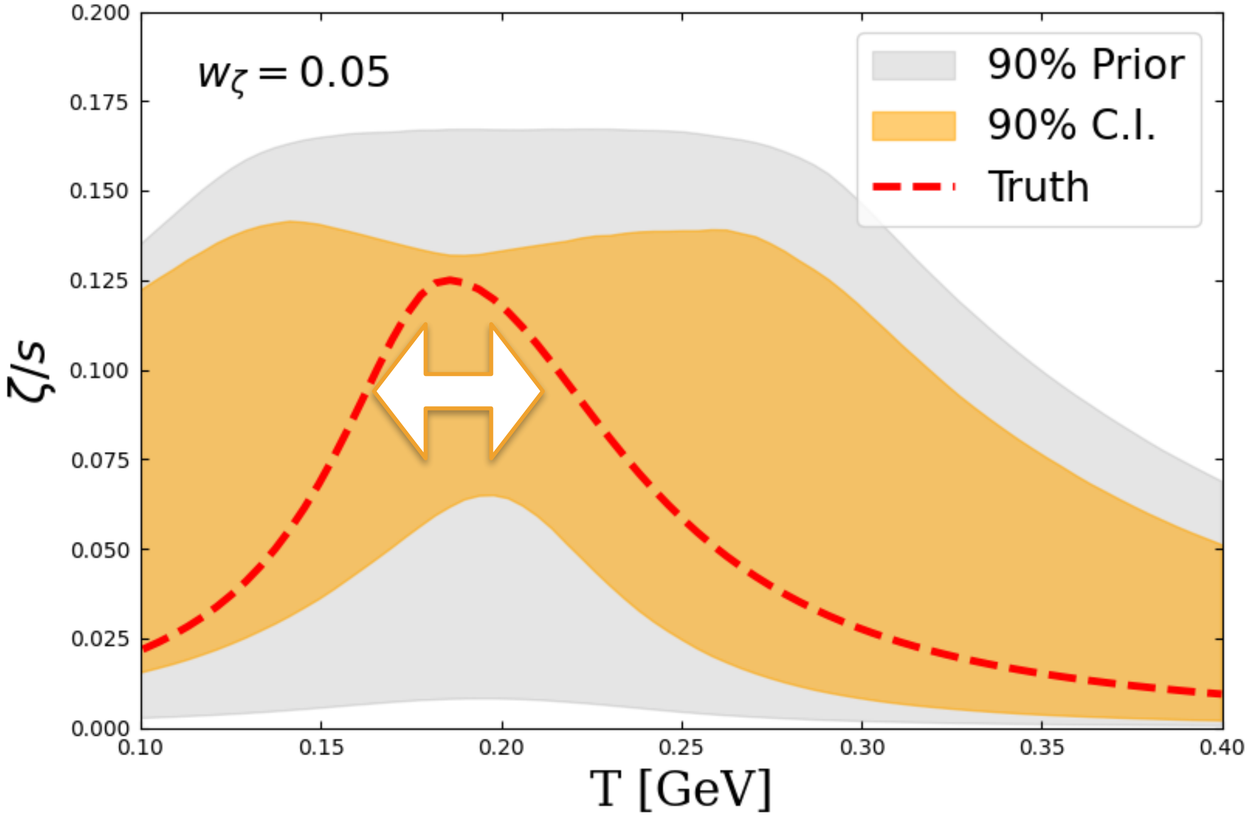

Model emulation and validation of sensitivity

- ~1000 observable bins → 20 principal components
- 400 parameter training points for Gaussian Process with ~2000 events each

Closure tests throughout parameter space:

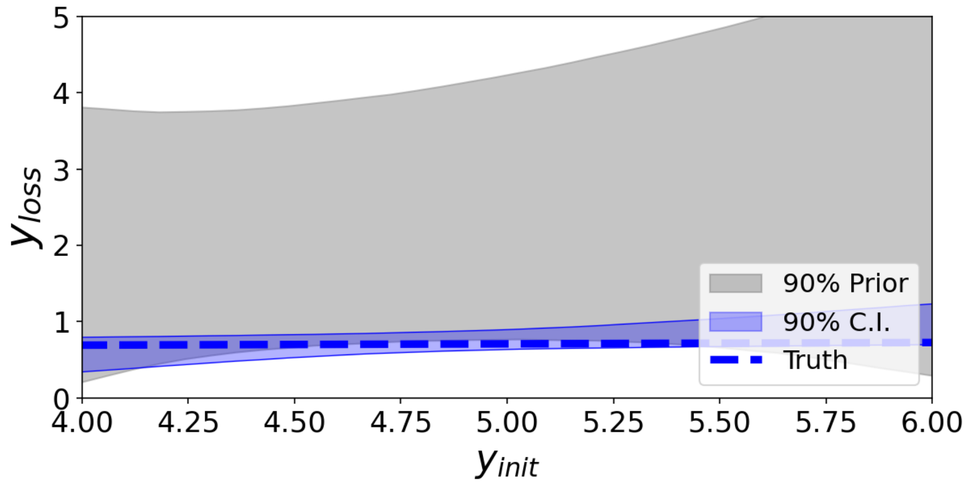

Closure tests around particular region of parameter space:

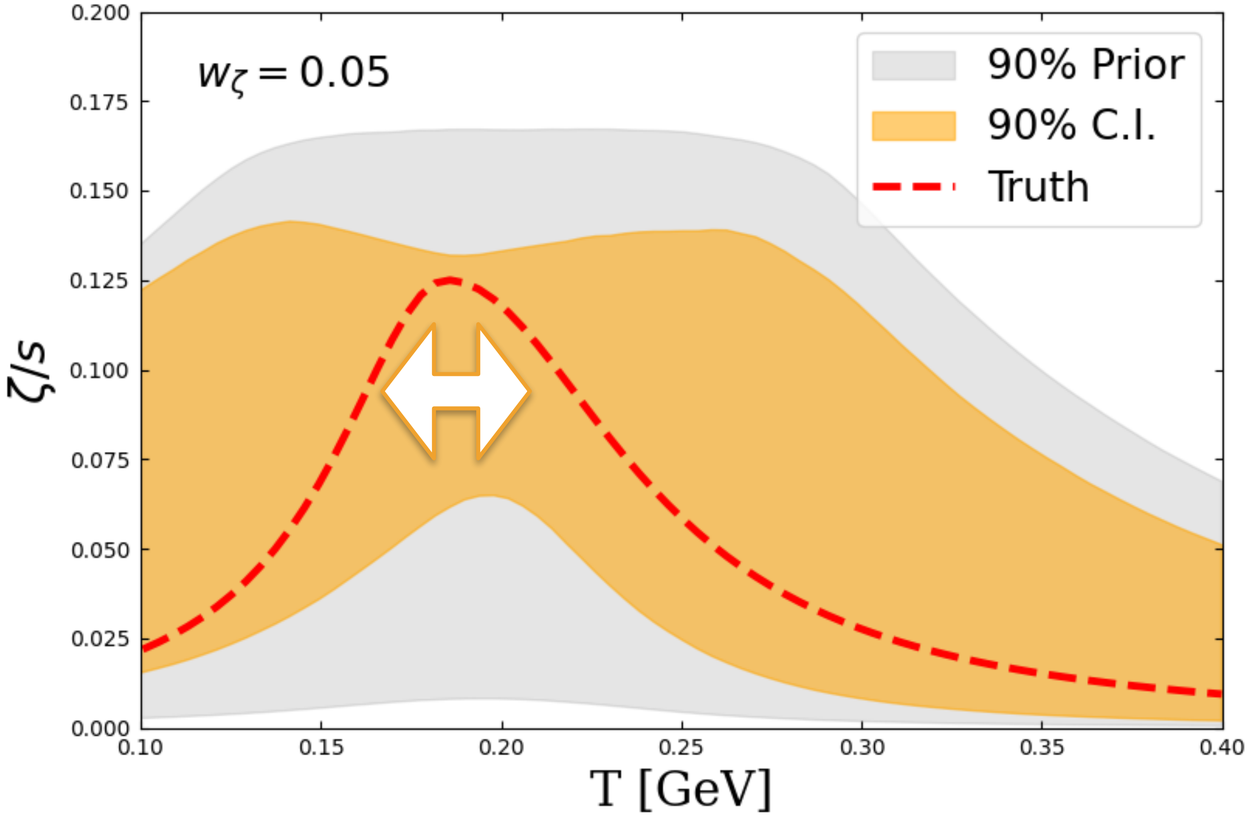

Model emulation and validation of sensitivity

- ~1000 observable bins → 20 principal components
- 400 parameter training points for Gaussian Process with ~2000 events each

Closure tests throughout parameter space:

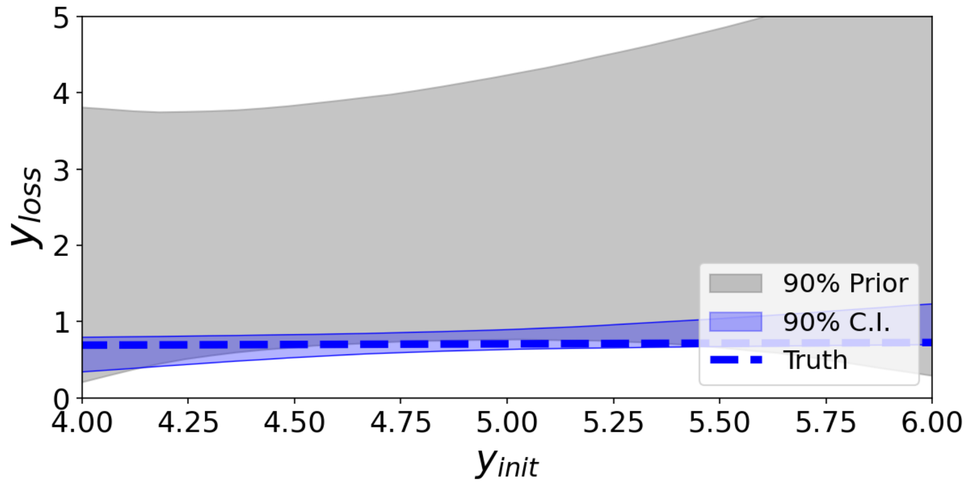

Closure tests around particular region of parameter space:

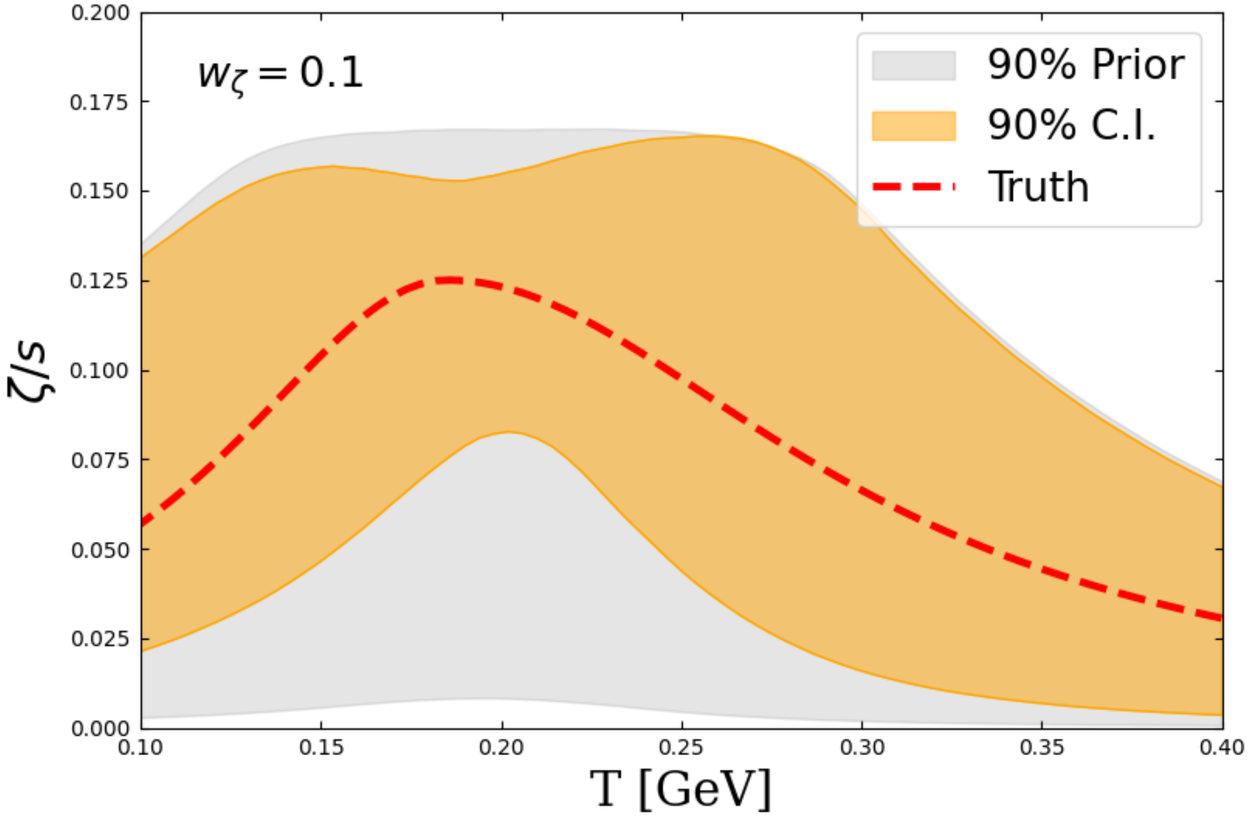

Model emulation and validation of sensitivity

- ~1000 observable bins → 20 principal components
- 400 parameter training points for Gaussian Process with ~2000 events each

Closure tests throughout parameter space:

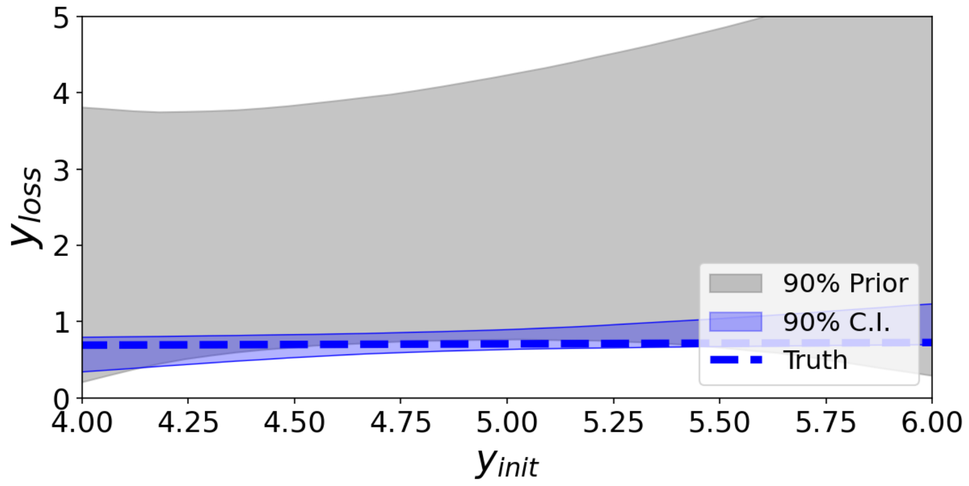

Closure tests around particular region of parameter space:

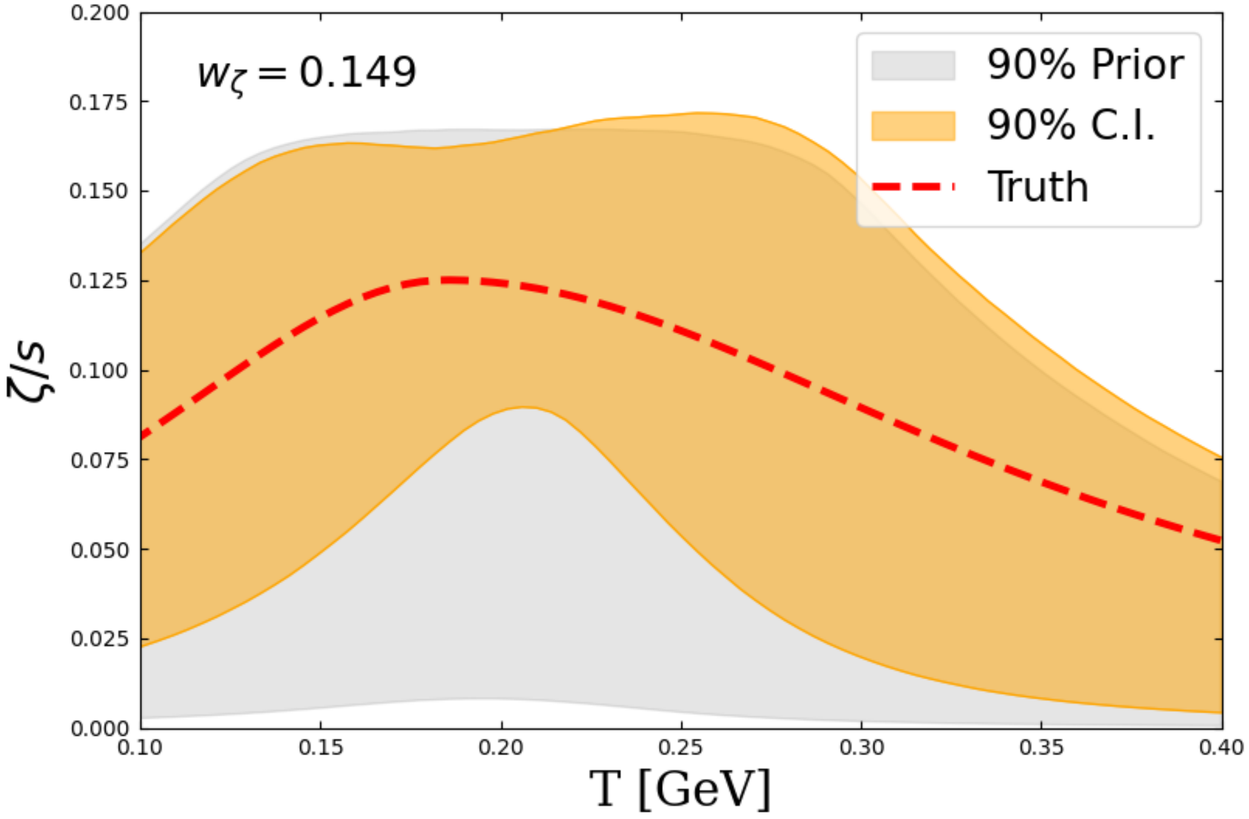

Relative contribution to covariance matrix from theory and experiment

$$\Sigma_{emu}/\Sigma_{exp}$$

d-Au $dN/d\eta$

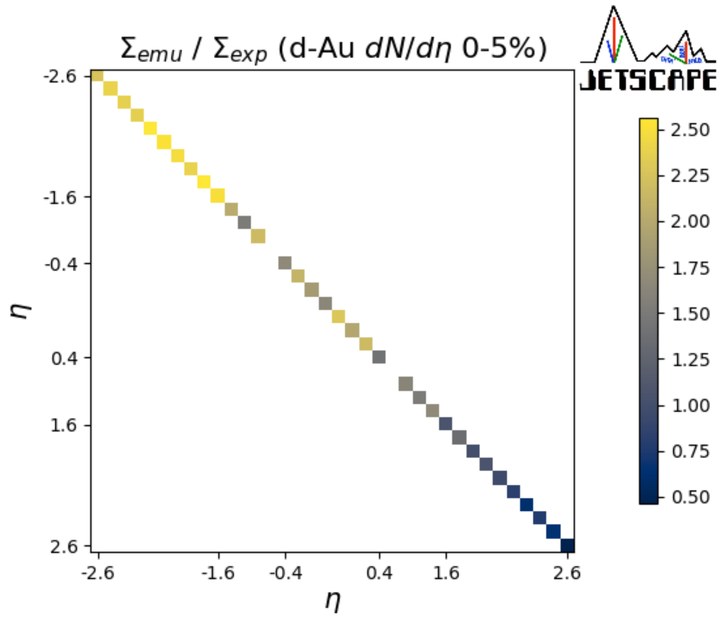

Au-Au $v_2(\eta)$

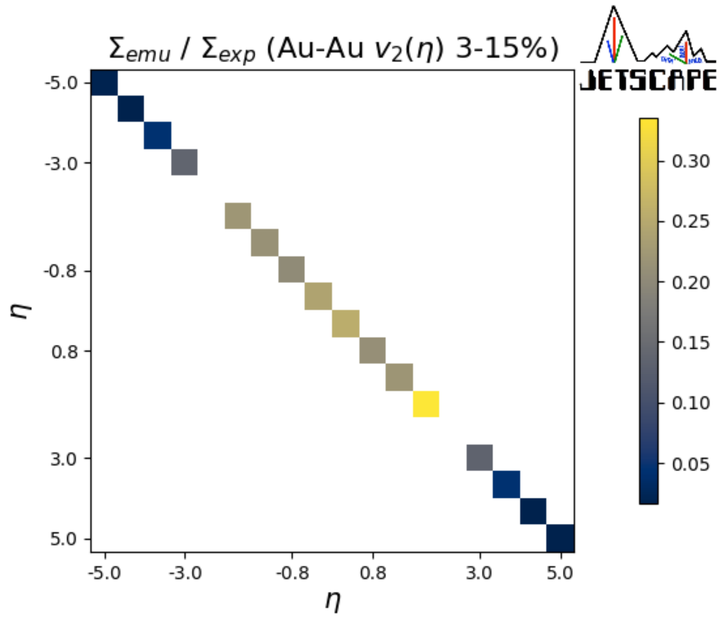

Au-Au $v_2(p_T)$

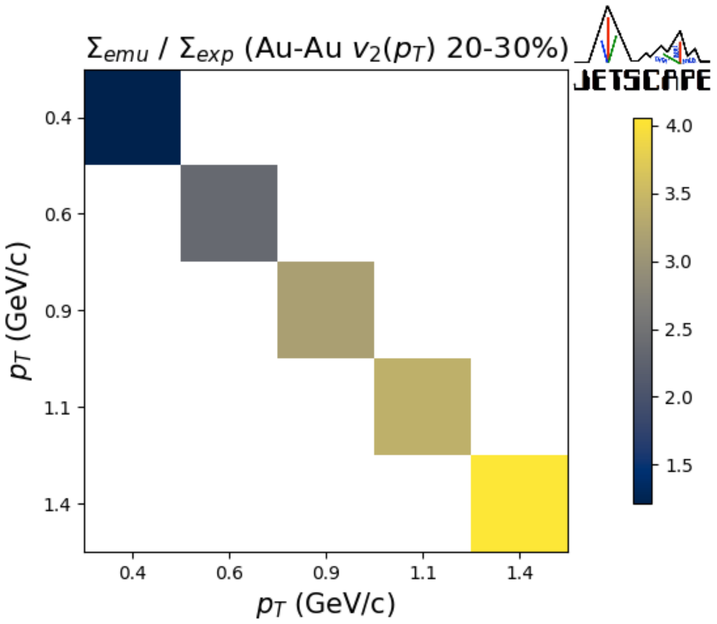

Correlations between observable bins from the emulator

$$Cov(y_i, y_j)/\sigma_i\sigma_j$$

d-Au $dN/d\eta$

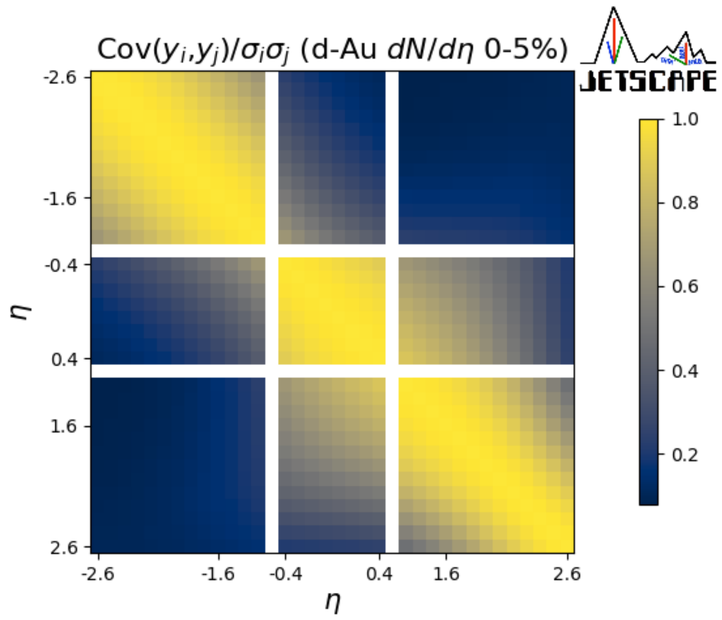

Au-Au $v_2(\eta)$

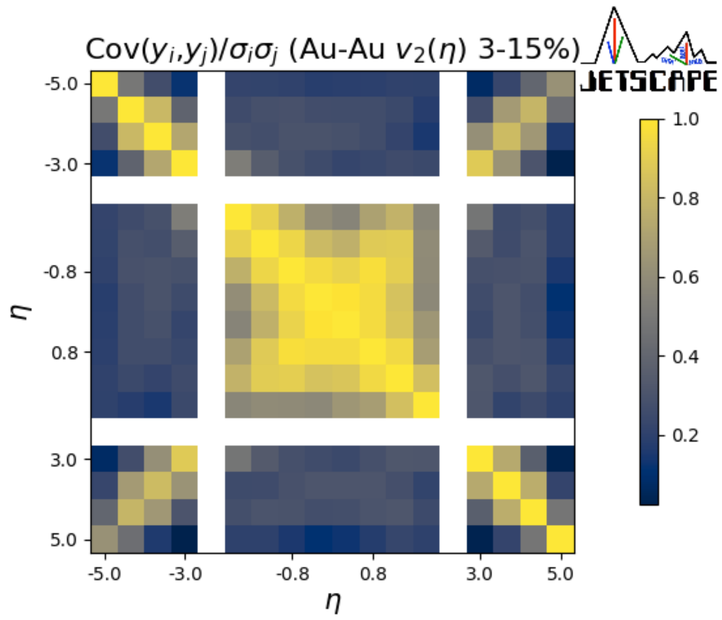

Au-Au $v_2(p_T)$

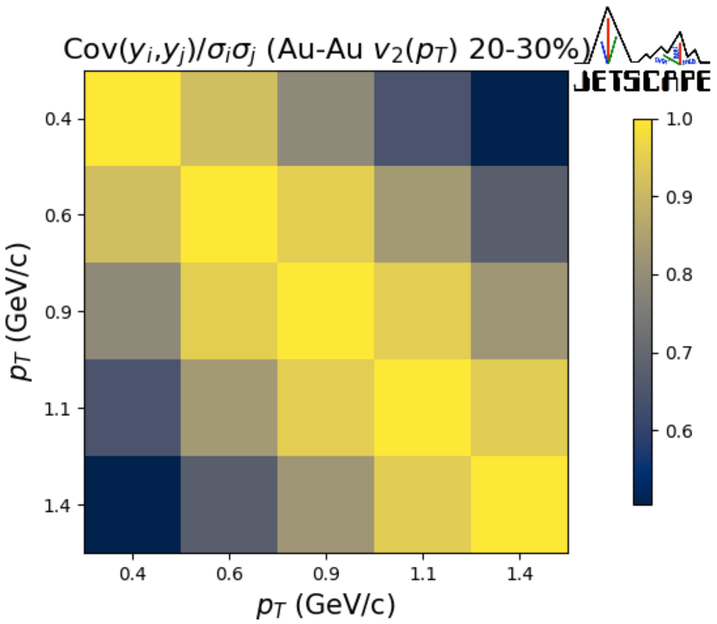

Emulator vs experimental covariance for all observables

$$\sigma_j^2 / y_j^{emu} y_j^{exp}$$

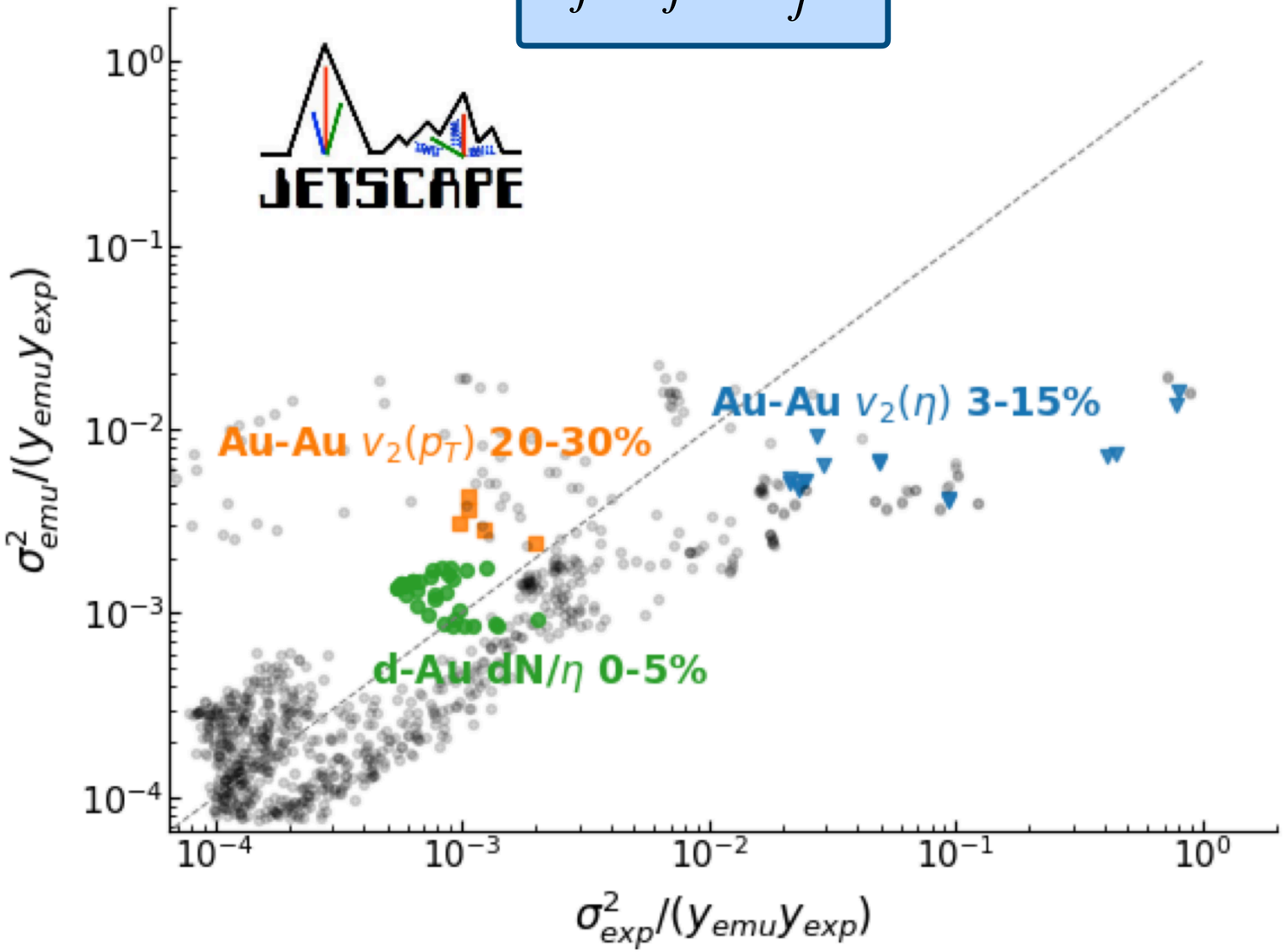

Observables from calibrated model

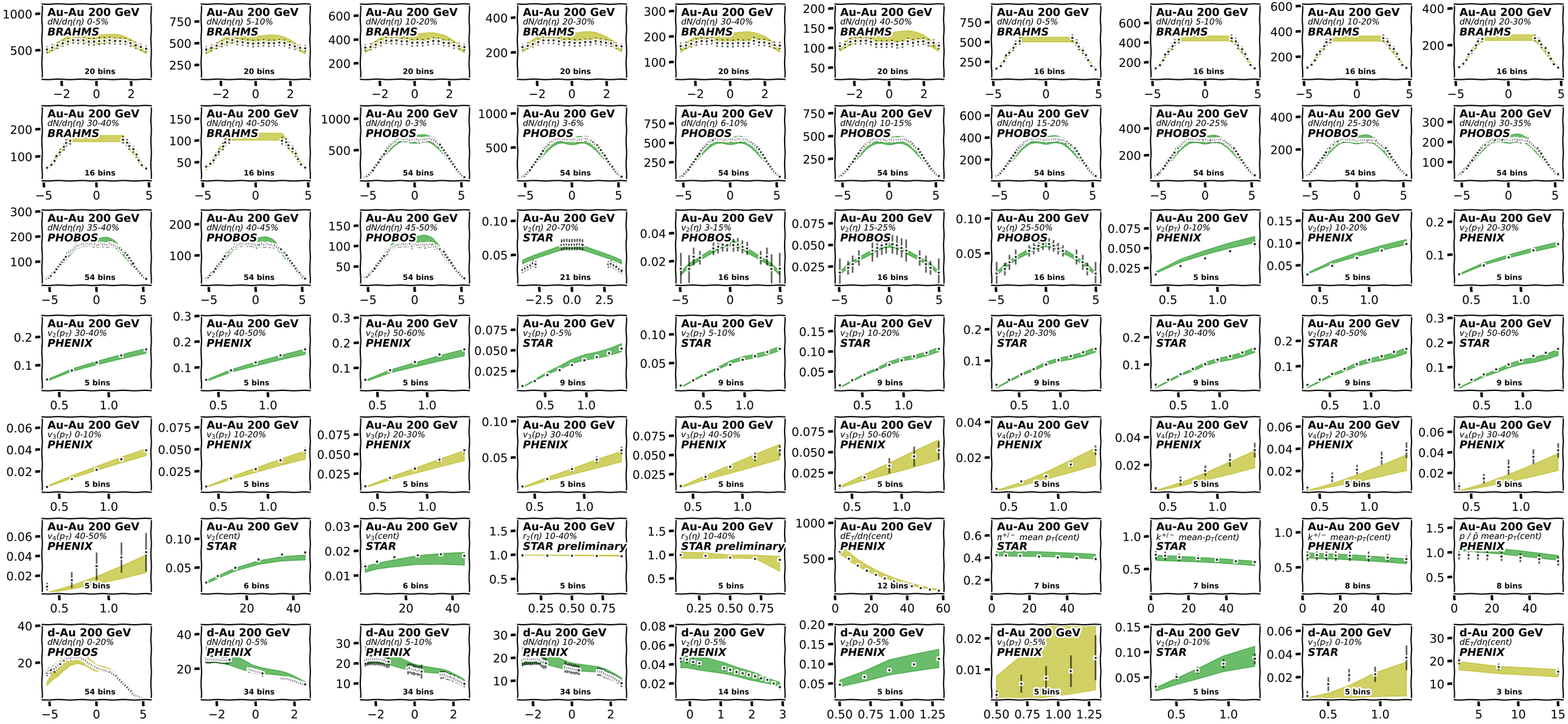

Observables from calibrated model

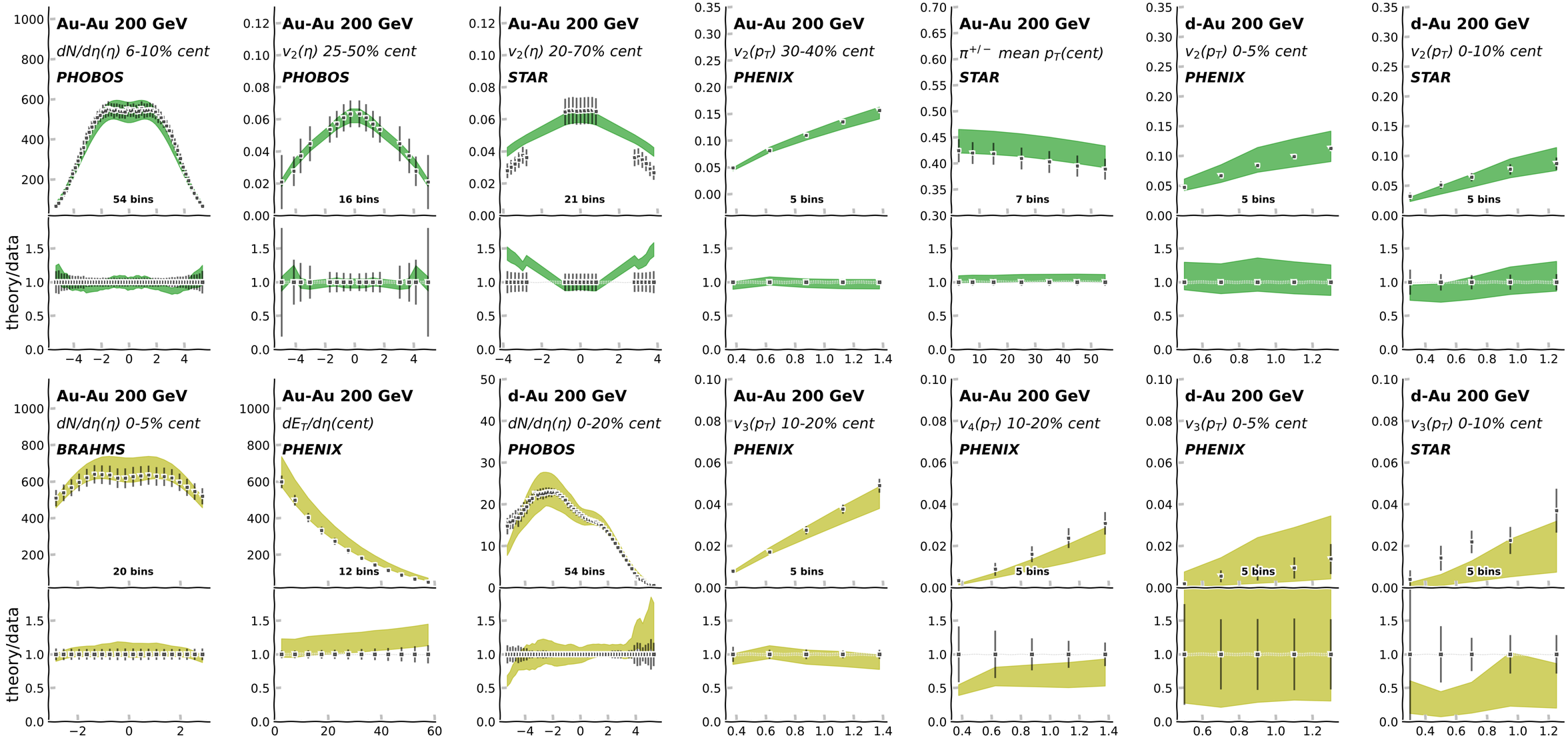

Observables from calibrated model

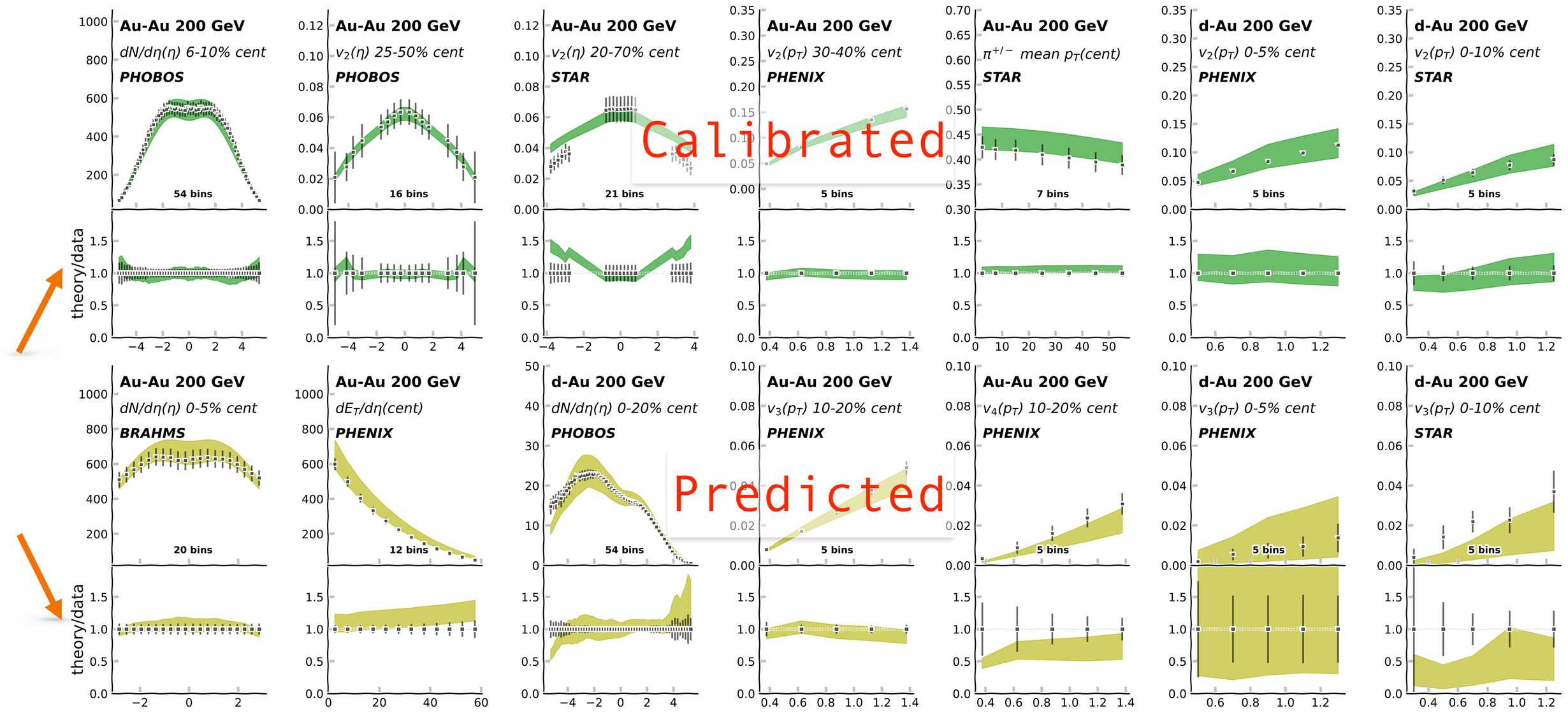

Observables from calibrated model

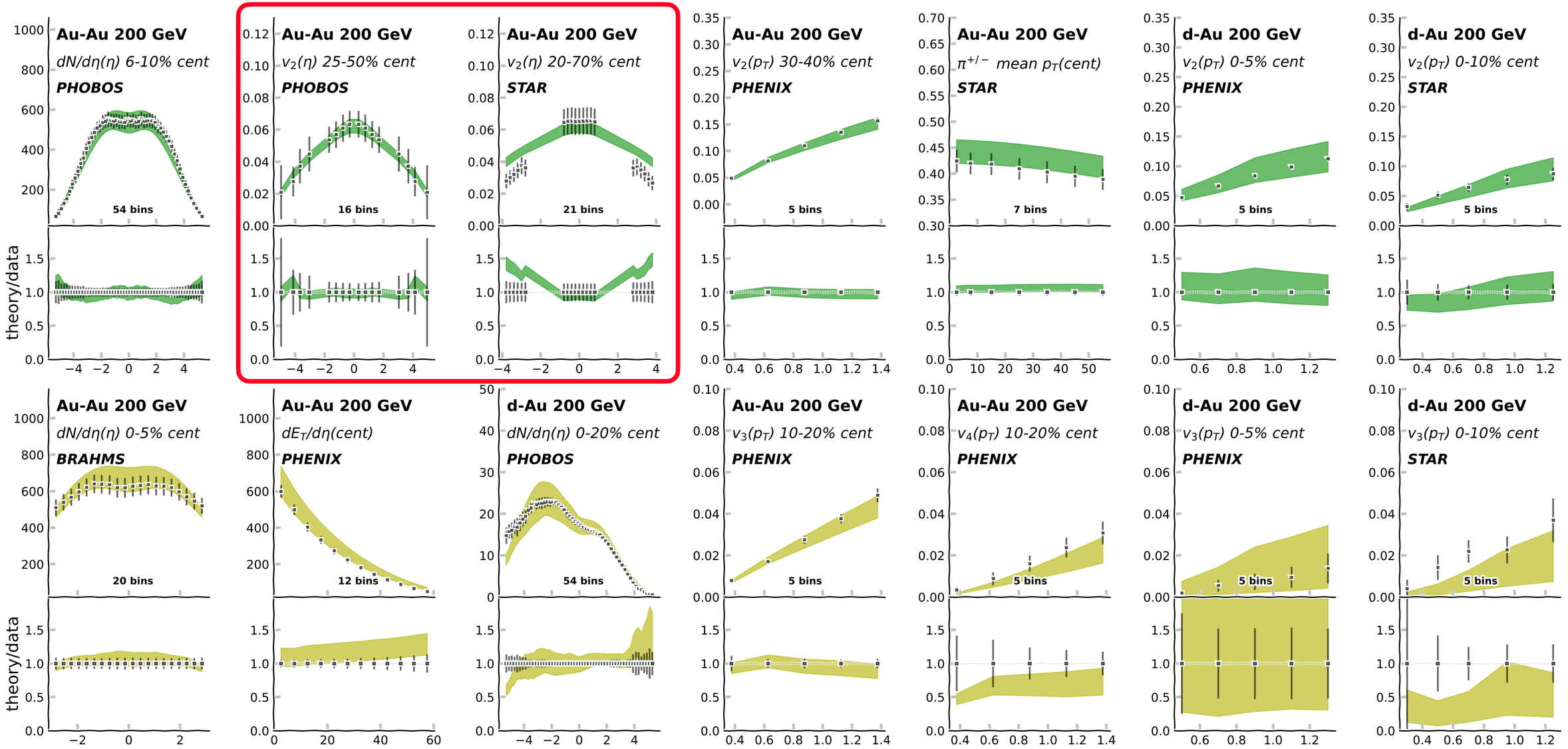

Observables from calibrated model

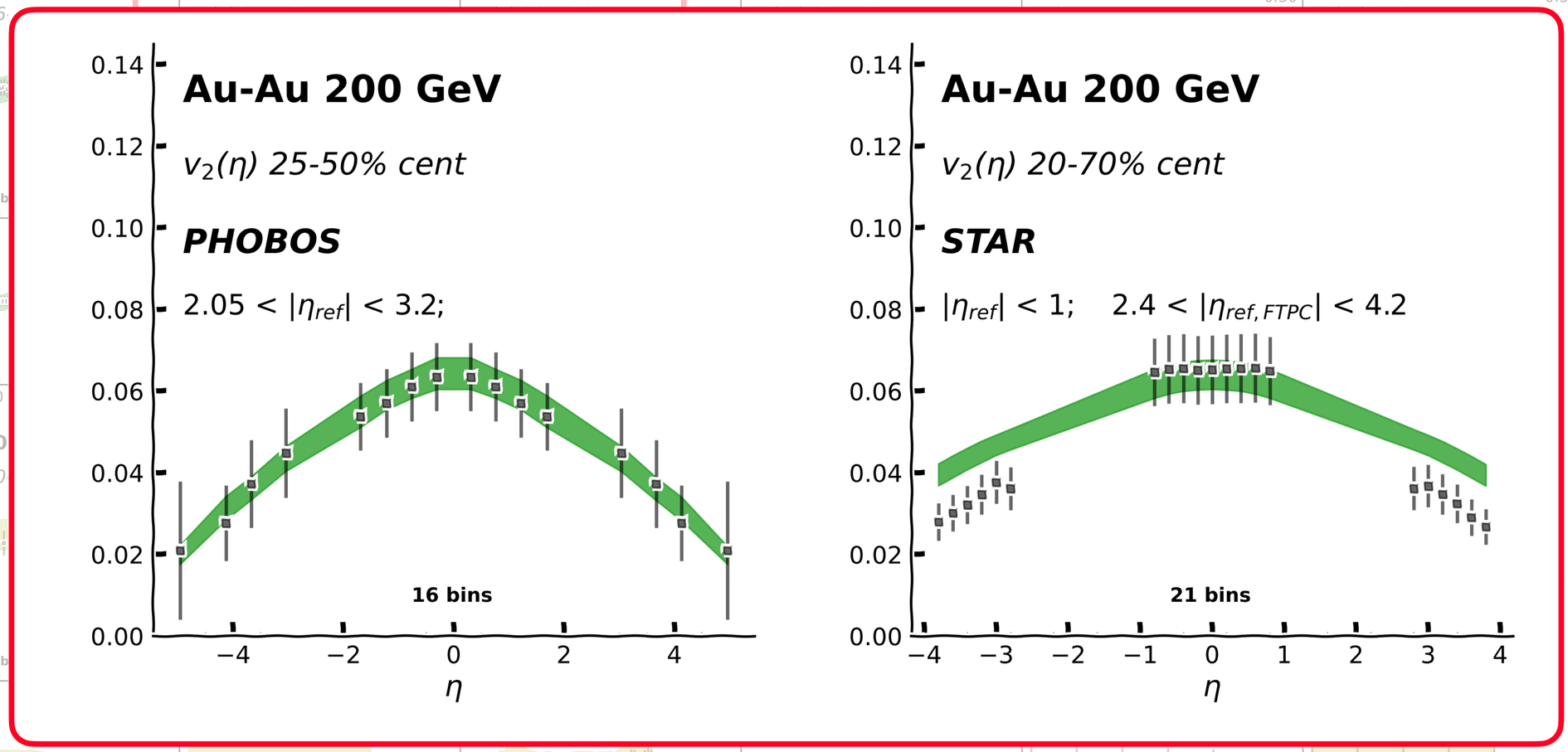

Observables from calibrated model

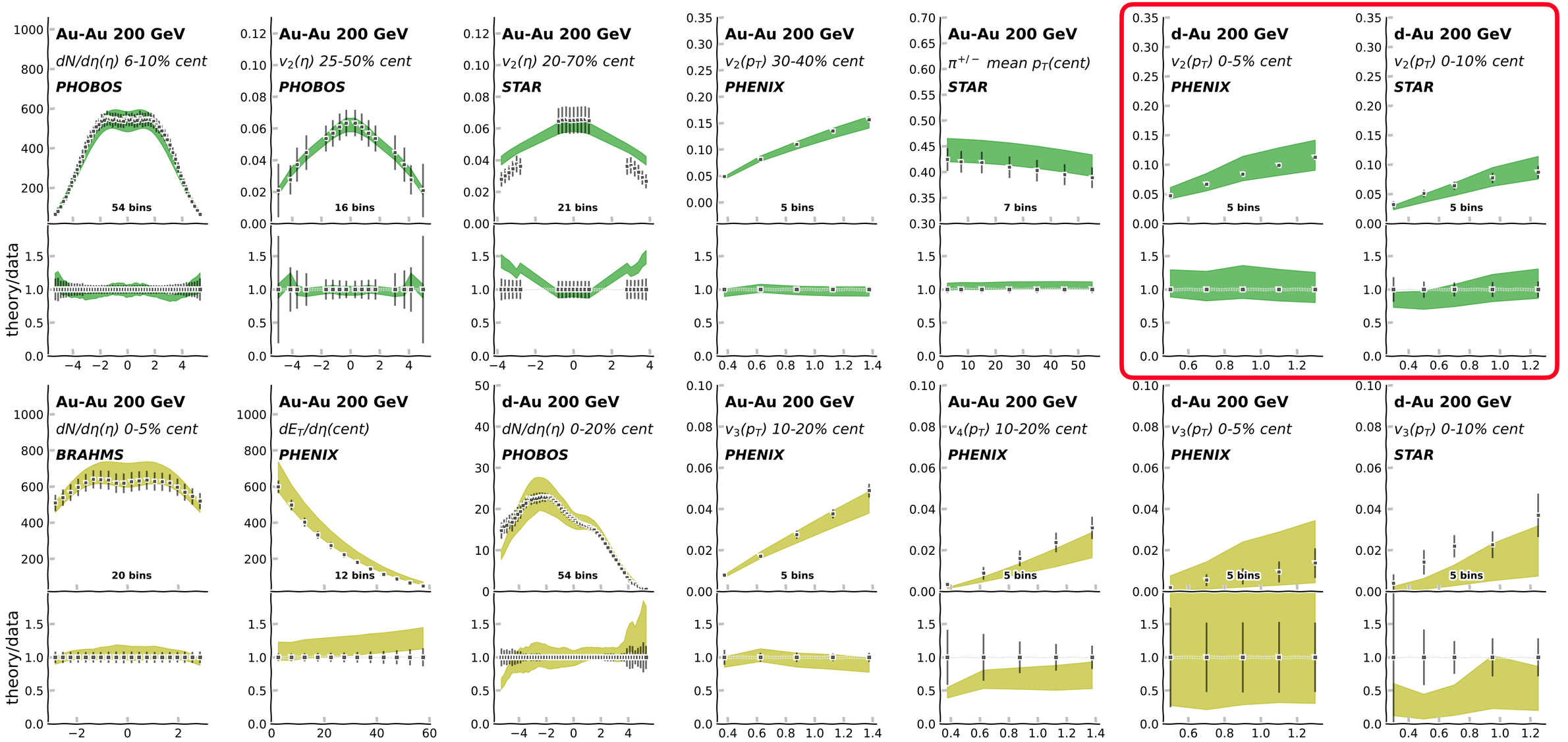

Observables from calibrated model

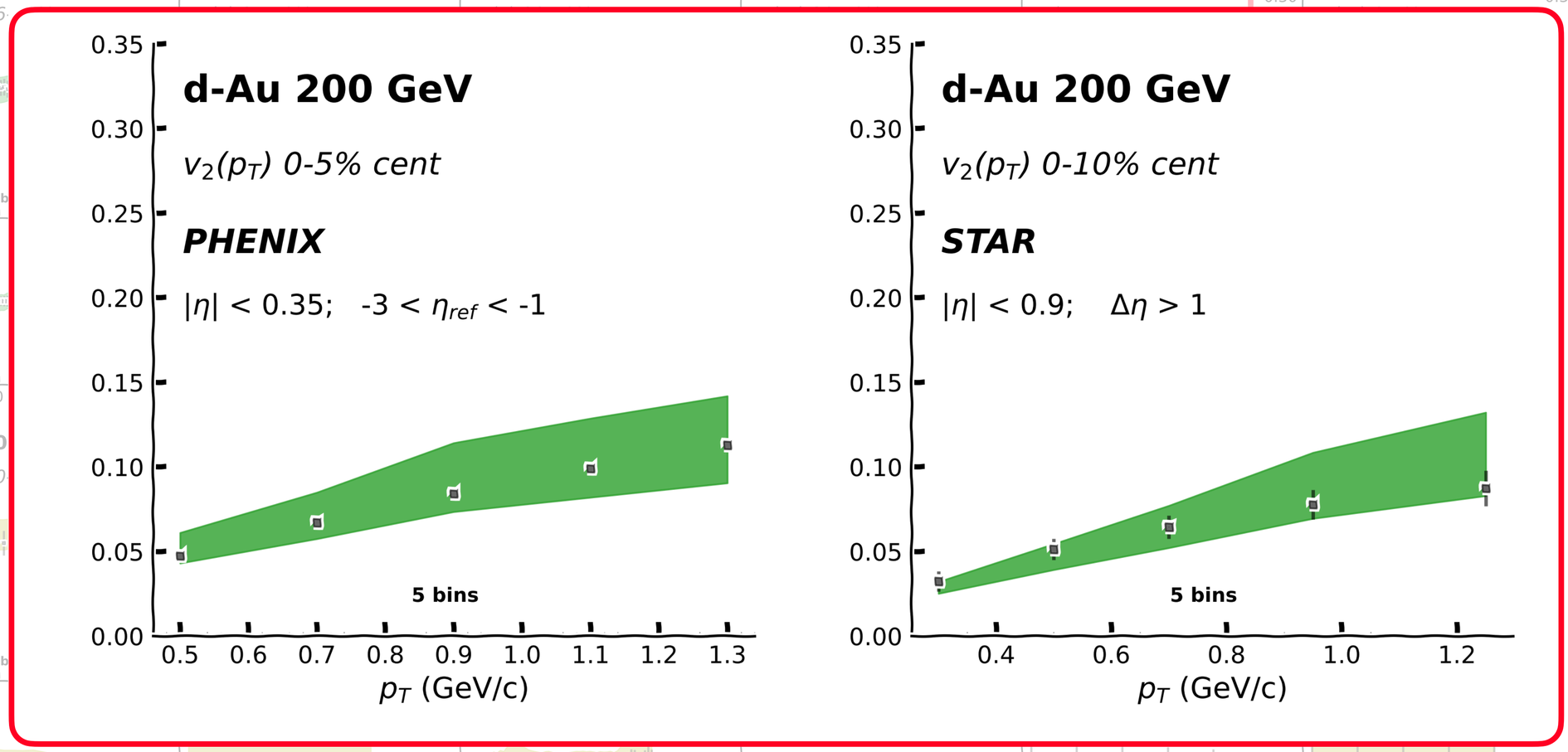

Observables from calibrated model

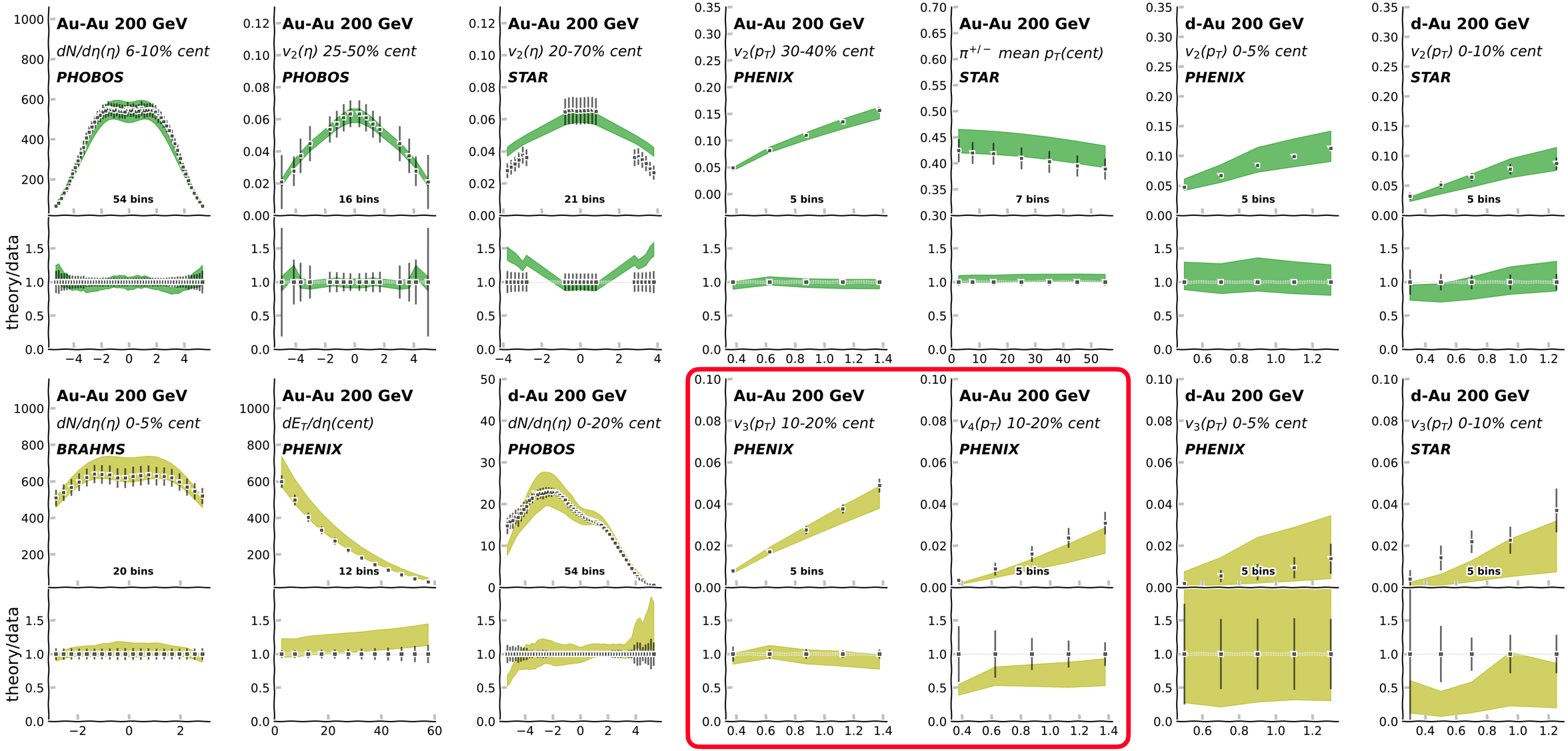

Observables from calibrated model

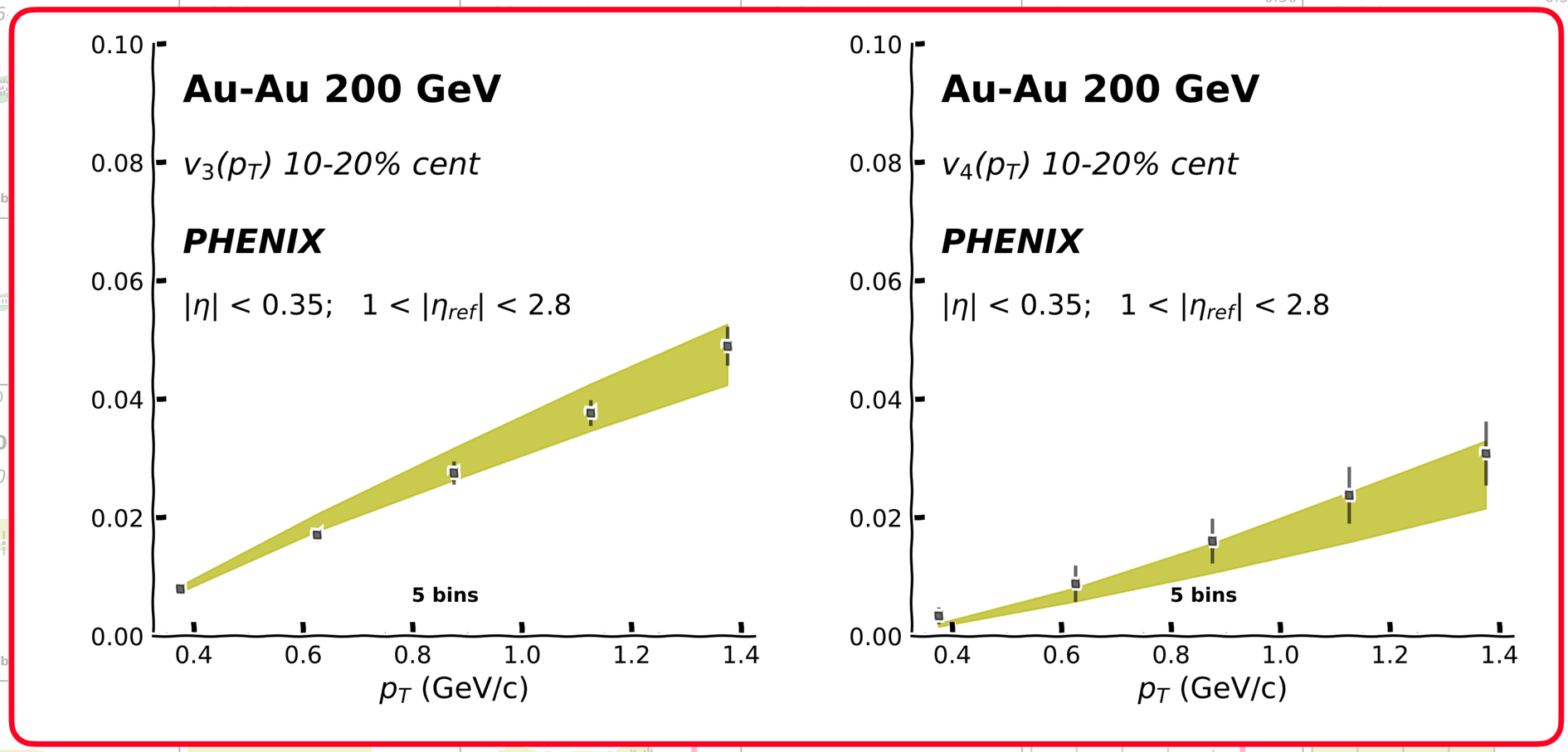

Observables from calibrated model

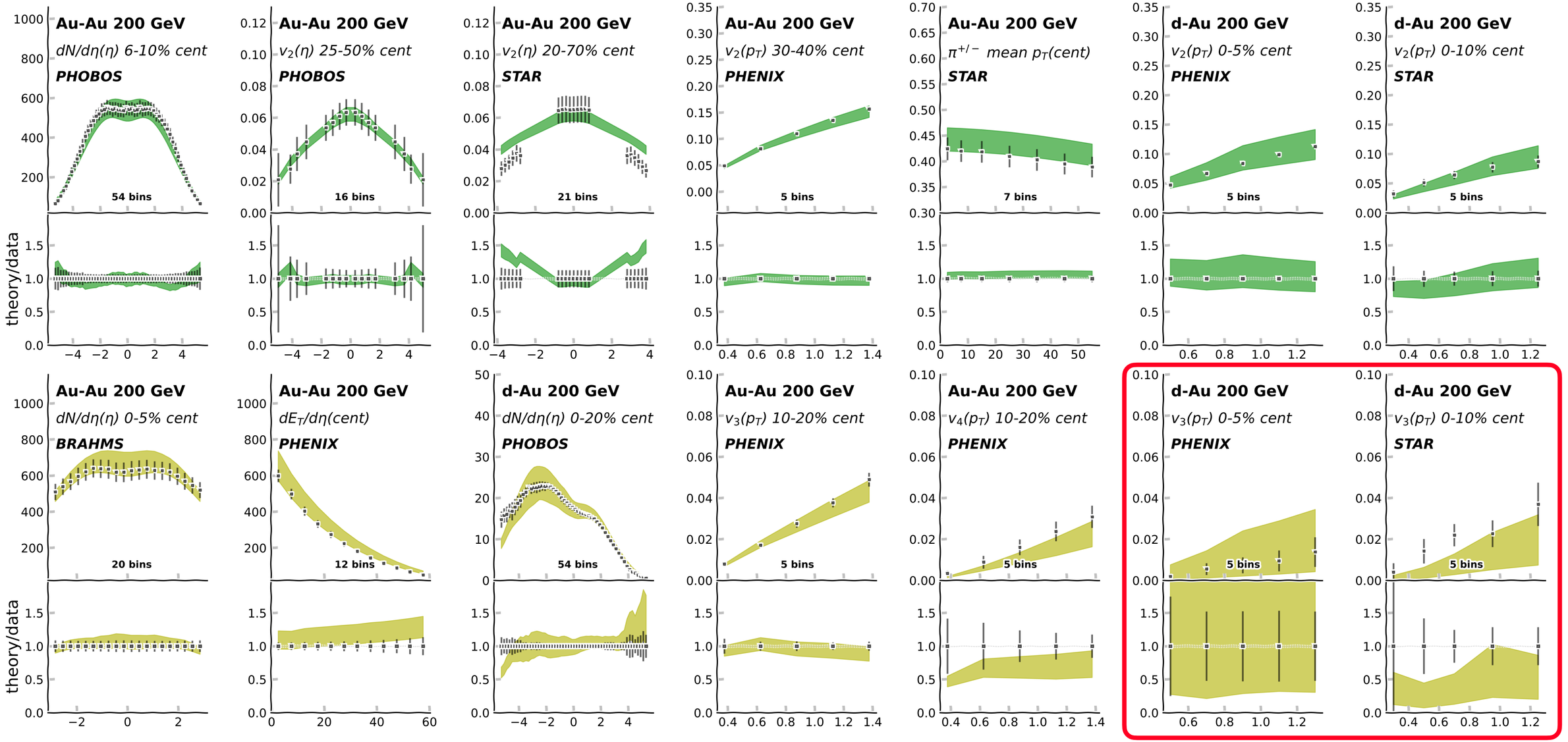

Observables from calibrated model

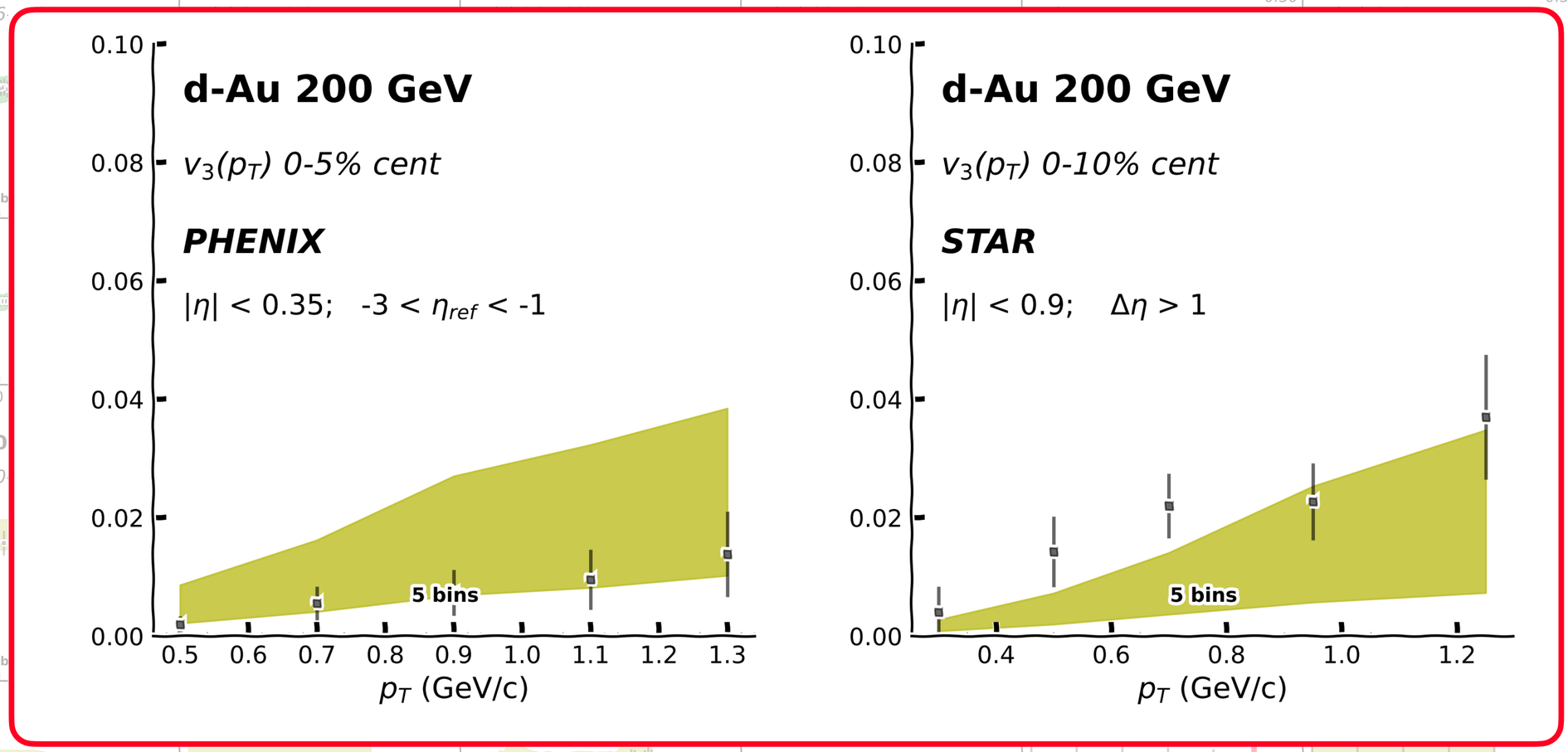

Constraints from forward/backward data

- Significant rapidity loss constraints provided by mid-rapidity data
- E_{loss} of nuclear fragments constrained by finite rapidity data
- Viscosity posteriors shifted to larger values
  - Preference for finite bulk viscosity at low T

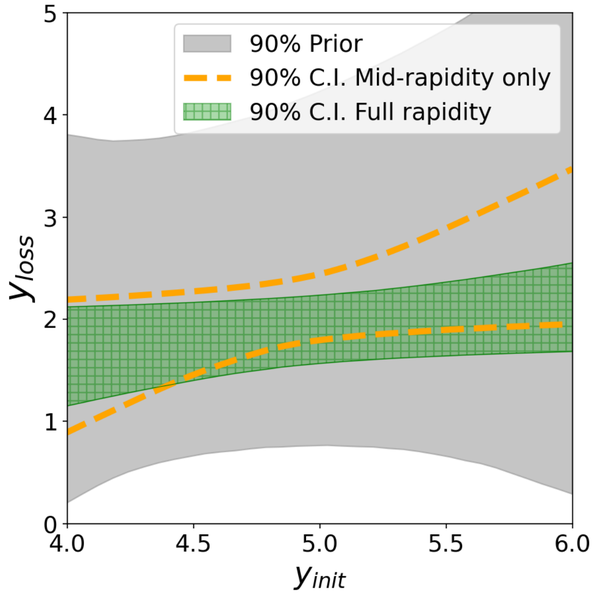

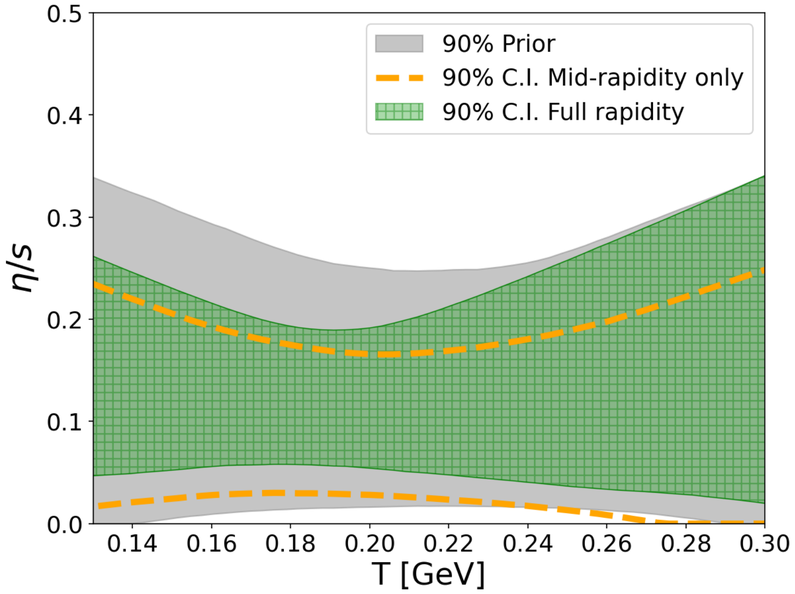

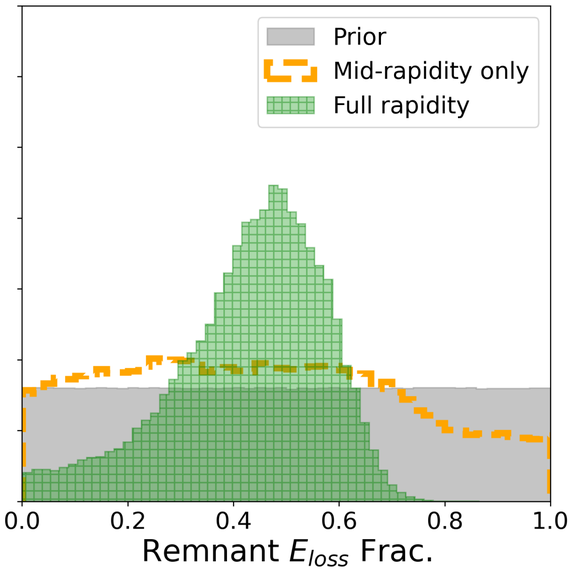

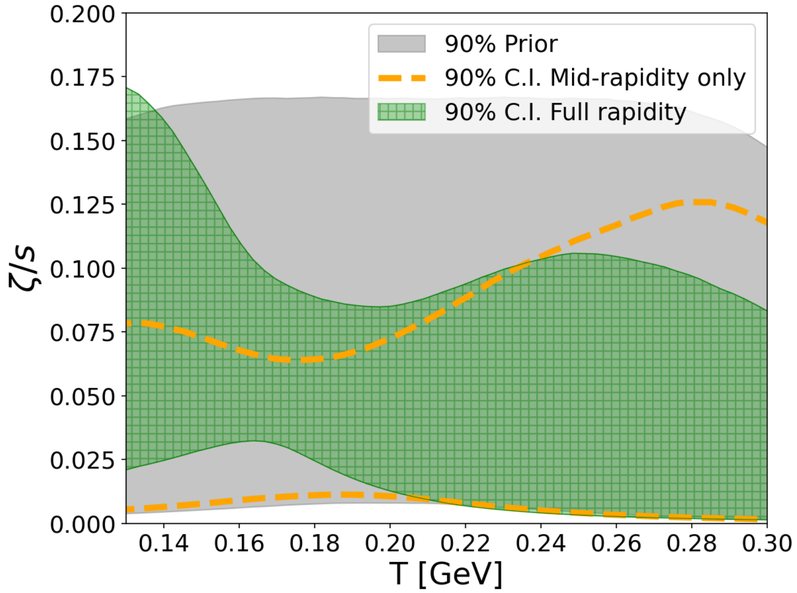

- Can we use the calibrated model to quantify the impact of generic experimental choices on observables?

- Two test cases:
  - Centrality selection for $dN/d\eta$
  - Reference region for $v_n(\eta)$

- Calculations using 5 high-statistics samples as a representation of the posterior

- Can we use the calibrated model to quantify the impact of generic experimental choices on observables?
- Two test cases:
  - Centrality selection for $dN/d\eta$
  - Reference region for $v_n(\eta)$
- Calculations using 5 high-statistics samples as a representation of the posterior

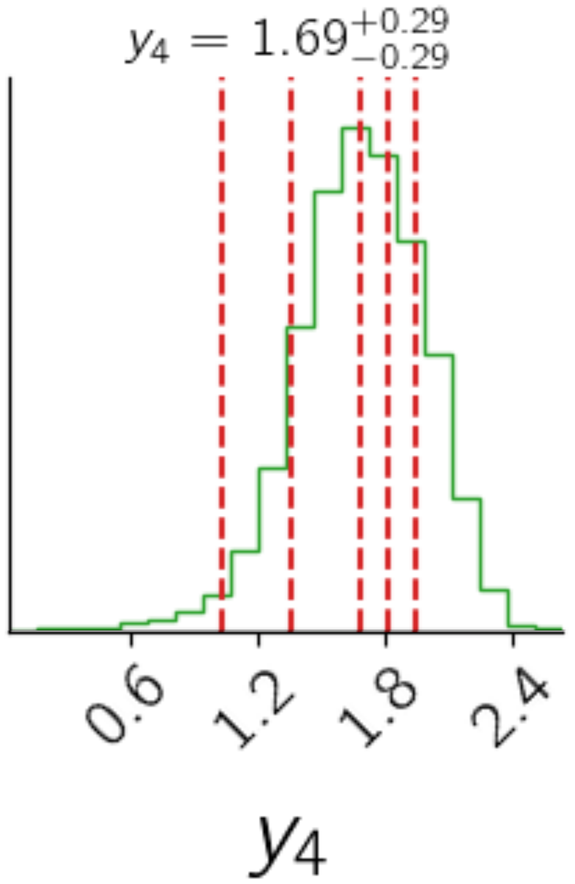

The effect of the centrality selection

- The effect of centrality selection region on dN/dη is small (<1%) in Au-Au but large (~20%) in d-Au

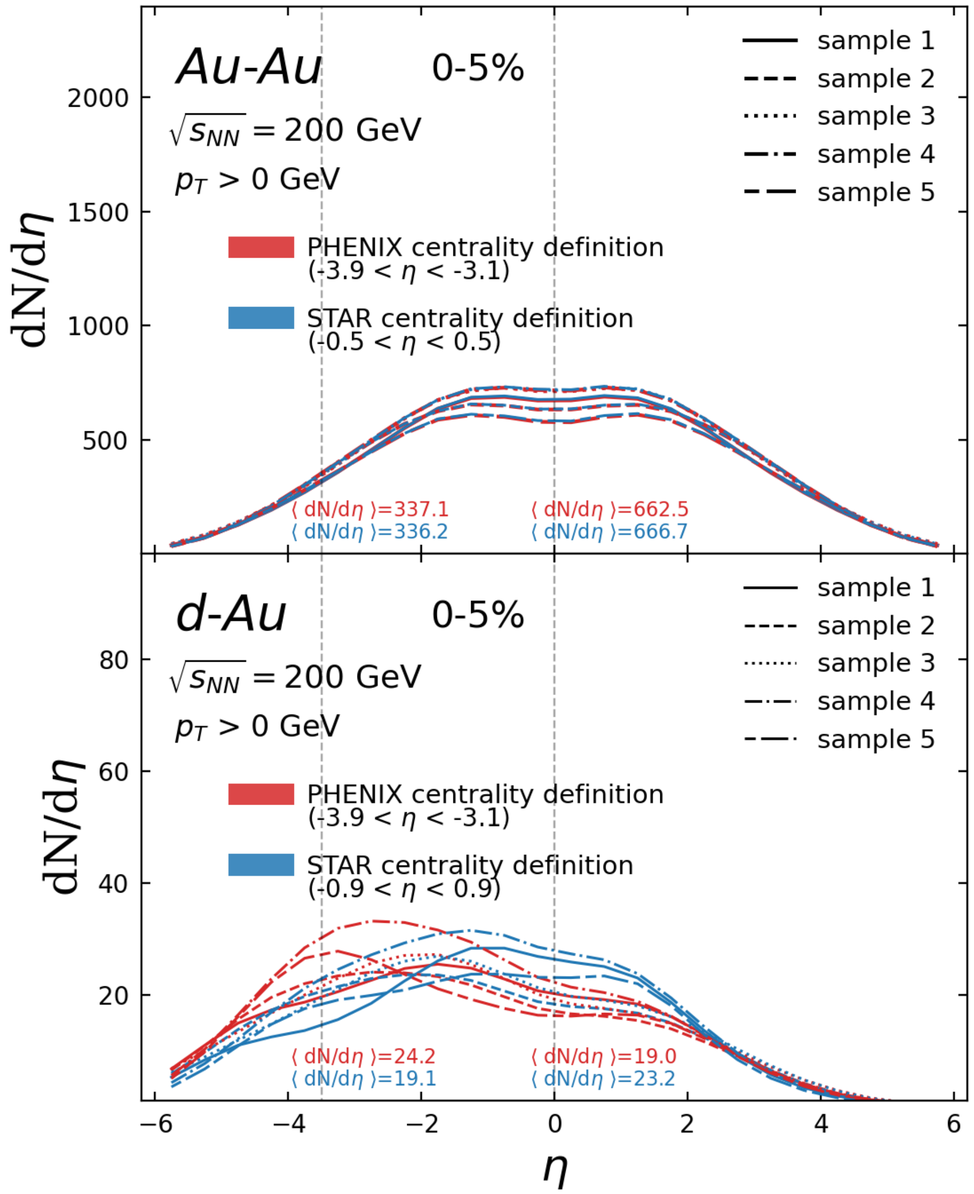

The longitudinal structure of flow - $v_2(\eta)$

- The effect of selection of the rapidity reference region on $v_2(\eta)$ is ~15% in both Au-Au and d-Au

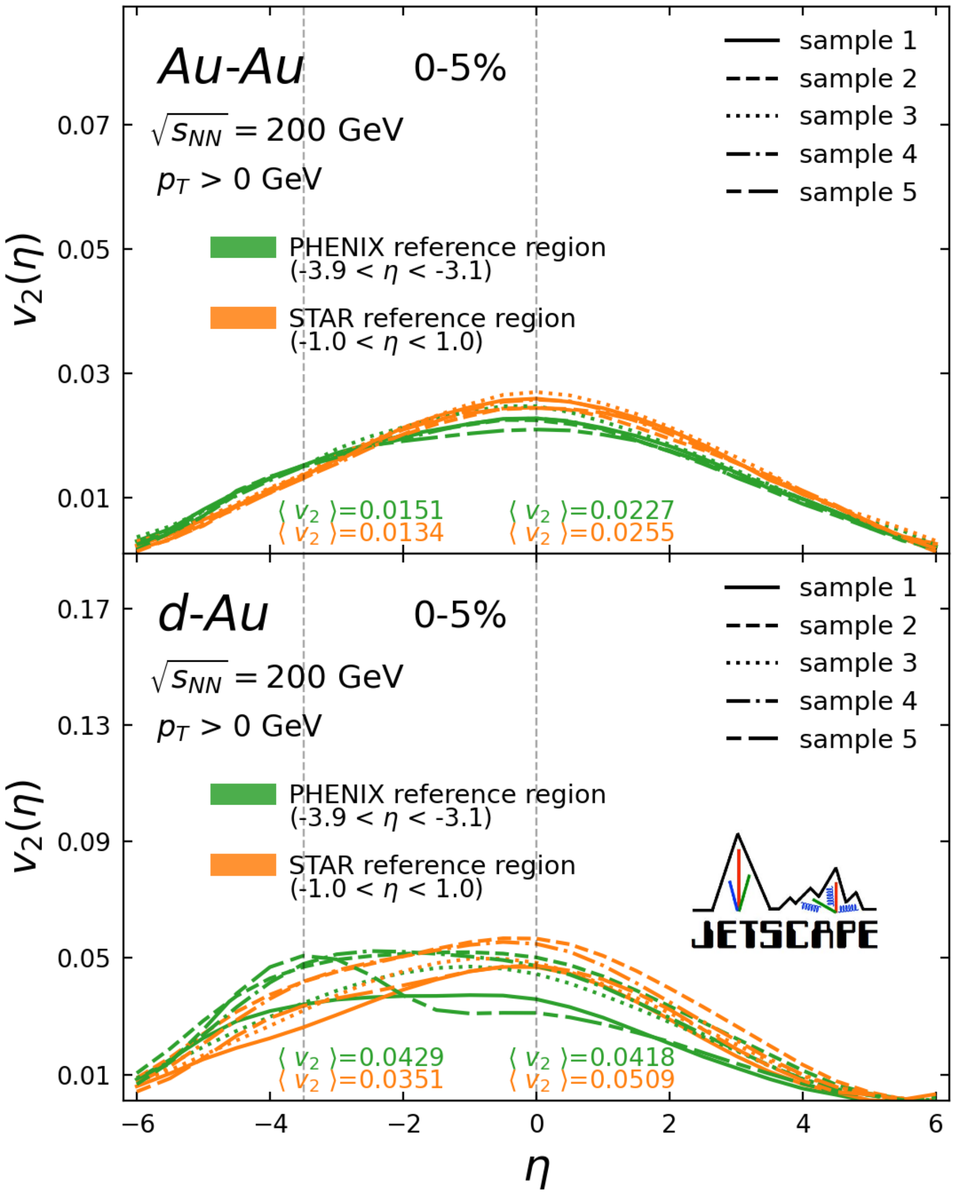

The longitudinal structure of flow - $v_3(\eta)$

- The effect of selection of the rapidity reference region on $v_3(\eta)$ is ~15-20% in Au-Au and ~50% in d-Au

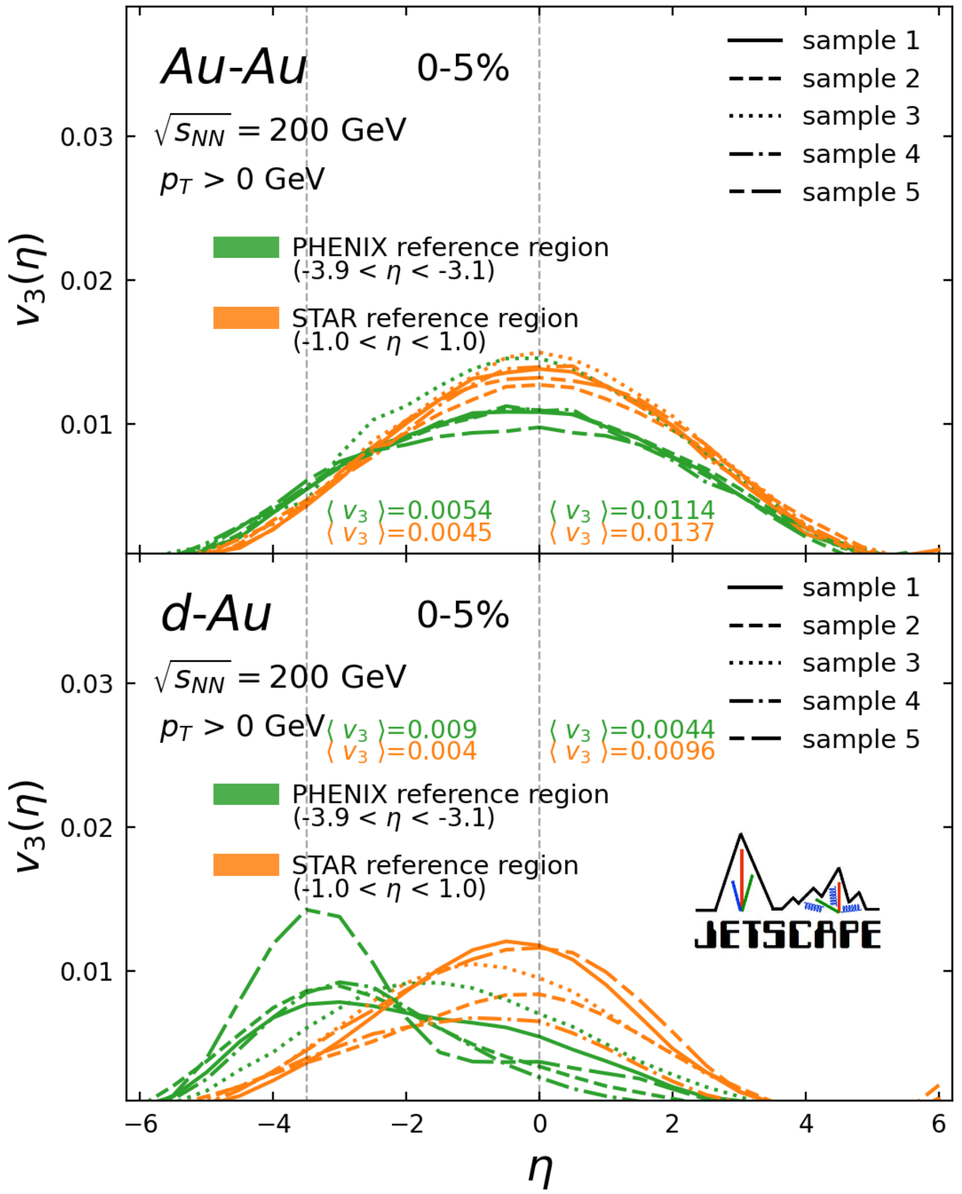

Comparison with data for additional small systems

p-Au, d-Au, ^3He-Au $v_n(p_T)$ from STAR & PHENIX

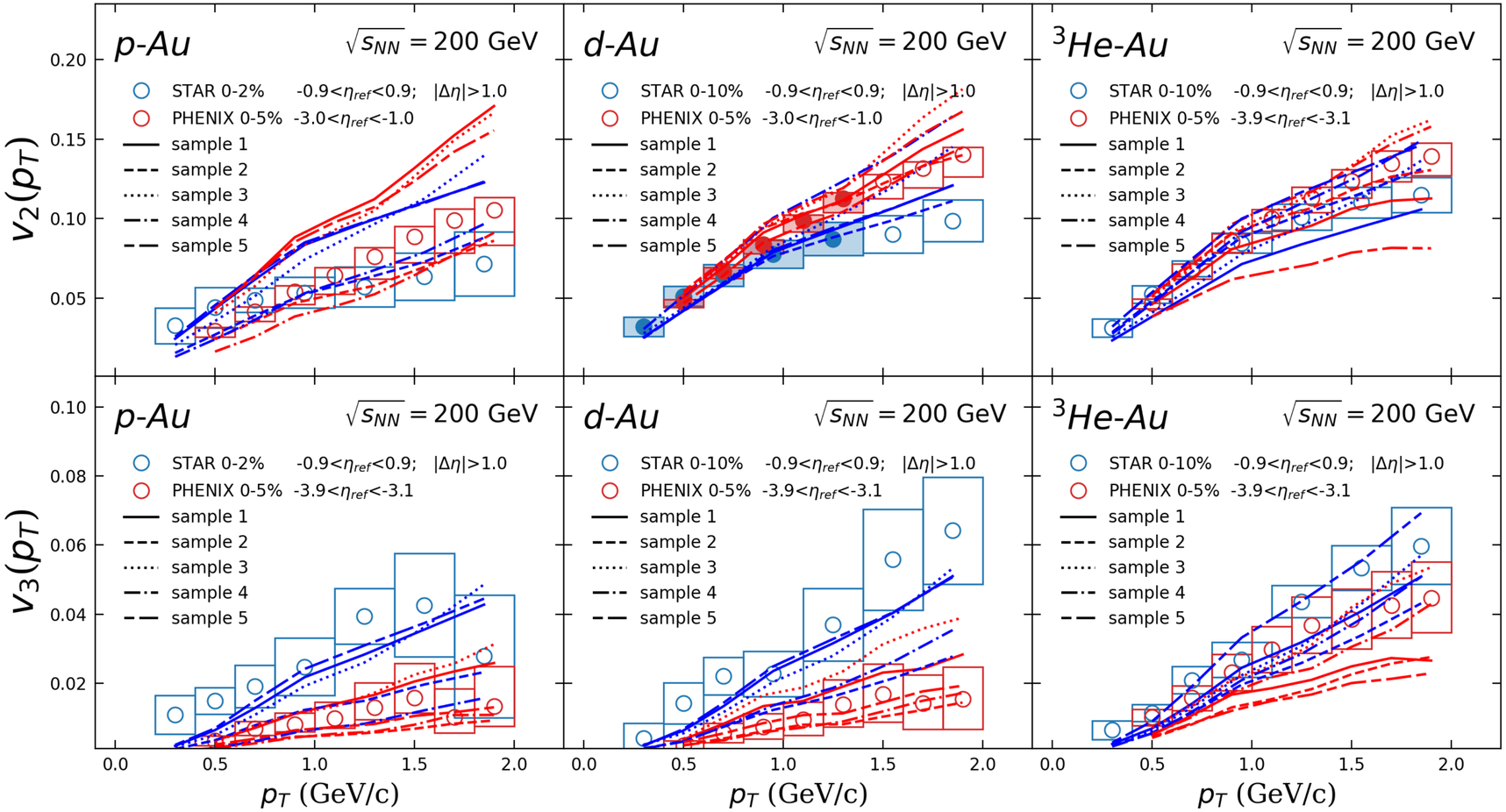

p-Au, d-Au, ^3He-Au $v_n(p_T)$ from PHENIX

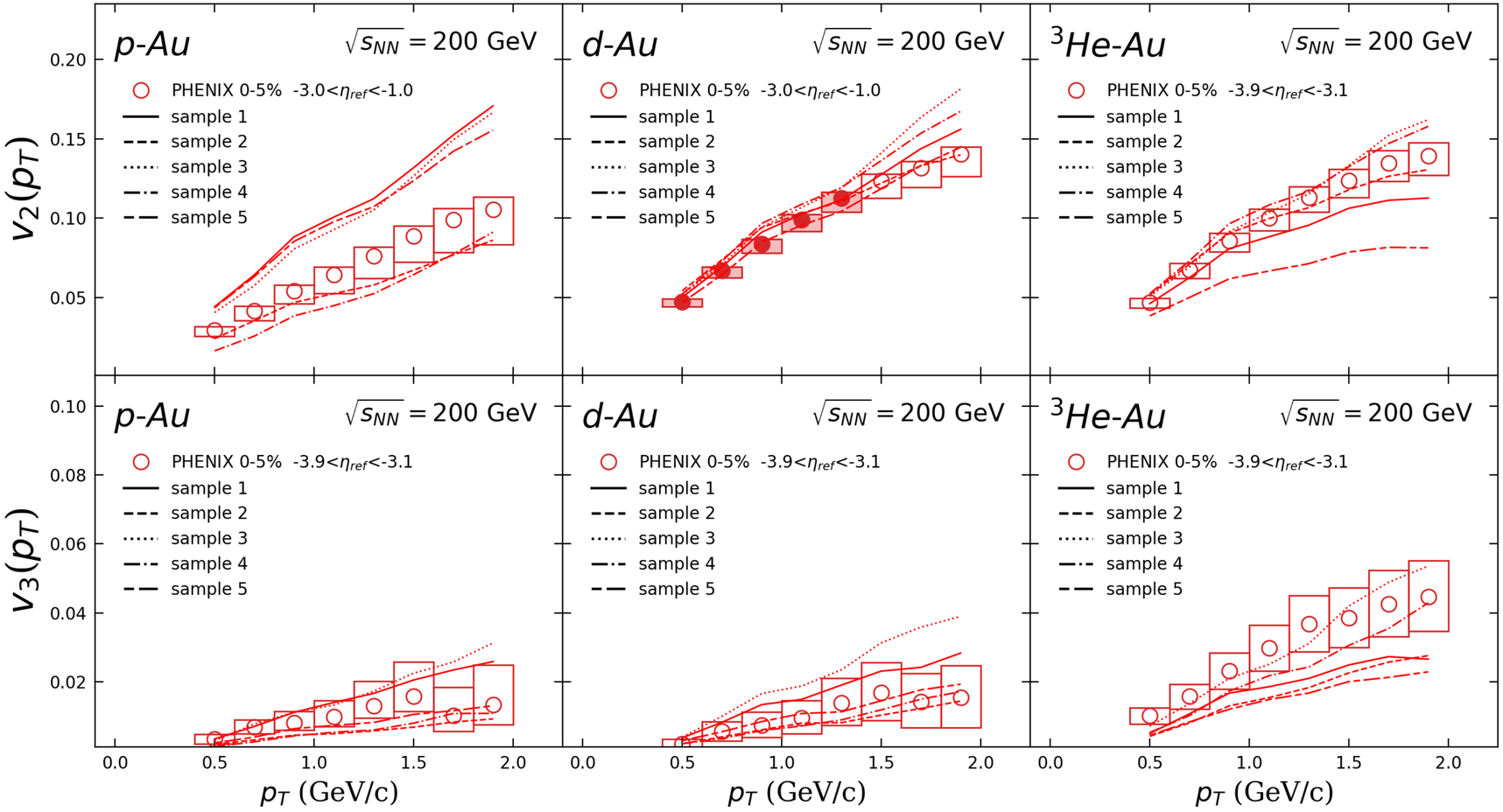

p-Au, d-Au, ^3He-Au $v_n(p_T)$ from STAR

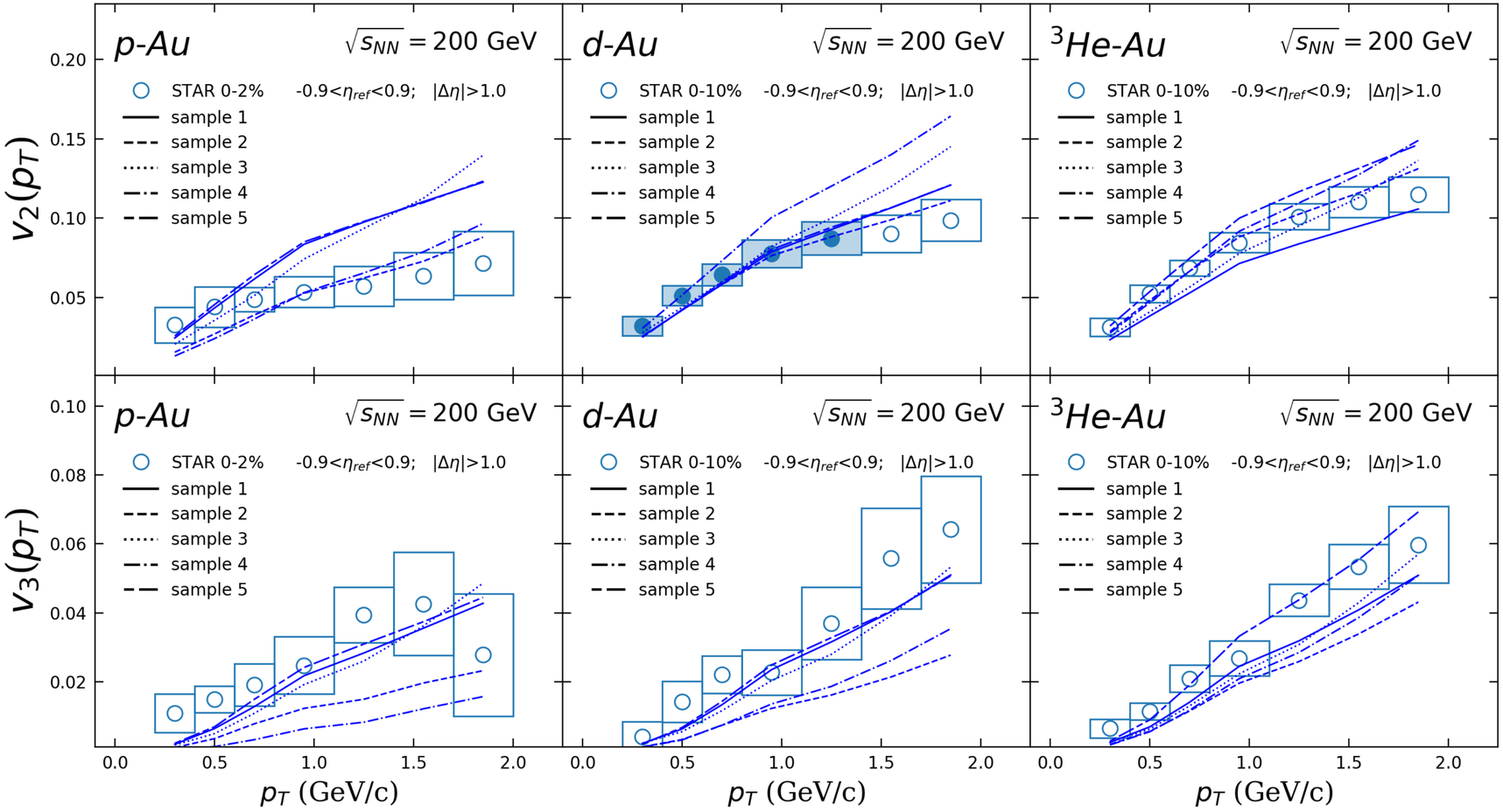

d-Au $v_3(p_T)$ from STAR

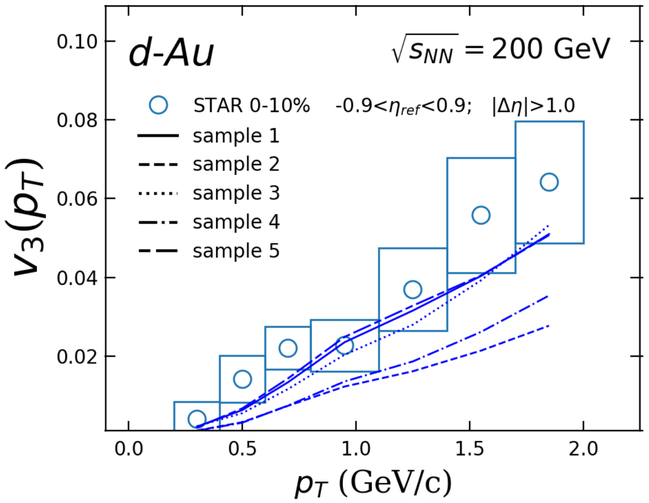

d-Au $v_3(p_T)$ from STAR & PHENIX

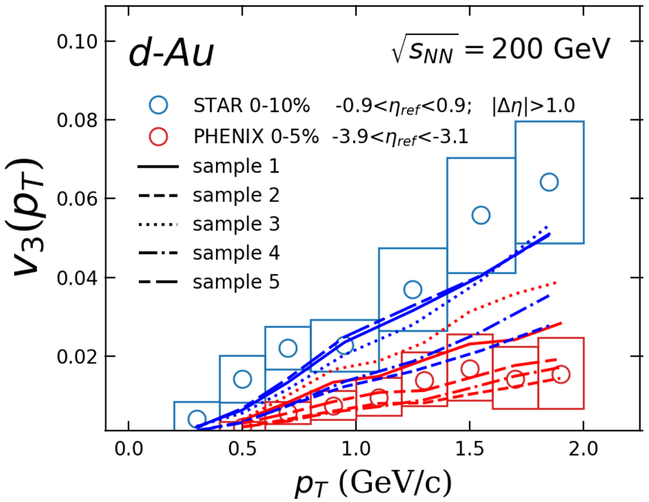

d-Au $v_3(p_T)$ from STAR & PHENIX

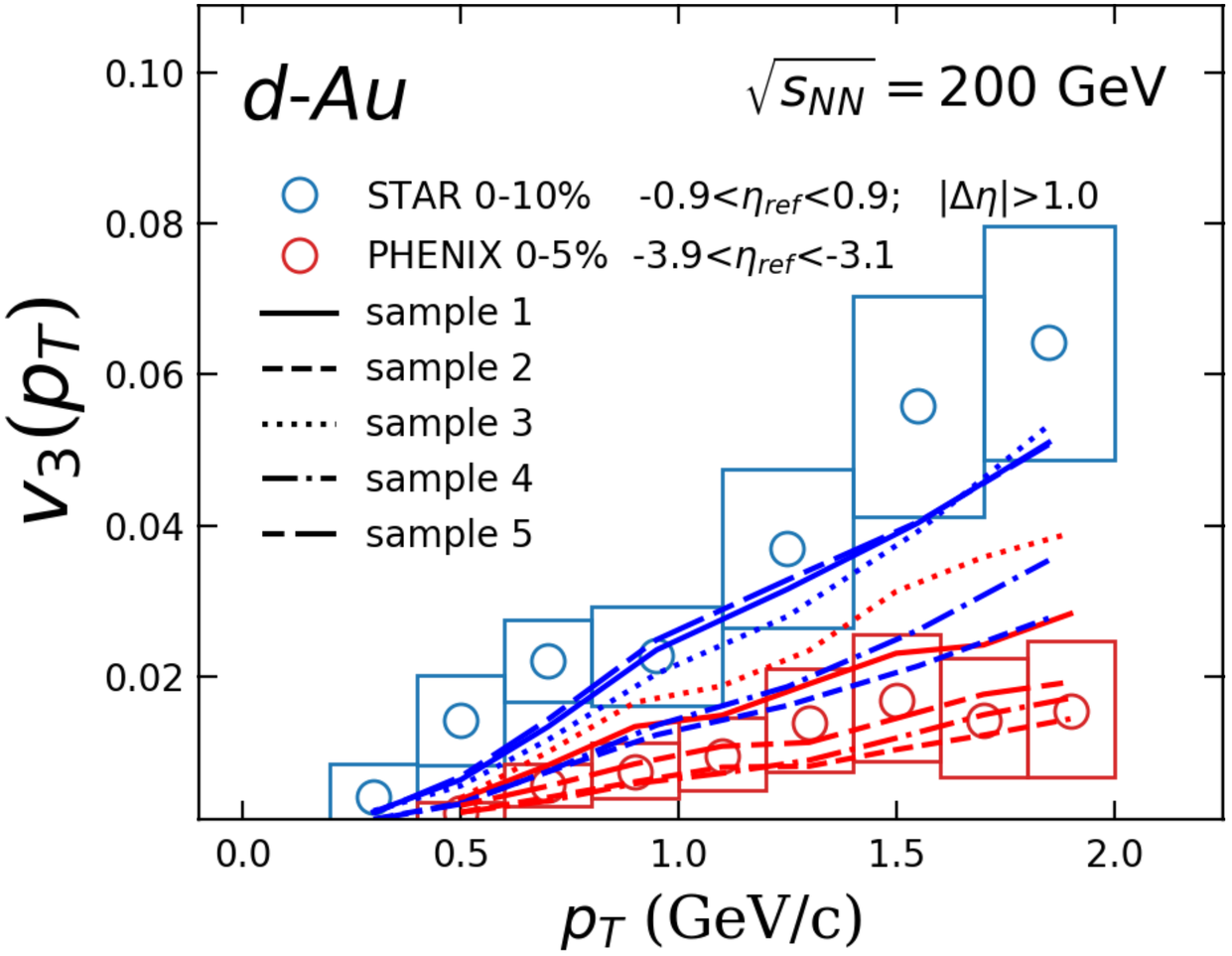

Conclusions and next steps

- Calibrated model successfully describes wide range of RHIC data in full rapidity range
- Including rapidity-dependent data leads to a preference for finite bulk viscosity
- Future analyses may work to quantify uncertainties from initial state and particlization models, covariance assumptions, and use LHC data
- Incorporating additional small systems (perhaps through transfer learning)
- Using calibration to gauge the usefulness of proposed measurements

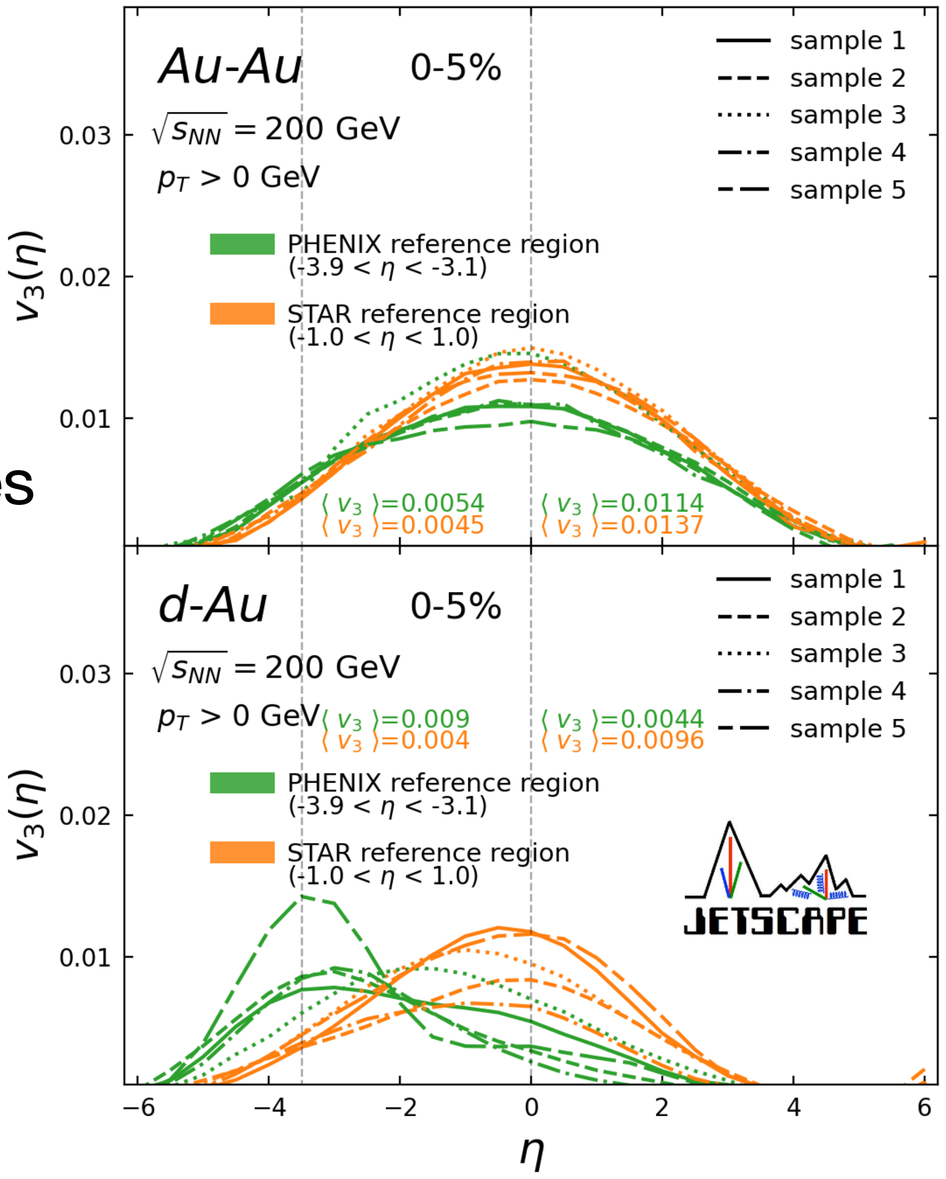

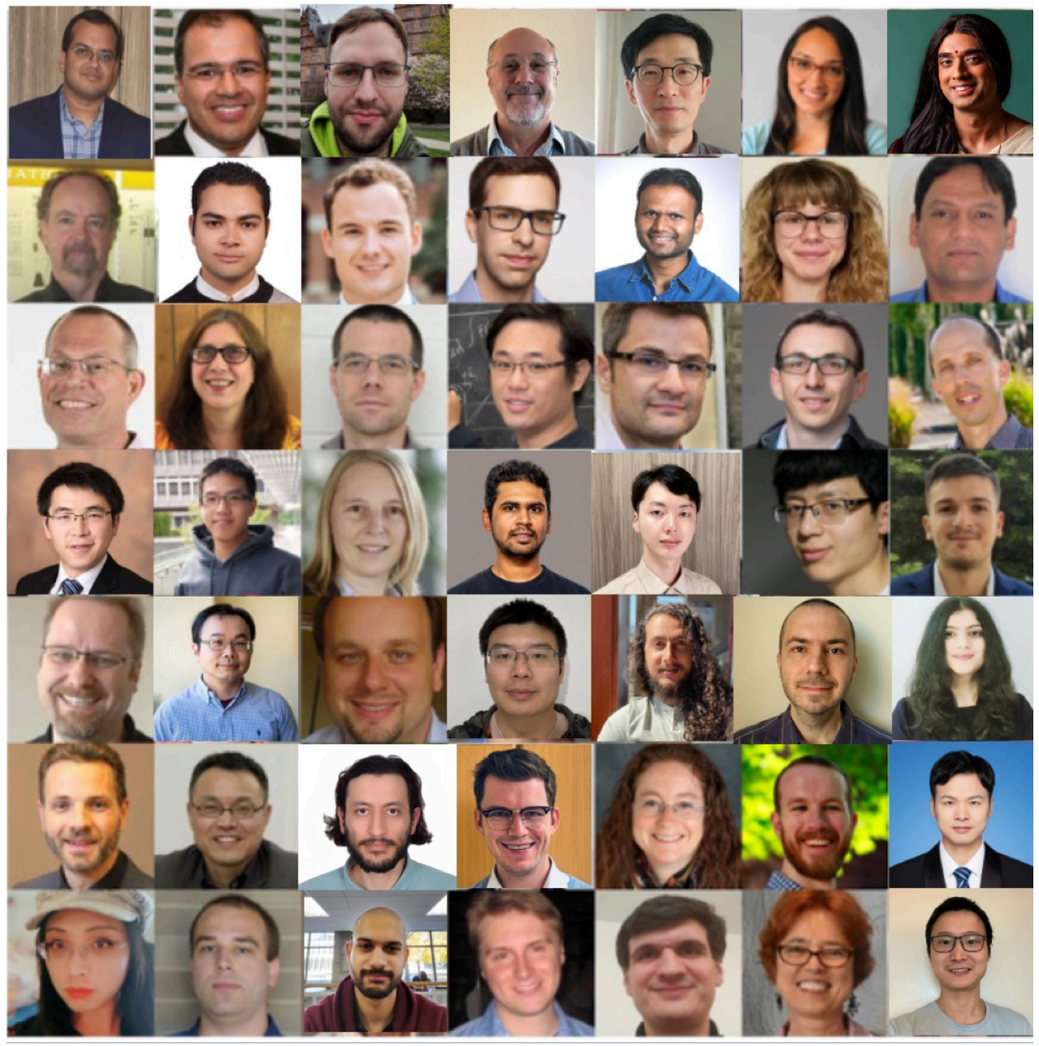

Special thanks to J-F Paquet, Matt Luzum, Julia Velkovska, Chun Shen, Mayank Singh, Gabriel Rocha, Shengquan Tuo, Matt Heffernan and the *JETSCAPE* Collaboration

THANK YOU !

Backup

Model emulation and performance

- Gaussian process emulator (GP) used as fast surrogate for full model
- Training simulations decomposed into principal components (PCs)
- Emulator performance improved by:
  - discretizing viscosity parameters
  - log-transform of $dN/d\eta$

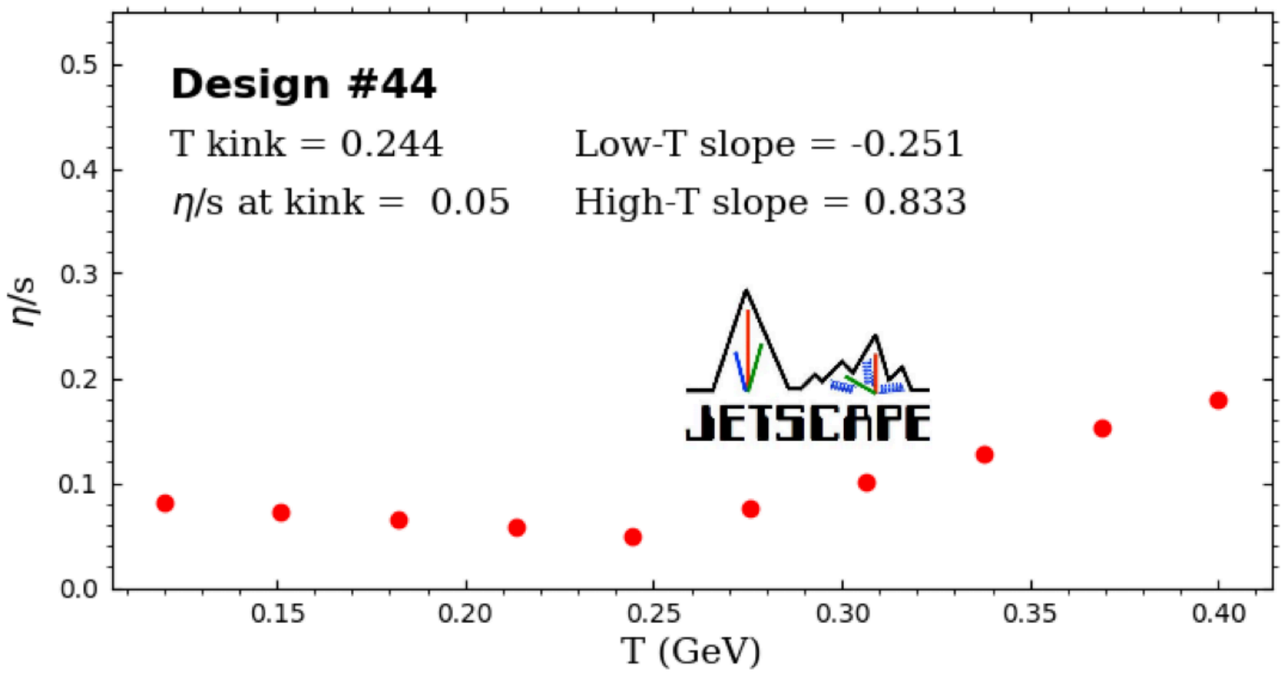

Model emulation and performance

- Gaussian process emulator (GP) used as fast surrogate for full model
- Training simulations decomposed into principal components (PCs)
- Emulator performance improved by:
  - discretizing viscosity parameters
  - log-transform of $dN/d\eta$

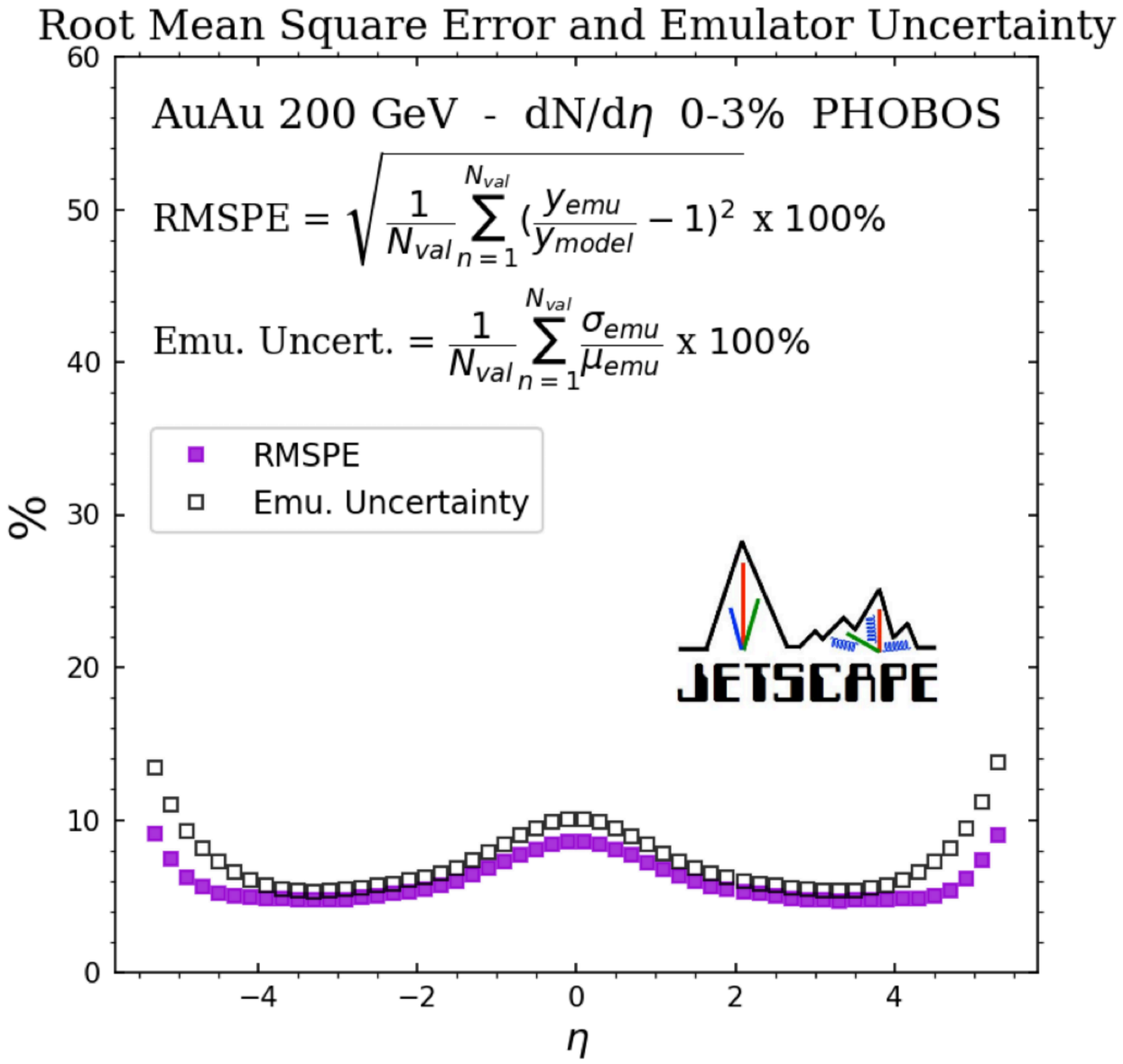

System dependence of constraints: viscosity parameters

- Somewhat consistent individual system posteriors (Au-Au and d-Au)
- Stronger indication of finite viscosity from Au-Au (particularly at low T)
  - $\langle p_T \rangle$, centrality dependence, and small experimental uncertainties ($v_2(p_T)$)

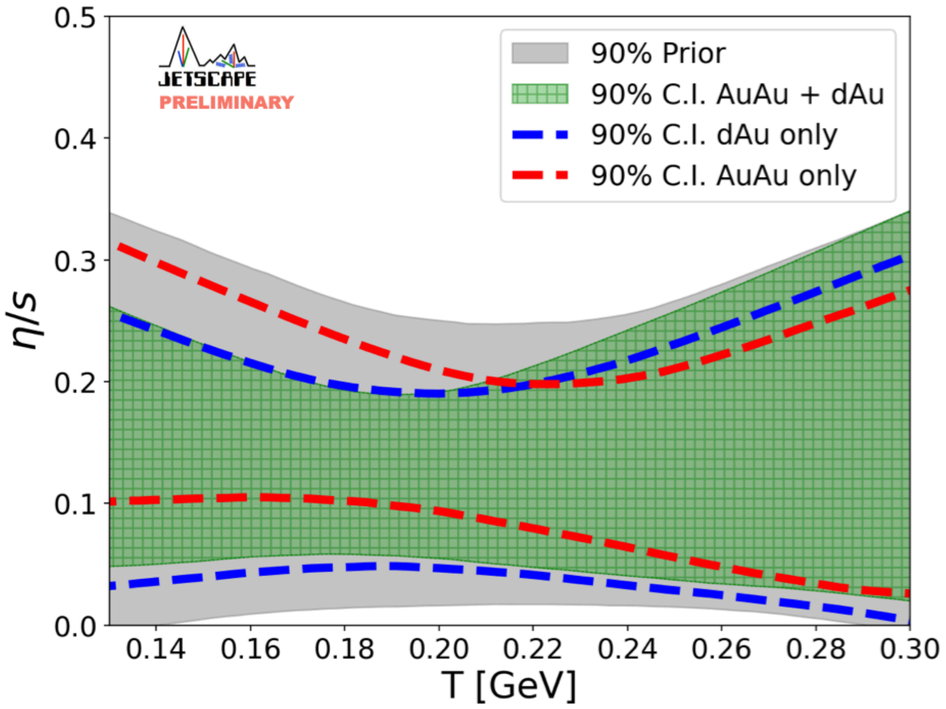

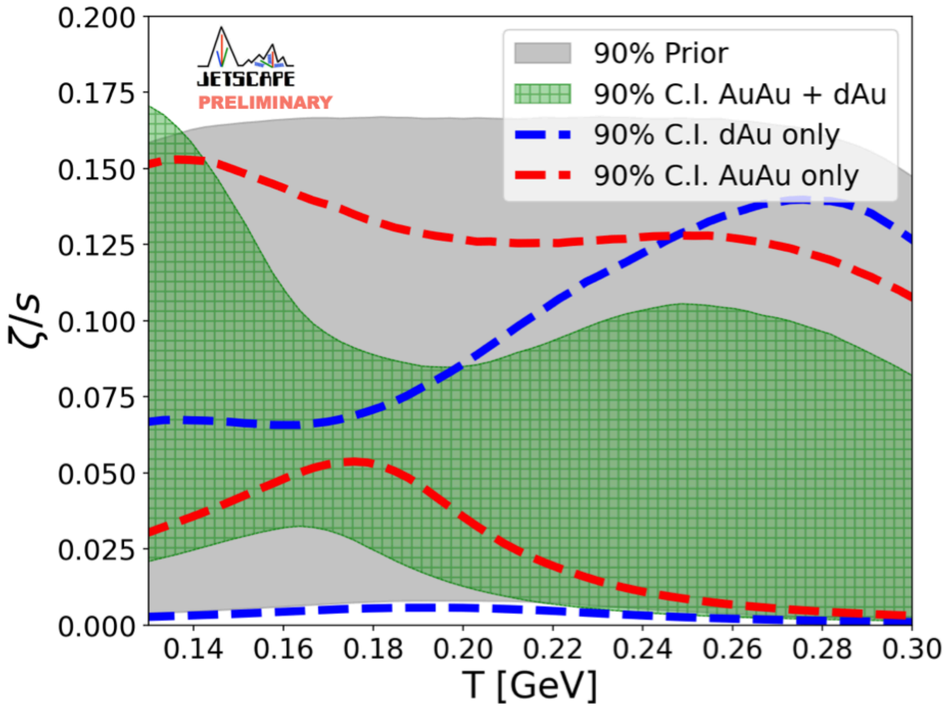

Full parameter posterior

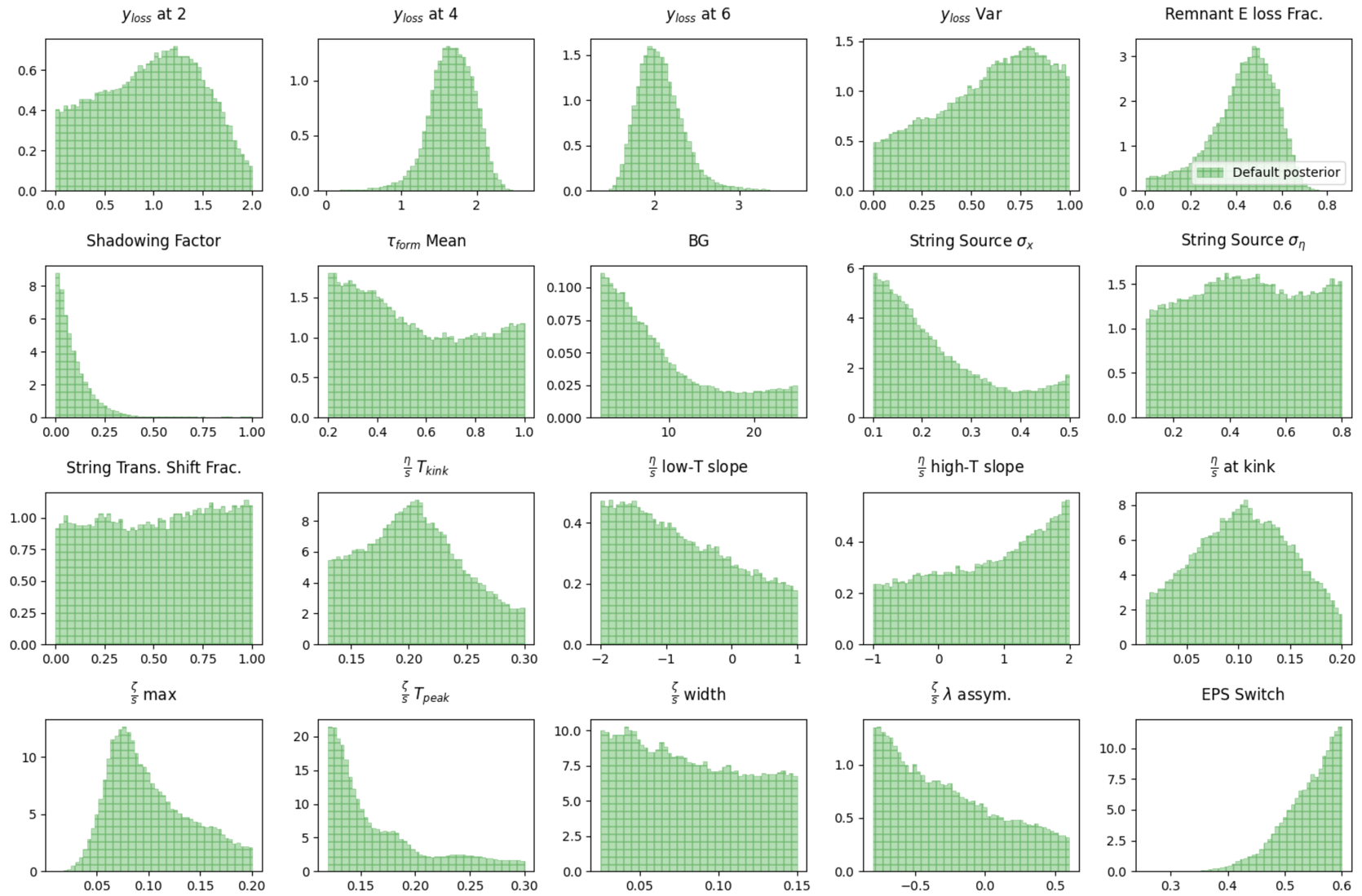

Full parameter posterior: system dependence

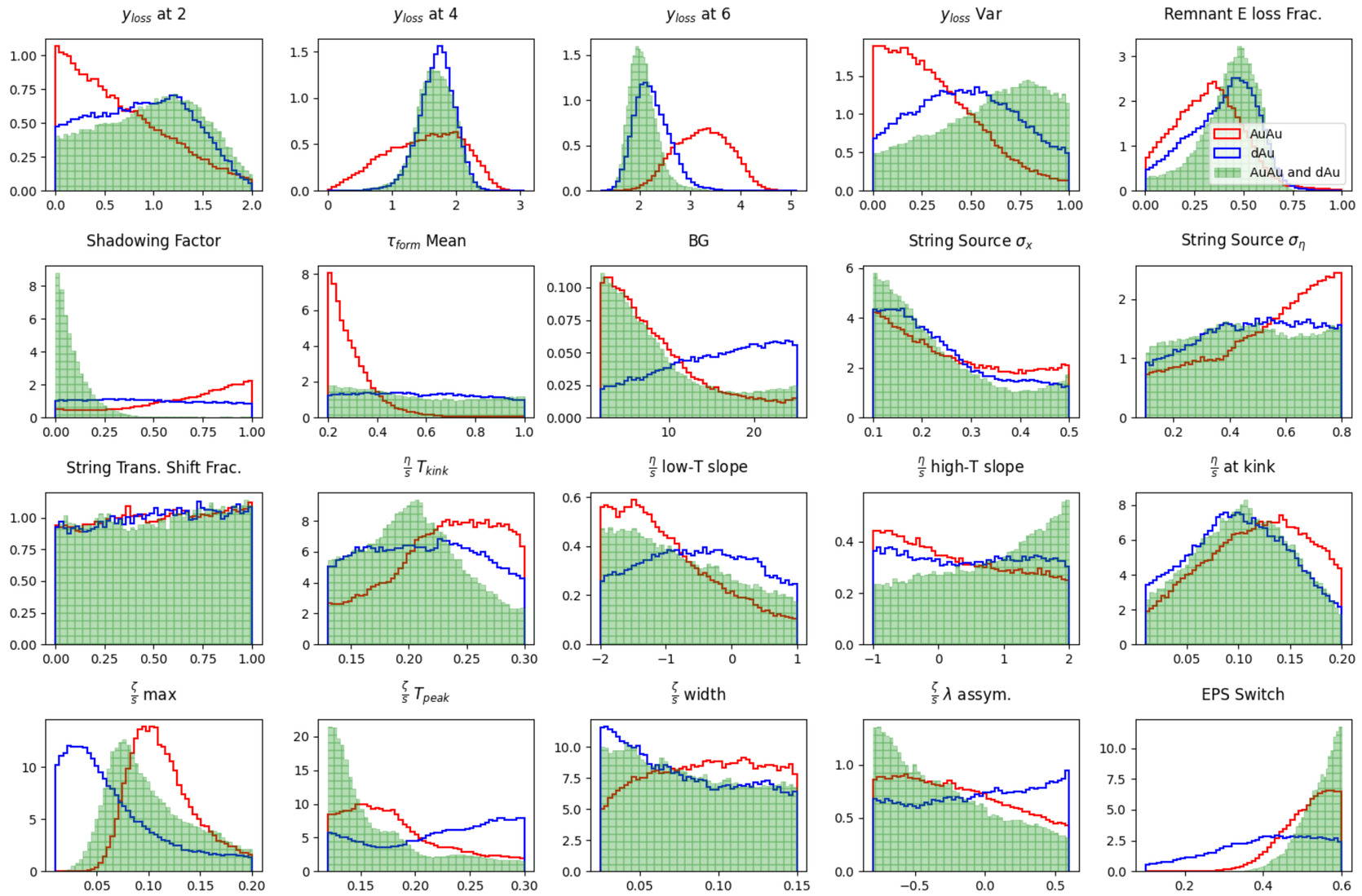

Model tension - $v_2(\eta)$ from STAR and $v_2(p_T)$ from PHENIX

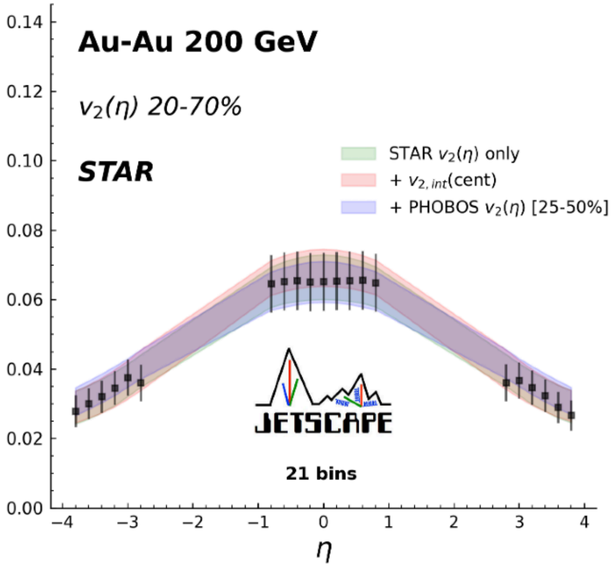

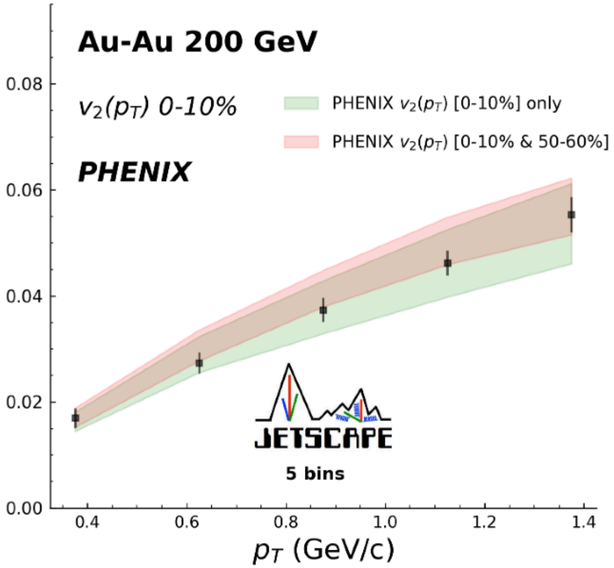

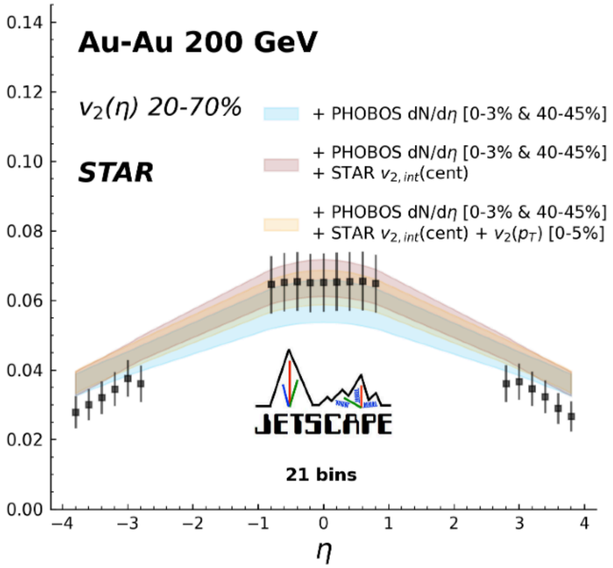

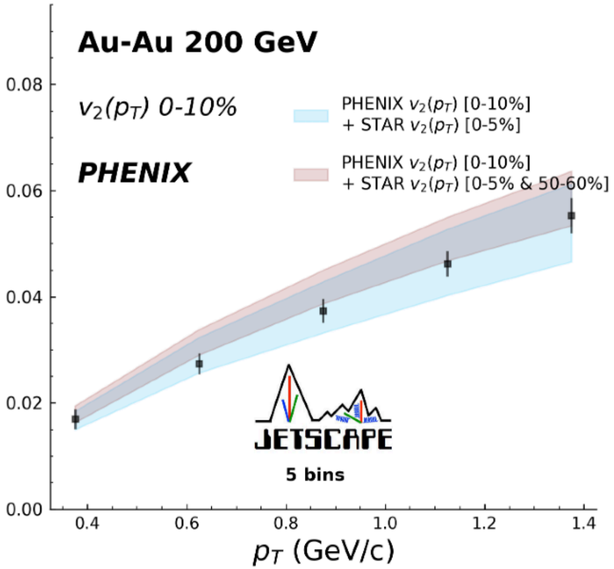

Sensitivity to parameters - bulk viscosity

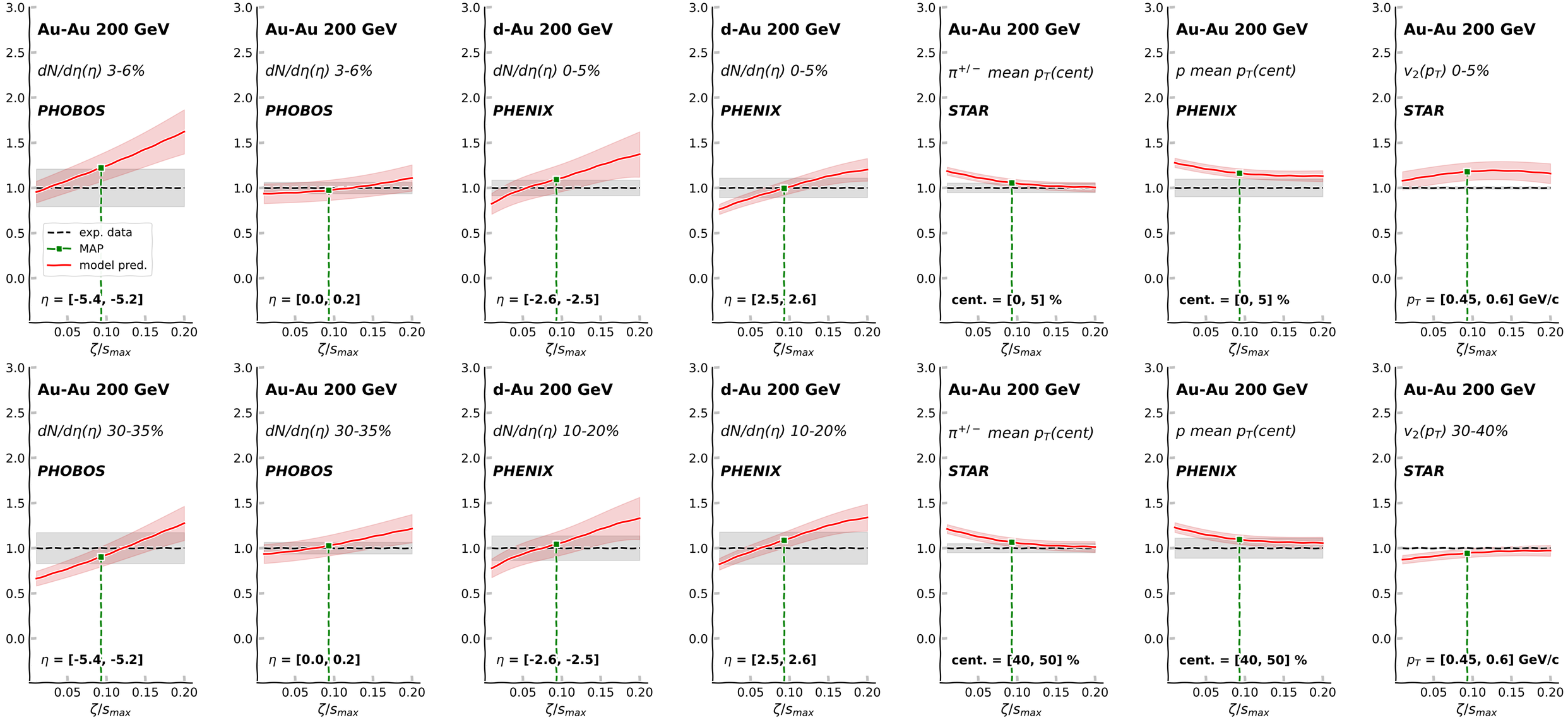

Summary of experimental data

	system	Experiment	cent.bins	data points
$dN_{ch}/\mathrm{d}\eta(\eta)$	Au-Au	PHOBOS	11	594
$v_2(\eta)$	Au-Au	PHOBOS	3	48
$v_2(\eta)$	Au-Au	STAR	1	21
$v_2(p_T)$	Au-Au	PHENIX	6	30
$v_2(p_T)$	Au-Au	STAR	7	63
v_2(cent.)	Au-Au	STAR	6	6
v_3(cent.)	Au-Au	STAR	6	6
π $\langle pT \rangle$(cent.)	Au-Au	STAR	7	7
k $\langle pT \rangle$(cent.)	Au-Au	STAR	7	7
k $\langle pT \rangle$(cent.)	Au-Au	PHENIX	8	8
p $\langle pT \rangle$(cent.)	Au-Au	PHENIX	8	8
$dN_{ch}/\mathrm{d}\eta(\eta)$	d-Au	PHOBOS	1	54
$dN_{ch}/\mathrm{d}\eta(\eta)$	d-Au	PHENIX	3	102
$v_2(\eta)$	d-Au	PHENIX	1	14
$v_2(p_T)$	d-Au	PHENIX	1	5
$v_2(p_T)$	d-Au	STAR	1	5
Total				978

The model parameters and their priors

Parameter	Collision Stage	Prior Range
$y_{loss,2}$	Initial State	[0,2]
$y_{loss,4}$	Initial State	[$y_{loss,2}$,4]
$y_{loss,6}$	Initial State	[$y_{loss,4}$,6]
$\sigma_{y_{loss}}$	Initial State	[0,1]
α_{rem}	Initial State	[0,1]
Shadowing Factor	Initial State	[0,1]
τ_{form} Mean	Initial State	[0.2,1]
B_G [1/GeV^2]	Initial State	[2,25]
String Source σ_x [fm]	Initial State	[0.1,0.5]
String Source σ_η	Initial State	[0.1,0.8]
String Trans. Shift Frac.	Initial State	[0,1]
$\frac{\eta}{s}$ T_{kink} [GeV]	Hydro	[0.13,0.3]
$\frac{\eta}{s}$ low-T slope	Hydro	[-2,1]
$\frac{\eta}{s}$ high-T slope	Hydro	[-1,2]
$\frac{\eta}{s}$ at kink	Hydro	[0.01,0.2]
$\frac{\zeta}{s}$ max	Hydro	[0.01,0.2]
$\frac{\zeta}{s}$ T_{peak} [GeV]	Hydro	[0.12,0.3]
$\frac{\zeta}{s}$ width	Hydro	[0.025,0.15]
$\frac{\zeta}{s}$ λ assym.	Hydro	[-0.8,0.6]
EPS Switch [GeV/fm^3]	Particlization	[0.1,0.6]

Parameter priors

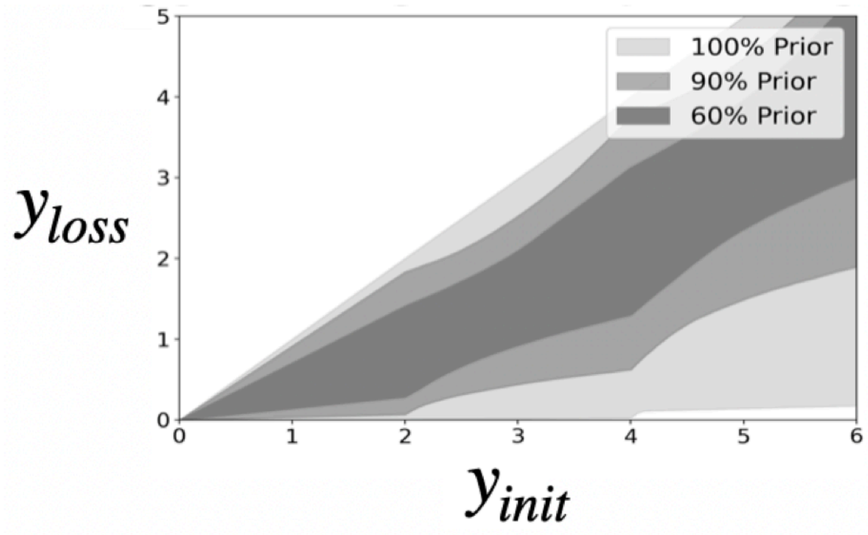

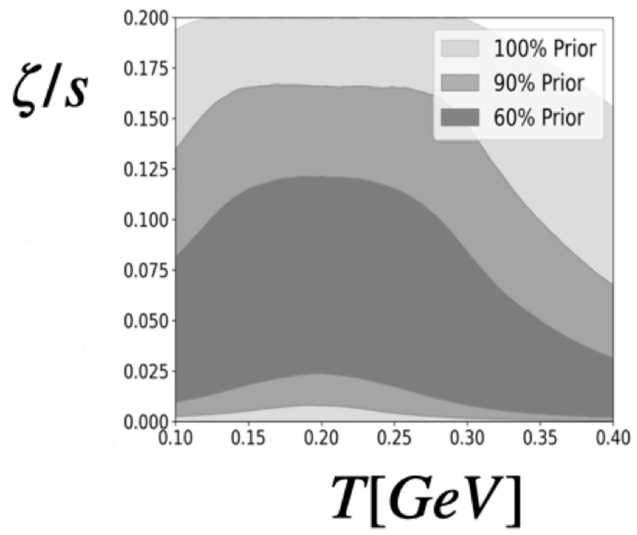

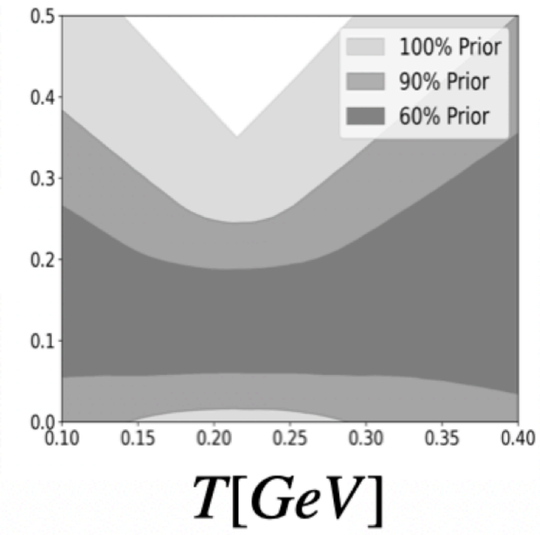

Impact of correlated errors on Bayesian fits in heavy ion physics

A simple model to investigate jet quenching and correlated errors for centrality-dependent nuclear-modification factors in relativistic heavy-ion collisions

" Fits to uncorrelated errors…closely track the measured data points, but when systematic error correlations are introduced, the most-probably fit functions undershoot the measured data. "

Soltz, Hangal, Angerami

Phys. Rev. C 111, 034911 (2025)

Observable sensitivity indices

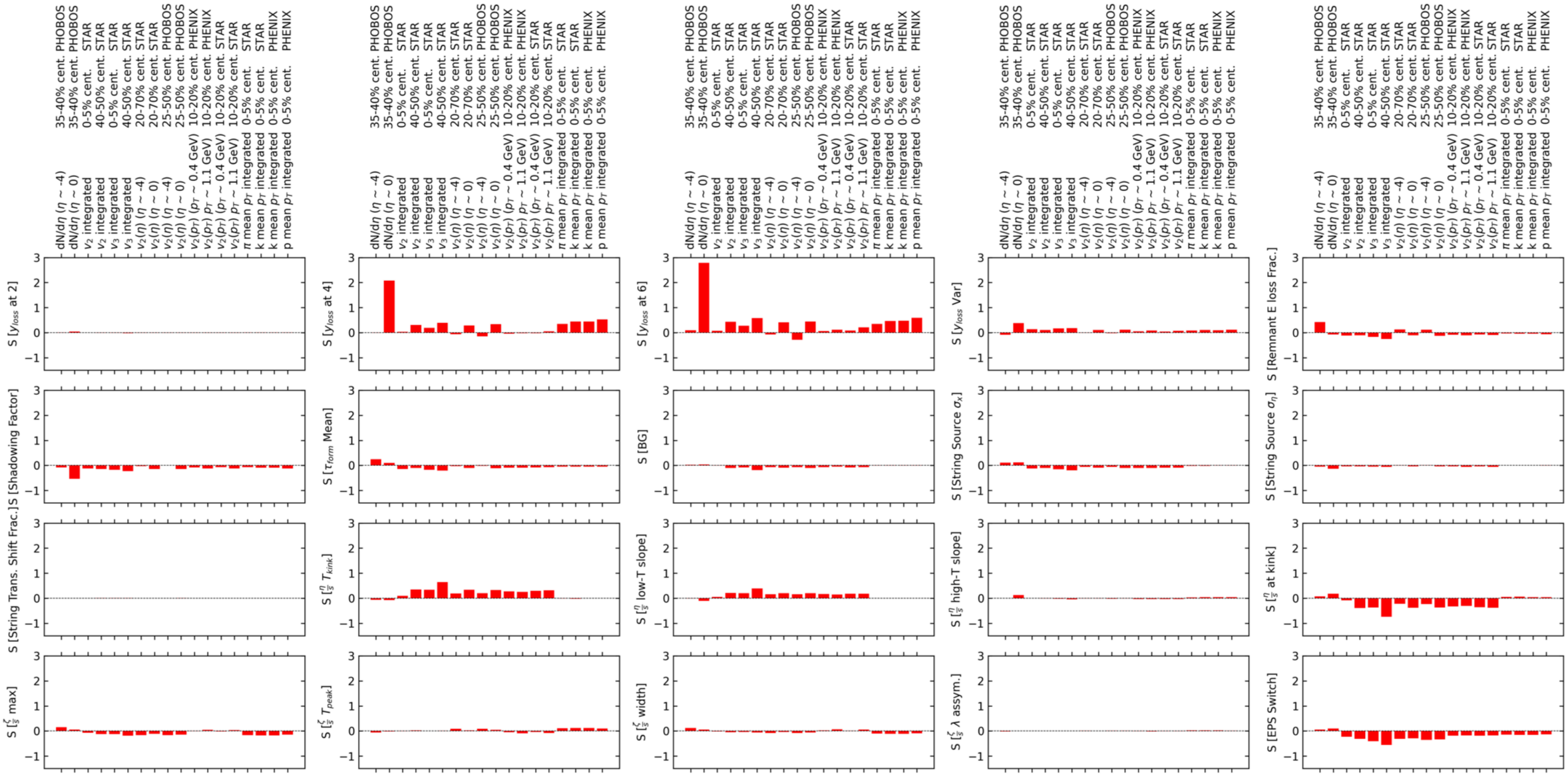

Calibrating on a single collision system

- Model constrained on only d-Au data describes Au-Au observables

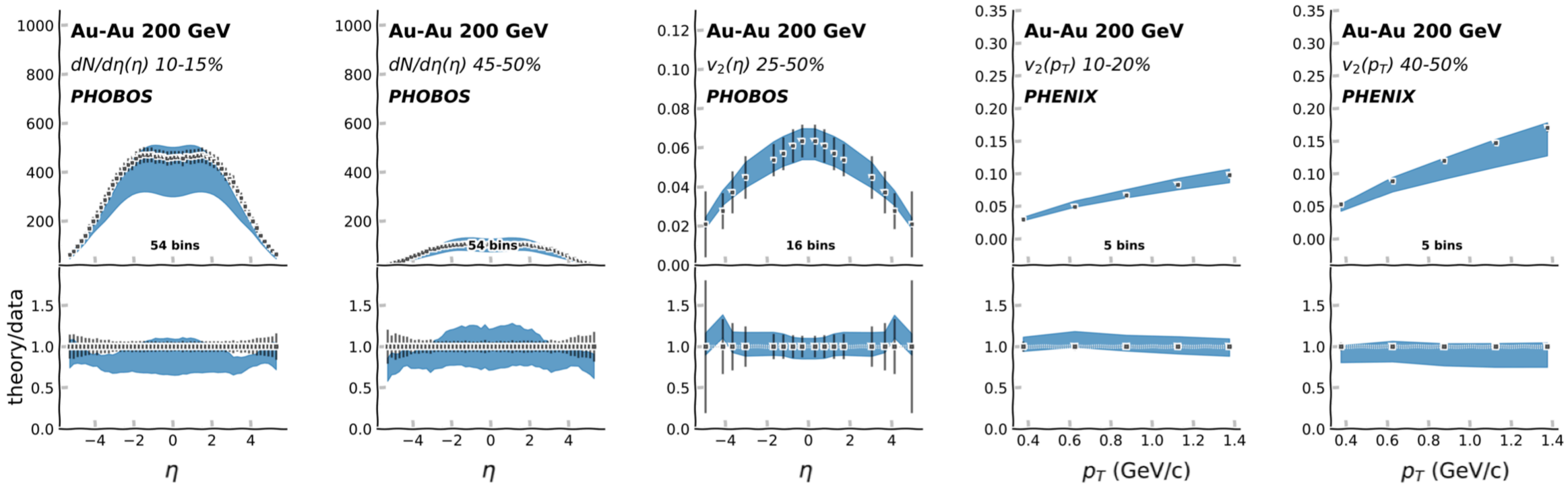

Observables from calibrated model: Au-Au-only fit

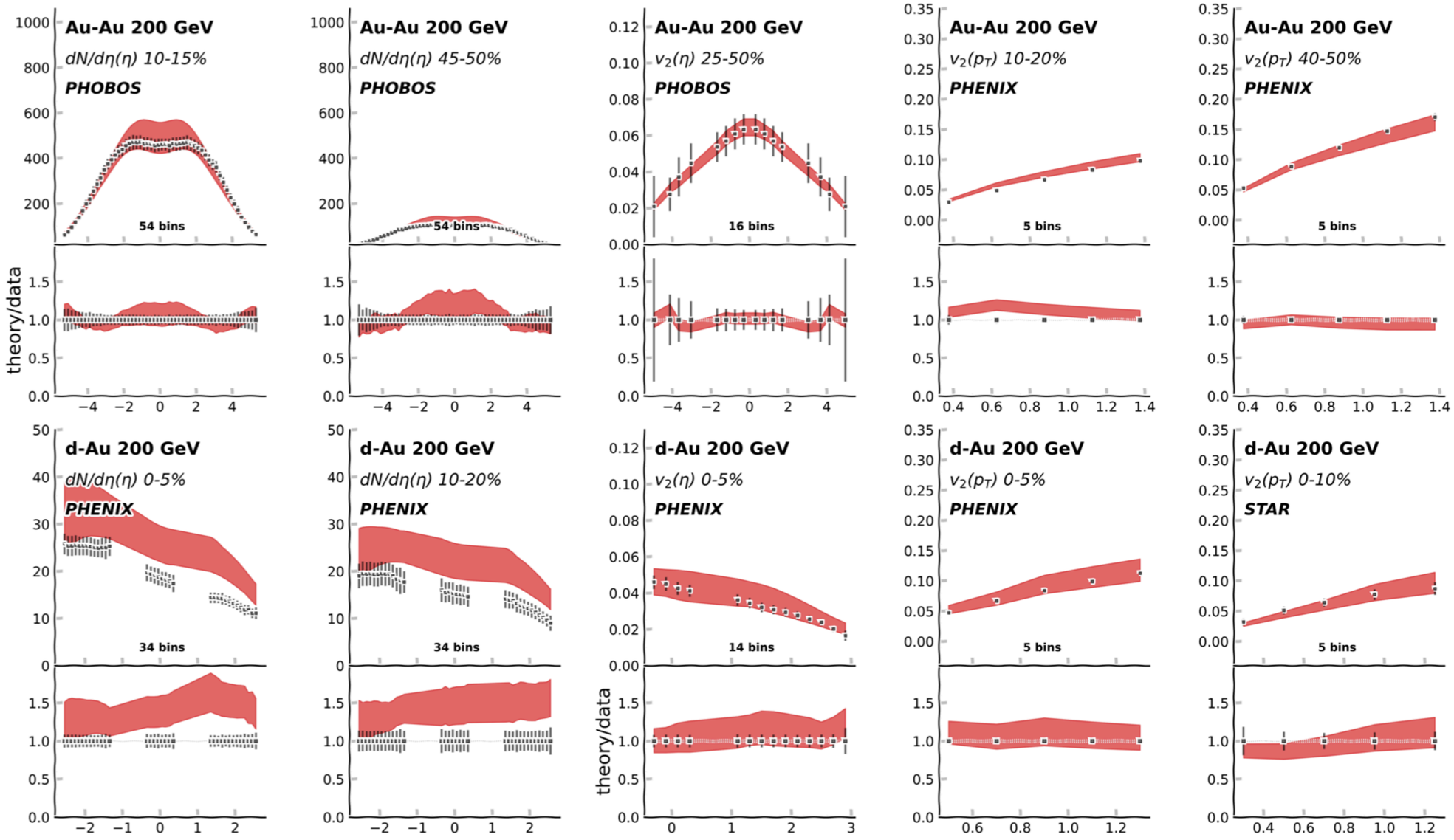

2pc $\Delta\phi$ distribution and correlation function

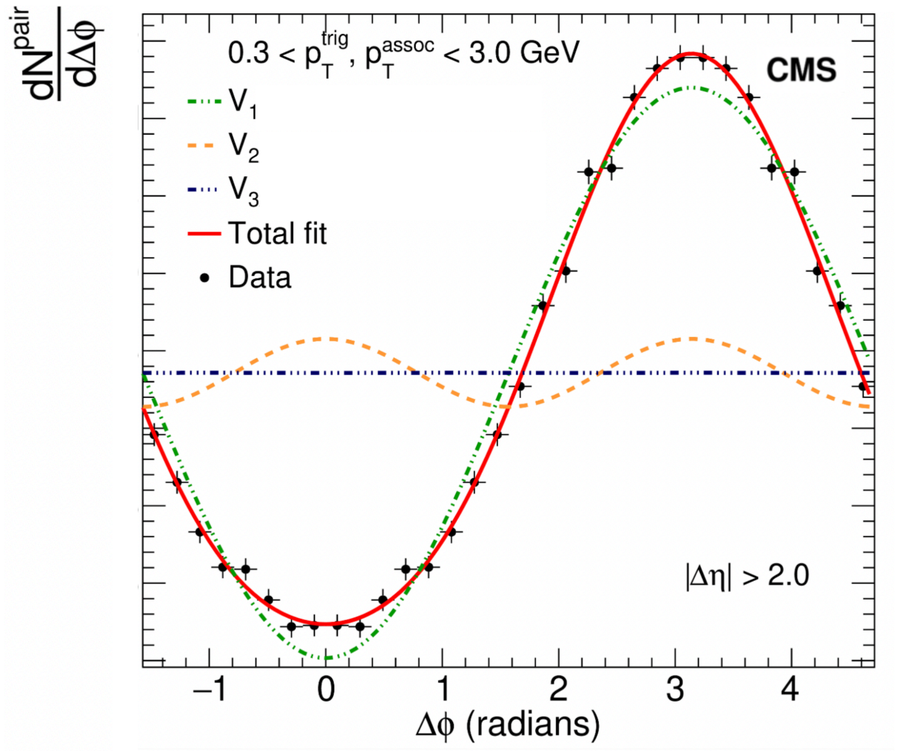

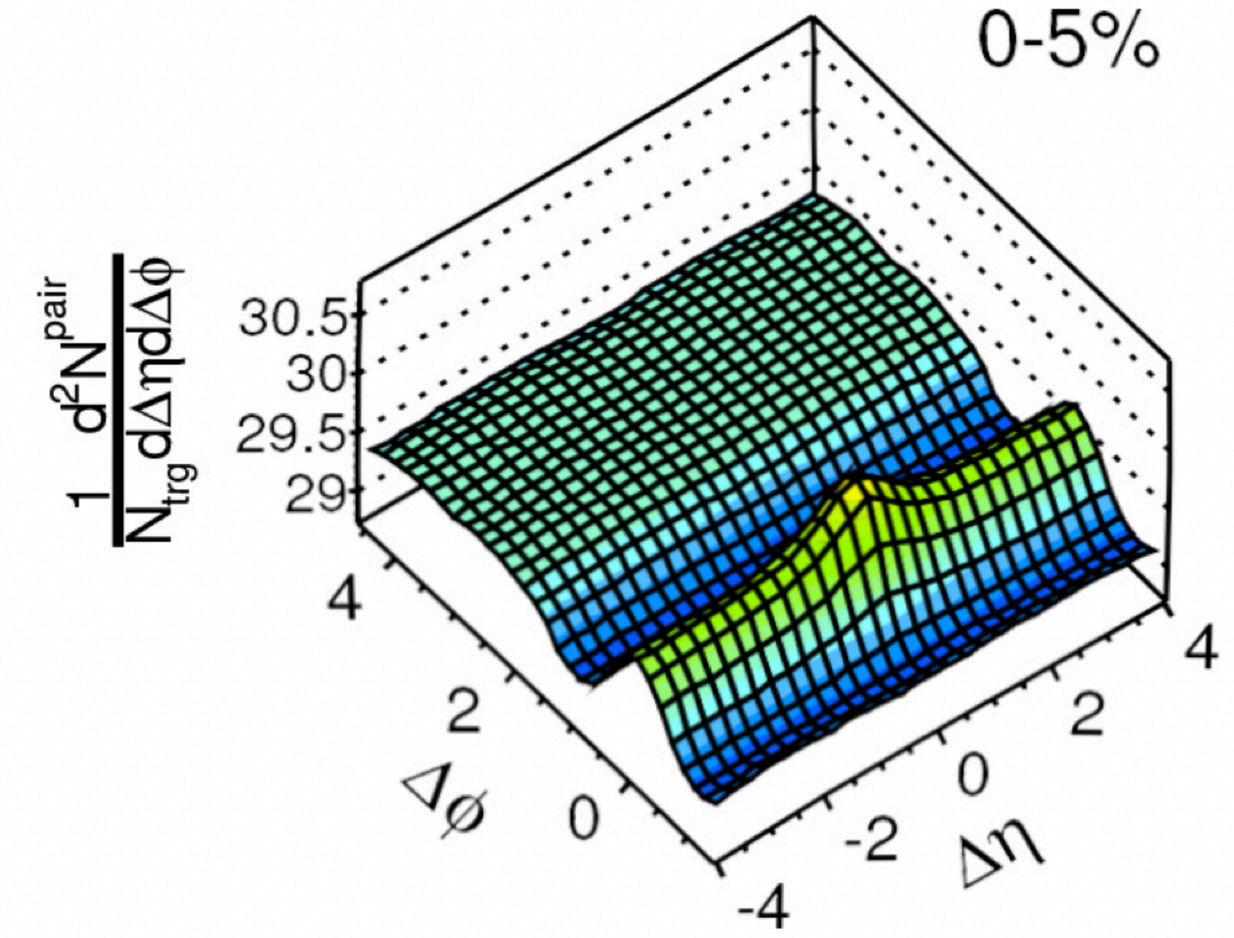

Likelihood function

$$\mathcal{P}(\boldsymbol{y}_e|\boldsymbol{\theta}, I) = \frac{1}{(2\pi|\boldsymbol{\Sigma}(\theta)|)^{N/2}} \exp\left[-\frac{1}{2}\Delta\boldsymbol{y}^T(\boldsymbol{\theta})\boldsymbol{\Sigma}^{-1}(\boldsymbol{\theta})\Delta\boldsymbol{y}(\boldsymbol{\theta})\right]$$

The Model: 3D Initial State and Hydrodynamics

Impose energy momentum conservation

α_{rem} (Remnant energy loss fraction)

Initial State

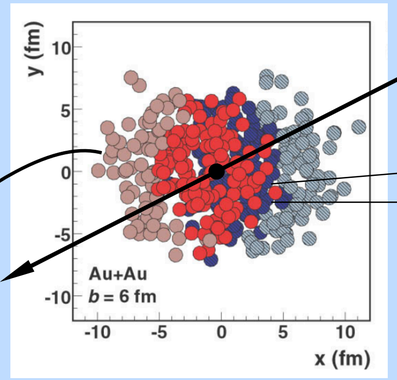

B_G

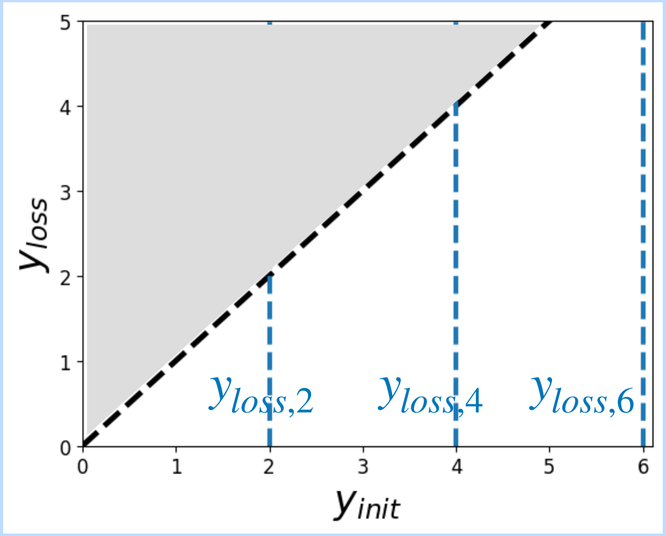

Schenke, Shen, Zhao.

Phys. Rev. C 105, 064905 (2022)

Phys. Rev. C 97, 024907 (2018)

3D MCGlauber

Hydrodynamics

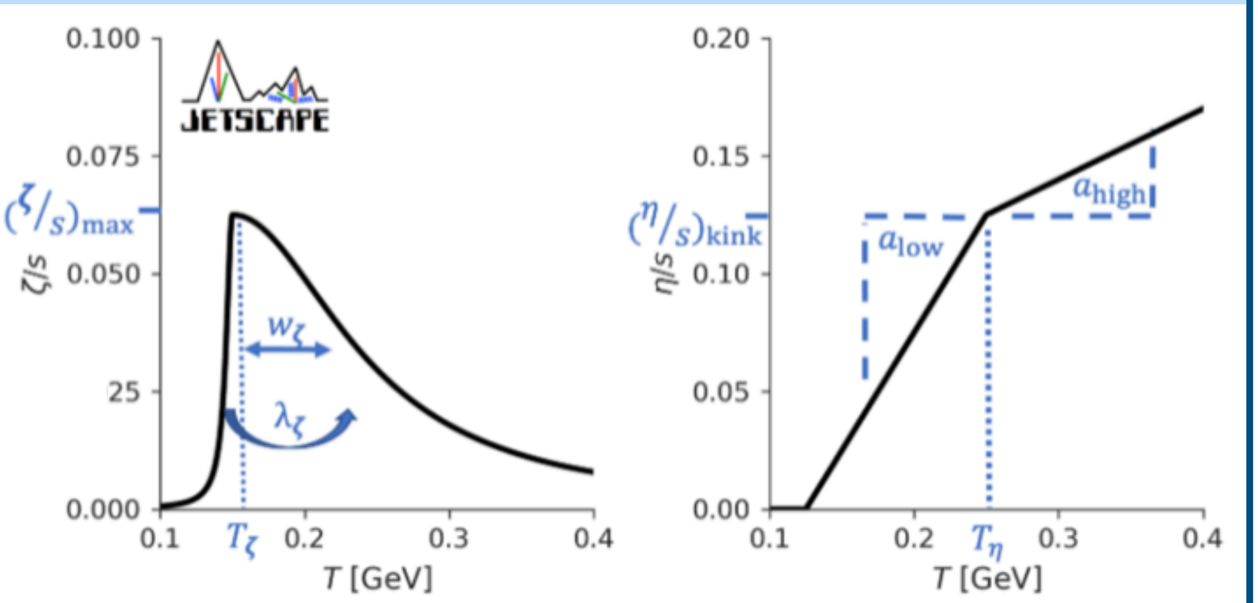

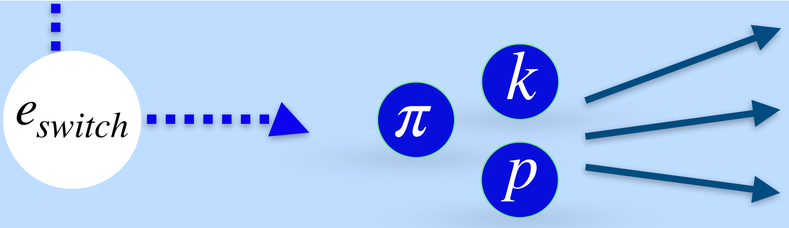

Hadronic Transport

MUSIC + UrQMD